On the Function of Somatic and Dendritic SK Channels in Cortical Pyramidal Neurons

A thesis submitted for the degree of Doctor of Philosophy of
The Australian National University

May 2014

By
Scott Lewis Jones

Australian National University

Eccles Institute of Neuroscience
The John Curtin School of Medical Research
The Australian National University
Canberra, Australia

STATEMENT

All the work described in this thesis is original and were performed between February 2010 and March 2014 under the supervision of Prof. Greg Stuart. A number of abstracts from presentations made at scientific meetings and one paper has been published as a result of the work described in this thesis:

ABSTRACTS

Jones, S. L. and Stuart, G. J. 2014. Action potential induced suppression of EPSPs by dendritic SK channels. Australian Neuroscience Society Meeting, Adelaide, SA, Australia.

Jones, S. L. and Stuart, G. J. 2012. Different calcium sources control somatic and dendritic SK channel activation in cortical pyramidal neurons. Federation of European Neurosciences Meeting, Barcelona, Spain.

Jones, S. L. and Stuart, G. J. 2012. Activation of SK channels in spines and dendrites by action potentials. Australian Neuroscience Society Meeting, Gold Coast, QLD, Australia.

PAPERS

Jones, S. L. and Stuart, G. J. 2013. Different calcium sources control somatic versus dendritic SK channel activation during action potentials. *J. Neurosci.* 33(50): 19396-19405.

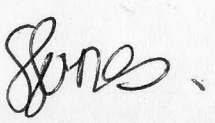

Scott L. Jones

ACKNOWLEDGEMENTS

I would firstly like to thank my supervisor Prof. Greg Stuart for his guidance and patience. His rigorous examination of concepts, ideas and arguments has taught me a great deal about how to think as a scientist.

I would also like to thank the members of my supervisory panel, Prof. John Bekkers and Dr. Maarten Kole, for their advice and helpful discussions.

Many thanks to Prof. Jens-Karl Eilers for helpful discussions on some aspects of the data in this study.

I would like to express thanks to my dear friends Tobias Bock and Dr. Jean-Didier Breton, for all of the helpful discussions we've had over the last four years and most importantly, never failing to make me laugh.

I would like to acknowledge my colleagues Dr. Mic Cavazzini, Dr. Fabio Longordo, Dr. Kaori Ikeda, Dr. Sepideh Keshavarzi, Minh-Son To and Stephen Rudinski for their good will, assistance and insights.

Thank you kindly to Garry Rodda for his outstanding technical support.

On a special note, I would like to thank my partner Janaya who has been an unwavering source of support and encouragement. There is not a day that goes by that I don't realise how lucky I am to have somebody such as her.

Finally I would also like to thank my family for their encouragement, support and inspiration. They've always taught me that those who dare to climb the mountains are the ones that get the greatest views.

SUMMARY

Small-conductance calcium-activated potassium (SK) channels play an important role in regulating neuronal excitability. Recent evidence indicates SK channels regulate NMDA receptor activation in dendritic spines and play a role in regulating synaptic plasticity. Using confocal fluorescent calcium imaging, we investigate the activation of SK channels in spines and dendrites of layer 5 (L5) cortical pyramidal neurons during action potentials (APs). The inhibition of SK channels with apamin results in a location-dependent increase in calcium influx into dendrites and spines during backpropagating APs (average increase ~40%). This effect was occluded by block of R-type voltage-dependent calcium channels (VDCCs), but not by inhibition of N- or P/Q-type VDCCs, or block of calcium release from intracellular stores. These results indicate that dendritic SK channels regulate calcium influx into dendrites and spines presumably by regulating the waveform of the backpropagating action potential. In addition, they show that SK channel activation is specifically controlled by calcium influx through R-type VDCCs, complimenting previous work indicating that SK channels are located within 25-50 nm of their calcium source, in a calcium nanodomain.

SK channels have also long been known to contribute to the medium afterhyperpolarization (mAHP) at the soma for many neuronal types, including L5 pyramidal neurons, where they regulate action potential output gain and the propensity for burst firing. During the experiments using confocal calcium imaging we noticed that the calcium indicator used, Oregon Green BAPTA-1,

which acts as a fast calcium buffer, blocked the SK mAHP. Subsequent experiments using low concentrations of the slow calcium buffer EGTA (1 mM) produced the same result, suggesting that somatic SK channels are not tightly co-localised with their calcium source. We estimate a coupling distance of greater than 150 nm, suggesting that calcium signaling between somatic SK channels and their calcium source occurs within a microdomain. Consistent with this idea, we show that all known subtypes of VDCCs except R-type were calcium sources for the apamin-sensitive mAHP at the soma.

Spike timing dependent plasticity (STDP) is a form of plasticity whereby the strength of connections between neurons in the brain are modulated following the pairing of postsynaptic APs with presynaptic activity within a narrow time window. The influx of calcium during EPSP-AP pairing is crucial to the induction of STDP. Given we show that dendritic SK channels can be activated by and influence calcium influx during bAPs, we investigated whether dendritic SK channel activation by bAPs can regulate STDP. We show that SK channels activated by bAPs significantly suppress EPSPs at negative timings for L5-L5 synaptic connections by dampening the activation of NMDA receptors. SK channels also suppressed EPSPs in layer 2/3 and hippocampal CA1 pyramidal neurons. Finally, we show that the induction of both LTP and LTD for L5-L5 synaptic connections is constrained by SK channel activation, presumably through their capacity to limit dendritic calcium influx during EPSP-AP pairing.

In conclusion, these findings provide new insights into the function of SK channels and the multifaceted role calcium plays in neuronal function.

Table of Contents

CHAPTER 1: GENERAL INTRODUCTION

GENERAL BACKGROUND

Single neurons in the brain receive thousands of synaptic inputs that are integrated in time and space to ultimately trigger an all-or-none action potential (AP). The mechanisms employed to achieve such integration are complex and varied, depending the site of synaptic input, neuronal morphology and the properties and distribution of ion channels in the dendritic tree.

Since the morphological investigations carried out by Santiago Ramon y Cajal in the late 19th and early 20th century, how neurons receive and process synaptic inputs has been under intense investigation and debate. It was Cajal (1911) that provided the foundational evidence for the neuron model, hypothesizing that single nerve cells, or neurons, function as individual units within the brain. In addition, Cajal's 'dynamic polarization' hypothesis proposed a theory for information flow in the brain, suggesting that neurons receive signals onto their dendritic tree, which then travel towards the soma and along the axon to terminate onto neighbouring neurons. These two concepts are still central to our current understanding of neurobiology.

Even though neurons display a variety of morphologies, almost all have dendritic and axonal compartments connected by the soma. Each of these compartments receives and processes information differently. The majority of synaptic inputs converge onto the dendritic tree, the morphology of which is

highly variable across neuronal types, ranging from the highly branched Purkinje neuron to the single branched olfactory sensing cell (Fiala & Harris, 1999). Synaptic inputs cause localized activation of ligand-gated ion channels within the postsynaptic membrane, which in turn, depending on the input type, evoke postsynaptic potentials (PSPs) that are either excitatory (EPSPs), causing depolarization, or inhibitory (IPSPs), causing hyperpolarization. The resulting PSP then propagates towards the axon, specialized for generating the AP due to a high density of voltage-gated sodium channels (Colbert & Johnston, 1996; Stuart *et al.*, 1997; Palmer & Stuart, 2006; Kole *et al.*, 2008). Generally, a multitude of excitatory inputs are required for the membrane potential to reach AP threshold. Furthermore, EPSPs attenuate significantly as they propagate through the dendritic tree, and can be significantly reduced by inhibitory input. Once initiated, APs propagate down the axon to trigger neurotransmitter release onto postsynaptic neurons, influencing their activity. In this way, groups of interconnected neurons form complex networks that perform multiple roles in information processing.

Signaling in Dendrites

A significant amount of integration and computation occurs in dendrites. Initially it was thought that the electrical behavior of dendrites could be entirely explained using passive cable theory, which uses the variables of membrane resistance (R_m), membrane capacitance (C_m) and axial resistance (R_i) to predict dendritic electrical properties (Rall, 1959). This extensive literature spanning many decades has not always been in agreement as physiological values for R_m, C_m and R_i were difficult to obtain and often based on electrical recordings

made at the soma (Spruston *et al.*, 1994). In addition, whilst passive properties play a significant role, it was later found that active conductances present within dendrites have the capacity to defy predictions of passive cable theory (Johnston *et al.*, 1996 for review). The advent of direct electrical recordings from dendrites (Stuart *et al.,* 1993) allowed a more precise description of dendritic properties and how they influence synaptic integration. A significant discovery was that APs are actively propagated antidromically from the axon into the dendritic tree of layer 5 (L5) cortical pyramidal neurons where voltage-gated sodium channels (VGSCs), expressed along the apical dendrite, facilitate the spread of APs into thinner distal dendrites (Stuart & Sakmann, 1994). This phenomenon of active backpropagation has also been demonstrated in other types of neurons including CA1 pyramidal neurons of the hippocampus (Spruston *et al.*, 1995), dopaminergic neurons in the substantia nigra (Hausser *et al.*, 1995) and layer 2/3 (L2/3) cortical pyramidal neurons (Larkum *et al.*, 2007). In addition, dendritic VGSCs can also mediate dendritic sodium spikes, which can trigger somatic APs and amplify backpropagating APs (bAPs) when APs and EPSPs are simultaneously evoked (Stuart *et al.*, 1997; Golding *et al.*, 1998; Stuart & Hausser, 2001). Other active dendritic events involving voltage-dependent calcium channels (VDCCs), called dendritic calcium spikes, have also been described in multiple cell types. These large calcium dependent electrical events are a crucial determinant of distal dendritic integration and have been observed both *in vitro* and *in vivo* where they propagate readily towards the soma and influence AP output (Schiller *et al.*, 1997; Larkum *et al.*, 1998; Schiller *et al.,* 2000, Losonczy & Magee, 2006; Larkum *et al.*, 2009; Smith *et al.*, 2013). Finally, activation of NMDARs can lead to the generation of NMDA

spikes, which have also been proposed to play a key role in active dendritic integration (Schiller *et al.*, 2000; Larkum *et al.*, 2009;Larvzin *et al.*, 2012).

Dendritic morphology is a key determinant of the electrical properties of dendrites, with increases in axial resistance and input impedance occurring as a function of distance from the soma due to decreases in dendritic diameter (Jack *et al.*, 1975; Rinzel & Rall, 1974; Spruston, 2008). As a consequence, EPSPs recorded at distal locations cause significantly larger local voltage changes than those at more proximal locations (Williams & Stuart, 2002; Nevian *et al.*, 2007). This may explain why excitatory synaptic responses at more distal locations have a more pronounced NMDAR component compared to responses at proximal locations (Branco & Hausser, 2011). Distal synaptic conductances have also been shown to be increased for a subset of inputs to CA1 pyramidal neurons (Magee & Cook, 2000; Nicholson *et al.*, 2006), which compensates for attenuation of EPSPs as they propagate to the soma, although has been shown not to occur in L5 pyramidal neurons (Williams & Stuart, 2002). The effectiveness of this "synaptic scaling" is limited due to the reduction in electrical driving force associated with large local EPSP amplitudes at distal locations. Collectively, the effects of increasing input impedance and synaptic scaling enhance the recruitment of voltage-dependent conductances such as VDSCs, VDCCs and NMDARs, and facilitates the initiation of dendritic spikes (Larkum *et al.*, 2009; Katz *et al.*, 2009). This allows distal synaptic inputs to influence somatic AP output despite the attenuation they individually undergo (which can exceed 100 fold) as they propagate to the soma.

As large excitatory events can be readily generated in distal dendrites, there are also mechanisms that dampen excitability in these dendritic regions. Hyperpolarization-activated cation (HCN) channels, mediating the current called I_h, are expressed in a somato-dendritic gradient along the apical dendrite of cortical L5 and hippocampal CA1 pyramidal neurons (Magee, 1998; Williams & Stuart, 2000; Berger *et al.*, 2001; Lorincz *et al.*, 2002; Kole *et al.*, 2006; George *et al.*, 2009), but are not present in layer 2/3 or CA3 pyramidal neurons (Lorincz *et al.*, 2002). I_h has a profound impact on dendritic excitability. HCN channels are active at resting membrane potentials, keeping dendritic input resistance relatively low, and deactivate with depolarisation provided by EPSPs and other regenerative events (Magee & Cook, 2000; Williams & Stuart, 2002). In addition, various voltage-dependent potassium channels, mediating the currents I_A, I_K and I_M, are also readily expressed in distal dendritic regions (Hoffman *et al.*, 1997; Bekkers, 2000; Korngreen & Sakmann, 2000; Johnston *et al.*, 2000; Losonczy *et al.*, 2008; Harnett *et al.*, 2013; but see Schaefer *et al.*, 2007). Therefore, even though both passive and active membrane properties at distal dendritic regions can act to facilitate excitatory signals, the presence of opposing conductances keeps dendritic excitability in check.

Dendritic spines

For most excitatory neurons, the majority of glutamatergic synapses are made onto small protuberances projecting from the dendritic shaft called dendritic spines. Each spine usually houses the postsynaptic terminal of a single glutamatergic synapse and thus the number of spines on a given excitatory neuron equates to the minimum number of excitatory inputs that neuron

receives, which varys according to brain region and species (Elston & DeFelipe, 2002; Ballesteros-Yanez, *et al.*, 2006).

Spines display considerable variability in both size and shape (Sorra & Harris, 2000) and are very plastic (Kasai *et al.*, 2010). Most of what we know about spines has been gathered from *in vitro* investigations where in both culture and acute slice preparations spines are highly dynamic (Engert & Bonhoeffer, 1999; Bonhoeffer & Yuste, 2002; Nagerl *et al.*, 2004). Although knowledge about the properties of spines *in vivo* is somewhat limited, recent investigations confirm the dynamicity and persistence of spines during memory formation (Trachtenberg *et al.*, 2002; Roberts *et al.*, 2010; Wilbrecht *et al.*, 2010) and storage (Yang *et al.*, 2009). Both *in vitro* and *in vivo* there are both stable and more plastic populations of spines and these populations change with experience (Nagerl *et al.*, 2007). Evidence suggests that thinner spines are more dynamic and might be available to contribute to learning and memory formation (Jourdain *et al.*, 2003; Holmaat *et al.*, 2005), whereas large spines are more stable and might be more important for memory storage (Holmaat *et al.*, 2006). In addition, spine maturation correlates strongly with synaptic strength and spine size (Matsuzaki *et al.*, 2001; Matsuzaki *et al.*, 2004; Zito *et al.*, 2009). Repeated focal activation of glutamate receptors on the dendritic shaft can also lead to rapid spine formation (Kwon & Sabatini, 2011). In addition, the continued activation of small spines often leads to enlargement and an increase in responsiveness (Matsuzaki *et al.*, 2004). These studies suggest that immature spines are generally small, dynamic and produce small

electrical responses, whereas mature spines, associated with memory retention, are large and produce strong electrical responses.

Electrical properties of dendritic spines

Due to their small size, obtaining experimental data from spines continues to be a significant challenge. As a result, investigations into the electrical properties of spines have largely been conducted *in silico* using analytical and/or computational approaches. These theoretical models can be grouped into passive and active, depending on whether they incorporate the contribution of dendritic voltage-gated conductances or not. Passive models of spines purely using cable theory to determine the electrical consequences of spine morphology highlighted the asymmetry between the spine head and the parent dendrite, created by the small local capacitance and the high input resistance of the spine head (Llinas & Hillman, 1969; Rall & Rinzel, 1971; Jack *et al.*, 1975; Rall, 1978; Koch & Poggio 1983a; Koch & Poggio 1983b; Koch & Zador, 1993). These studies predict that dendritic voltage changes will invade spines without attenuation, whereas EPSPs propagating from the spine to the dendrite are likely to attenuate appreciably depending largely on the magnitude of the spine neck resistance. In addition, the high input resistance and small capacitance of the spine head means that the amplitude of EPSPs in spines is likely to be enhanced compared to EPSPs generated directly into the dendritic shaft (Rall & Rinzel, 1971; Koch & Zador, 1993).

These early passive models predicted that if the spine neck resistance is high it could augment attenuation from the spine head to the parent dendrite (Chang

1952; Llinas & Hillman 1969; Rall & Rinzel, 1971; Jack *et al.*, 1975) by reducing EPSC driving force in the spine head. It was also proposed that alterations to spine neck length, and thereby resistance, might impact on synaptic strength (Crick 1982; Rall 1978). Initial estimates based on models incorporating ultrastructural and diffusional coupling information predict a spine neck conductance of between 2 and 1000 nanosiemens (nS) (Harris & Stevens 1988; Svoboda *et al.*, 1996). These predictions of neck conductance are much higher than measured synaptic conductances, which are on the order of 0.2-1 nS (Bekkers *et al.*, 1990), although may be underestimated due to the use of somatic voltage clamp measurements (Williams & Mitchell, 2008). These initial studies suggested only a modest filtering effect of the spine neck and that spines work primarily as biochemical rather than electrical compartments (Wickens, 1988; Koch & Zador, 1993; Svoboda *et al.*, 1996). Spines also add a significant amount of membrane to the dendritic tree (Wilson, 1986), which lowers dendritic input impedance and ultimately slows temporal dynamics of electrical events (Jaslove, 1992).

As discussed previously, dendrites are not passive structures (Stuart & Sakmann 1994; Stuart *et al.*, 1999) and thus results from passive models provide only a first approximation. A high spine head input resistance, for example, would be expected to be more effective at recruiting voltage-dependent conductances such as VGSCs and NMDARs during EPSPs as the EPSPs will be larger. Such ideas led to the notion that EPSPs in spines could generate regenerative events ("spikes") that could spread to neighbouring spines (Coss & Perkel 1985; Perkel 1982; Perkel & Perkel, 1985; Shepherd *et*

al; 1985). In addition, it is thought that VGSCs must be present in spines and contribute electrogenically to support the observed extent of action potential backpropagation in L5 pyramidal neurons (Tsay & Yuste, 2002).

The development of optical techniques has facilitated experimental measurements from spines both *in vitro*, in cultures and acute slices, as well as *in vivo*. Photolysis of caged calcium and neurotransmitters such as glutamate and GABA, in addition to fluorescent voltage and calcium imaging have given considerable experimental access to the study of the physiology of spines, as will be discussed below.

Two-photon glutamate uncaging has provided some evidence to support spine compartmentalisation, showing that EPSP amplitude as measured at the soma is inversely proportional to spine neck length (Araya *et al.*, 2006). In addition, other studies have shown that voltage dependent conductances can be differentially activated in the spine head compared to the dendritic shaft. This is true of VDCCs (Bloodgood & Sabatini, 2009), and is also thought to be the case for TTX-sensitive VGSCs (Araya *et al.*, 2007). Spine neck geometry is also suspected to change with neuronal activity (Bloodgood & Sabatini, 2005; Tonnesen *et al.*, 2014), suggesting that electrical compartmentalization of spines is dynamic. A recent study, using fluorescent calcium imaging as a proxy for spine and dendritic voltage, estimated a ~45 fold amplification of the voltage in spines compared to dendrites during synaptic input (Harnett *et al.*, 2012). In addition, in a subset of spines, inhibitory $GABA_A$ inputs can perturb calcium transients evoked by EPSPs and bAPs in spines, with minimal effects on

neighbouring spines or the dendritic shaft (Chiu *et al.*, 2013). To date, the current experimental evidence suggests spine neck resistances range from ~50 to 500 MΩ (Svoboda *et al* 1996; Palmer & Stuart, 2009; Harnett *et al* 2012; Tonnesen *et al.*, 2014). Depending on spine location within the dendritic tree, and therefore dendritic input impedance, this range of spine neck resistances is high enough to isolate spine voltages from the parent dendrite (Gulledge *et al.*, 2012).

Although the utilization of somatic whole-cell patch clamp electrophysiology and fluorescent calcium imaging has revealed much about the electrical properties of spines, such techniques do not allow direct observation of spine voltage. The continued development of fluorescent voltage imaging has provided and will continue to provide more direct information regarding spine electrophysiology. A few studies using this technique have confirmed that bAPs invade spines with no voltage loss (Palmer & Stuart, 2009; Holthoff *et al.*, 2010; Acker *et al.*, 2011) and that voltage attenuation occurs for EPSPs propagating from the spine to the dendrite at least in a subset of spines (Palmer & Stuart, 2009). Unfortunately this technique has been limited by poor signal-to-noise properties necessitating sacrifices in temporal resolution and excessive averaging to obtain fluorescence signals (Antic *et al.*, 2003; Palmer & Stuart, 2009; Holthoff *et al.*, 2010); this can lead to errors in kinetic measurements due to under sampling and restricts investigation to voltage changes greater than 10-20 mV.

The recent development of higher sensitivity voltage-sensitive dyes tuned to multi-photon excitation (Acker *et al.*, 2011), in addition to a new DiO/DPA FRET

based method (Bradley *et al.*, 2009), now allow high temporal resolution fluorescence transients to be obtained from dendritic spines with single trial resolution. These new techniques will help resolve whether spines act as electrical compartments when activated synaptically by providing direct measurements of the membrane potential in spines during EPSPs.

Calcium dynamics in dendritic spines

The amplitude and time course of calcium signals in spines are dependent on many factors including the activation and inactivation kinetics of calcium sources, calcium extrusion mechanisms, endogenous calcium binding proteins and spine morphology. Many studies have shown that almost all of these factors vary from spine-to-spine. Much of the recent evidence has come from fluorescent calcium imaging combined in many instances with glutamate uncaging as this allows direct stimulation of individual spines and simultaneous monitoring of changes in intracellular calcium concentration.

Calcium-sensitive dyes, unlike voltage sensitive dyes, have very good signal-to-noise properties and are commercially available in a range of sensitivities. Calcium signals can be used as a proxy for somatic AP firing in addition to dendritic shaft and spine depolarization during various electrical events such as bAPs and EPSPs, as well as regenerative events such as NMDA and dendritic calcium spikes both *in vitro* and *in vivo* (Yuste & Denk, 1995; Schiller *et al.*, 2000; Holthoff *et al.*, 2004; Kampa & Stuart, 2006; Holboro *et al.*, 2010; Jia *et al.*, 2010; Harnett *et al.*, 2012; Larvzin *et al.*, 2012; Xu *et al.*, 2012; Harnett *et al.*, 2013; Smith *et al.*, 2013). In addition, this technique has also allowed the

study of spine calcium sources and continues to elucidate the mechanisms involved in the induction and regulation of synaptic responses during plasticity. Even though fluorescent calcium imaging is a powerful experimental tool, effects of altering intracellular calcium buffering must be considered (Yasuda *et al.* 2004). Whilst overwhelming endogenous calcium buffers and binding proteins can be advantageous for investigating calcium sources activated in response to a particular stimulus, this can lead to errors in the calculation of changes in free calcium concentration (Higley & Sabatini, 2008) and when evaluating calcium extrusion mechanisms (Holthoff *et al.*, 2002).

The dynamic nature of dendritic spines is very much dependent on the influx of calcium caused by synaptic input alone or in combination with bAPs and/or other types of dendritic electrical events (Alvarez & Sabatini, 2007). Whilst there is still some debate as to whether the spine neck resistance can isolate the spine electrically, it is well established that it can isolate the spine biochemically, restricting rises in calcium during synaptic stimulation to the activated spine head (Koch & Zador, 1993; Yuste & Denk, 1995; Bloodgood *et al.*, 2009). This compartmentalization aids in the specificity of calcium dependent processes required for plasticity induction (such as CaMKII activation), which is limited to stimulated spines (Lee *et al.*, 2009).

Spine calcium sources

NMDARs

Calcium influx through NMDARs contributes a large component of the calcium influx into spines during synaptic input in many types of spiny neurons including

cortical (Koester & Sakmann, 1998; Yuste *et al.*, 1999; Nevian & Sakmann, 2006; Schiller *et al.*, 1998) and hippocampal (Kovalchuk *et al.*, 2000; Bloodgood & Sabatini, 2007; Sabatini *et al.*, 2002) pyramidal neurons, spiny stellate neurons (Nevian & Sakmann, 2004), olfactory granule cells (Egger *et al.*, 2005) and striatal medium spiny neurons (MSNs) (Carter & Sabatini, 2004).

In CA1 pyramidal neurons, NMDARs located in spines consist of heterodimers of the NR1 and NR2A or NR2B subunits. The presence of NR2A or NR2B containing NMDARs varies from spine to spine but there expression is segregated as many spines express either NR2A or NR2B but not both (Janssen *et al.*, 2005). In addition, functional evidence indicates that the contribution of NR2A and NR2B NMDARs to spine head calcium influx varies considerably between spines (Sobczyk *et al.*, 2005). This indicates that the composition of NMDARs is not only regulated during development, but also on a synapse-by-synapse basis. Given NR2B containing NMDARs deactivate more slowly (Moyner *et al.*, 1994), they will contribute much more to synaptically evoked calcium transients (Sobczyk *et al.*, 2005). In addition, they are coupled to different signaling cascades to NR2A containing NMDARs (Barria & Malinow, 2005; Sobczyk & Svoboda, 2007), indicating that plasticity induction may differ across populations of spines depending on which NMDAR subtype is present (Massey *et al.*, 2004; Liu *et al.*, 2004; Bartlett *et al.*, 2007).

NMDARs can be readily modulated by phosphorylation and calcium mediated inactivation. Several studies have indicated that protein kinase A (PKA) activity can influence the permeability of calcium through NMDARs (Sobczyk *et al.*,

2005; Skeberdis *et al* 2006; Sobczyk & Svoboda, 2007). Repetitive activation of NR2B containing NMDARs can lead to the activation of a serine/threonine phosphatase that can dramatically decrease calcium influx through NR2B containing NMDARs (Sobczyk & Svoboda, 2007). The influx of calcium can also directly lead to inactivation of NMDARs (Legendre *et al.*, 1993; Rosenmund & Westbrook 1993; Rosenmund *et al.*, 1995). These are all examples of negative feedback mechanisms where calcium influx, principally via NMDARs, can either directly or indirectly regulate NMDAR activation during periods of intense synaptic activity.

The strongest modulator of NMDAR activation however is the membrane potential itself due to the voltage-dependent block mediated by extracellular magnesium (Moyner *et al.*, 1992; Mayer *et al.*, 1984; Nowak *et al.*, 1984), the extent of which is also dependent on subunit composition (Moyner *et al.*, 1994). At resting membrane potentials magnesium block is incomplete and even though NMDAR currents evoked at resting potentials often do not lead to significant EPSPs, the small volume of the spine head and the large driving force for calcium results in significant calcium influx (Bloodgood & Sabatini, 2007). A few studies have provided evidence for AMPAR mediated depolarization being sufficient to partially relieve magnesium block, particularly in CA1 pyramidal neurons (Ngo-Ahn *et al.*, 2005; Grunditz *et al.*, 2008; Holboro *et al.*, 2010), although recent modeling studies indicate that the extent to which this is expected to occur in spines is unclear (Gulledge *et al.*, 2012).

NMDAR activation is also boosted by bAPs, which invade dendrites and spines, as discussed above. This wave of depolarization is sufficient to transiently relieve magnesium block and enhance synaptic calcium influx. The interaction of bAPs with NMDAR activation has been shown in many cell types including cortical and CA1 pyramidal neurons (Koester & Sakmann, 1998; Yuste *et al.*, 1999 Kovalchuk *et al*, 2000; Sabatini *et al.*, 2002; Nevian & Sakmann, 2006; Schiller *et al.*, 1998; Nevian & Sakmann, 2004; Egger *et al.*, 2005; Carter & Sabatini, 2004; Kampa *et al.*, 2006; Kampa & Stuart, 2006; Bloodgood & Sabatini, 2007; Holboro *et al.*, 2010) and is presumably important for the induction of spike-timing dependent plasticity (STDP), which is discussed later.

AMPARs

AMPA receptors can impact on calcium influx in two ways, either indirectly by enhancing NMDAR or VDCC activation via depolarization, or directly via calcium permeable AMPARs. Calcium permeable AMPARs lack GluR2 subunits and are commonly expressed in many GABAergic interneuron subtypes in addition to neurons in the cerebellum (for review see Cull-Candy *et al.*, 2006) and striatal MSNs (Carter & Sabatini, 2004). GluR2 lacking AMPARs were thought not to be present at synapses on excitatory neurons, however, there have been several demonstrations of their involvement in homeostatic and Hebbian synaptic plasticity in hippocampal pyramidal neurons (Thiagarajan *et al.*, 2005; Plant *et al.*, 2006; Gainey *et al.*, 2009). Another study, also in CA1 pyramidal neurons, showed that GluR2 lacking AMPARs are located perisynaptically in the spine head and invade the synapse upon the induction of LTP (Yang *et al.*, 2010). For cortical pyramidal neurons, calcium permeable AMPARs are expressed very early in development but expression decreases

substantially in the first postnatal weeks leading to a switch to calcium impermeable AMPARs (Kumar *et al.*, 2002). Overall, research into calcium permeable AMPARs is in its infancy and many facets of their function remain unclear. One general theme has however emerged, that in excitatory neurons they seem to be present in synapses only transiently after the induction of plasticity but are unlikely to be involved in the persistence of plasticity.

VDCCs

Backpropagating AP-evoked calcium influx into spines is mediated by VDCCs. There is a considerable amount of spine-to-spine variability with regard to the number of VDCCs present in individual spines, with number ranging from 1 to 20 (Sabatini & Svoboda, 2000). The calcium channel subtypes mediating calcium influx also differ across different neuronal types, with T-type VDCCs in olfactory granule cell spines (Egger *et al.*, 2005), T-type and P/Q-type VDCCs in Purkinje cell spines (Isope & Murphy, 2005; Kulik *et al.*, 2004), L-type, R-type and T-type VDCCs in spines in striatal MSNs (Carter & Sabatini, 2004), L-type P/Q-type and low-voltage- activated VDCCs in spines on layer 2/3 cortical neurons (Koester & Sakmann, 2000), L-type and R-type VDCCs in rat hippocampal CA1 pyramidal neuron spines (Sabatini & Svoboda, 2000; Yasuda *et al.*, 2003; Hoogland & Saggau, 2004) and L-type, N-type, R-type and T-type VDCCs in the spines of these neurons in mice (Bloodgood & Sabatini, 2007)

Intracellular calcium stores

Calcium release from intracellular stores also occurs in spines. A few studies have shown that calcium-induced calcium release occurs as a result of synaptically evoked calcium influx (Emptage *et al.*, 1999; Kovalchuk *et al.*,

2000) and during EPSP-AP pairing (Wang *et al.*, 2000, Larkum *et al.*, 2003). The activation of metabotropic glutamate receptors has also been shown to cause IP_3-dependent release (Finch & Augustine, 1998; Nakamura *et al.*, 1999), which has been shown to be important for the induction of LTD (Aiba *et al.*, 1994; Huber *et al.*, 2001; Bender *et al.*, 2006; Nevian & Sakmann, 2006). In addition, aside from calcium release, intracellular calcium stores play an important role in calcium clearance after events such as bAPs and EPSPs. As a result, inhibition of SERCA pumps responsible for store filling result in a prolonged decay of calcium signals in spines and the dendritic shaft (Markram *et al.*, 1995; Sabatini *et al.*, 2002).

SPIKE-TIMING DEPENDENT PLASTICITY

Changes in synaptic strength are thought to underlie learning and memory. The first experimental evidence for long-term changes in synaptic strength was shown in the hippocampus of rabbits, where tetanic stimulation of the perforant path input to the dentate gyrus led to long-term potentiation (LTP) of these connections (Bliss & Lomo, 1973). Long-term depression (LTD) of synaptic inputs was demonstrated soon after (Lynch *et al.*, 1977). The requirements for the induction of LTP and LTD are reminiscent of a memory model described by Donald Hebb some 30 years earlier. His central idea was that connected neurons that are active at the same time will strengthen their connections. This led to one of the central dogmas of brain plasticity; the notion that "neurons that fire together, wire together" (Hebb 1949). The NMDAR was soon found to be a prime candidate for the detection of presynaptic activity, as it is only active when presynaptic activity leading to glutamate release occurs at the same time

as postsynaptic activity, which acts to relieve the voltage-dependent block of NMDARs by magnesium ions (Mayer *et al.*, 1984; Nowak *et al.*, 1984). Many forms of LTP and LTD have been found to be NMDAR dependent, although there are exceptions, with strong NMDAR activation associated with a large influx of calcium leading to LTP, whereas moderate NMDAR activation and less calcium influx usually leads to LTD (Bliss & Collingridge, 1993).

A specific form of synaptic plasticity, called spike-timing dependent plasticity (STDP) involves the pairing of presynaptic and postsynaptic APs. The sign and magnitude of the changes in synaptic strength are correlated with AP timing in connected neurons (Bi & Poo, 1998; Abbott & Nelson, 2000). Whilst NMDAR activation is crucial to the induction of STDP in many instances, mainly for LTP, spike timing-dependent LTD in some cases involves the activation of metabotropic glutamate receptors (Birtoli & Ulrich, 2004) and VDCCs (Nevian & Sakmann, 2006), as well as endocannabinoid release from the postsynaptic cell (Safo & Regher, 2005; Sjostrom *et al.*, 2003).

Typically, inputs that are activated before the postsynaptic AP (positive timing) are potentiated. In contrast, inputs activated soon after the postsynaptic AP (negative timing) are depressed. This could be interpreted as synapses that have led to the generation of the postsynaptic AP are potentiated, whereas those that couldn't have contributed to AP generation are depressed. The retrograde signal to the synapse indicating that a postsynaptic AP has occurred is the backpropagating voltage transient associated with the AP itself (Magee & Johnston, 1997; Stuart, 2001). These large dendritic depolarisations are

sufficient to relieve the magnesium block of NMDARs (Vargas-Caballero *et al*, 2003; Kampa *et al*., 2004), essential for the induction of STDP (Bi & Poo, 1998; Koester & Sakmann, 1998).

The relative timing of the postsynaptic AP to glutamate binding to the NMDARs is a crucial determinant of NMDAR activation and hence calcium influx (Kampa *et al*, 2004; Kampa *et al*., 2006; Koester & Sakmann, 1998; Nevian & Sakmann, 2004). The magnitude of this postsynaptic calcium influx controls which signaling cascade(s) will be activated and consequently determines the magnitude and sign of plasticity (Dan & Poo, 2004). The threshold calcium influx during pairing events for the induction of plasticity varies across different cell types. STDP induced in hippocampal cultures and L2/3 neurons in acute slices can be evoked by pairing events consisting of single post and pre synaptic APs (Bi & Poo, 1998; Froemke *et al*., 2005). In contrast, for L5 pyramidal neurons, bursts of postsynaptic APs are required to generated LTP (Markram *et al*., 1997; Sjostrom & Hausser, 2006; Kampa *et al*., 2006; Letzkus *et al*., 2006). The reason for these differences are unclear but it seems that in order to induce LTP in L5 neurons prolonged NMDAR activation is required.

In contrast to LTP, LTD is more readily induced in multiple neuronal types by repeated pairing events at negative timings consisting of single APs (Nevian & Sakmann, 2006; Bi & Poo, 1998; Froemke *et al*., 2005; Bender *et al*., 2006). However, the mechanism(s) underlying LTD induction are more complex. Whilst there is considerable evidence for the induction of LTD being NMDAR dependent, there is also a substantial number of studies showing NMDAR

independent mechanisms principally involving mGluR and VDCC activation leading to IP_3-dependent calcium release from intracellular stores, endocannabinoid synthesis and release, and activation of presynaptic endocannabinoid (CB1) receptors (Gerdeman *et al.*, 2002; Robbe *et al.*, 2002; Sjostrom *et al.*, 2004; Nevian & Sakmann, 2006). LTD induction in L5 pyramidal neurons does appear to be NMDAR independent but requires sufficient calcium influx for endocannabinoid release (Sjostrom *et al.*, 2004) and induction protocols consisting of single APs are insufficient to evoke LTD in these neurons (Sjostrom *et al.*, 2001).

Another variable impacting on the induction of STDP is the location of the active synapses as the attenuation of bAPs from proximal to distal dendritic locations (Stuart *et al.*, 1997) impacting on the induction of STDP at distal synapses. Three studies have shown that in cortical pyramidal neurons distal inputs are more prone to undergo LTD (Froemke *et al.*, 2005; Sjostrom & Hausser 2006; Letzkus *et al.*, 2006), which can be converted to LTP during dendritic depolarization associated with dendritic calcium spikes or strong synaptic stimulation (Sjostrom & Hausser 2006; Letzkus *et al.*, 2006). This switch from LTD to LTP is due to enhanced NMDAR activation and consequential calcium influx at distal locations during these large electrical events (Sjostrom & Hausser, 2006; Letzkus *et al.*, 2006).

Overall, there are a myriad of mechanisms that can lead to STDP. Amidst this mechanistic diversity it is clear that calcium influx plays a vital role. The regulation of calcium influx during EPSPs and bAPs through the various

calcium sources present in spines at the synapse is therefore of interest as it may play a role in the control of STDP.

CALCIUM-ACTIVATED POTASSIUM CHANNELS

One way calcium can impact on the excitability of neurons is via the activation of calcium-activated potassium (K_{Ca}) channels. The two main types of K_{Ca} channel, BK and SK channels are named after their single channel conductance. BK channels (where 'B' stands for big) have a large single channel conductance on the order of 100-200 pS (Coetzee *et al.*, 1999; Sah & Davies, 2000), whereas SK channels (where 'S' stands for small) have a much smaller single channel conductance of 8-20 pS (Hirschberg *et al.*, 1999). A third type of K_{Ca} channel of intermediate conductance (IK channels) have also recently been found to regulate AP firing in cerebellar Purkinje neurons (Engbers *et al.*, 2012).

BK channels

BK channels are expressed in multiple types of neurons in the brain, including cerebellar Purkinje neurons (Womack & Khodakhah, 2002), CA1 pyramidal neurons (Marrion & Travalin, 1998) and cortical L5 pyramidal neurons (Kang *et al.*, 1996; Sun *et al.*, 2003; Yu *et al.*, 2010). The function of BK channels in these neurons is to generate the fast AHP (fAHP) that controls the width of somatic APs (Lancaster & Nicoll, 1987; Storm, 1987; Shao *et al.*, 1999; Faber & Sah, 2003). In addition to their somatic actions, however, BK channels in L5 and CA1 pyramidal neurons are also expressed along the apical dendrite

(Benhassine & Berger, 2005) and play a role in dendritic excitability (Golding *et al.*, 1999; Benhassine & Berger, 2009).

BK channels are gated both by the binding of calcium and the membrane voltage (Marty, 1981; Lattore *et al.*, 1989). Due to the relatively low binding affinity for calcium (1-10 μM), BK channels typically form complexes with VDCCs and display coupling distances on the nanometer scale called nanodomains. The precise VDCC subtype driving BK channel activation varies between cell types, with L-type (Lancaster & Nicoll, 1987; Storm 1987a, 1987b) and N-type (Marrion & Travalin, 1998) important in hippocampal pyramidal neurons, P/Q-type in cerebellar Purkinje neurons (Edgerton & Reinhart, 2003; Womack *et al.*, 2004), L and N-type in frog hair cells (Roberts *et al.*, 1990; Roberts, 1993; Roberts, 1994), N-type in frog peripheral axon terminals (Robitaille *et al.*, 1993; Yazejian *et al* 1997; Yarejian *et al.*, 2000; Sun *et al.*, 2004) and P/Q and L-type in chromaffin cells (Solaro *et al.*, 1995; Prakriya *et al.*, 1996; Prakriya & Lingle, 1999). There have also been a few demonstrations of coupling over distances greater than 100 nm, called microdomains in chromaffin cells (Prakriya *et al.*, 1996; Prakriya & Lingle, 2000) and CA3 pyramidal neurons (Hu *et al.*, 2001).

SK channels

There are three subtypes of SK channel, named SK1, SK2 and SK3. Of these, only SK1 and SK2 are readily expressed in the cortex, and only SK2 is readily found in the hippocampus (Sailer *et al.*, 2002). SK3 is expressed mainly in subcortical areas such as the hypothalamus, thalamus, and the midbrain

(Kohler *et al.* 1996; Stocker & Pedarzani, 2000; Ballesteros-Merino *et al.*, 2014). In L5 pyramidal neurons the expression of SK channel subtype is location dependent with SK1 expressed prominently in distal apical dendrites and SK2 mostly expressed at the soma and basal dendritic regions (Sailer *et al.*, 2002).

SK channels lack voltage dependence and do not have a calcium-binding domain, and hence are not directly gated by calcium ions. Calmodulin acts as a highly affinity calcium sensor that transduces the binding of calcium, through a sequence of conformational changes, to the activation of coupled SK channels (Xia *et al.*, 1998; Keen *et al.*, 1999). Relatively low calcium concentrations are required to active SK channels, on the order of 0.3-2 μM (Xia *et al.*, 1998; Pendarzani *et al.*, 2001), and thus calcium influx associated with electrical events such as APs and EPSPs is sufficient to lead to strong activation.

Functionally, somatic SK channels mediate the medium afterhyperpolarisation (mAHP) in many types of neurons including, cerebellar Purkinje neurons (Womack & Khodakhah, 2003), vagal motorneurons (Sah & MacLachlan, 1991), neurons in the basolateral amygdala (Faber & Sah, 2002) and L5 pyramidal neurons (Schwindt *et al.*, 1988). The function of somatic SK channels in CA1 pyramidal neurons however is controversial (Stocker *et al.*, 1999; Gu *et al.*, 2005; Gu *et al.*, 2008). The mAHP is active within the time window of ~2-100 ms after a single or burst of APs and dampens regular and burst firing of somatic APs. SK channels that mediate the mAHP are generally tightly coupled to their calcium source, which is variable across cell types, with L-type VDCCs activating SK channels in CA1 pyramidal neurons and T-type VDCCs involved

in SK channel activation in midbrain dopaminergic neurons (Wolfart & Roeper, 2002).

Dendritic SK channels have been shown to dampen EPSPs in CA1 pyramidal neurons (Ngo-Ahn *et al.*, 2005), L5 pyramidal neurons in prefrontal cortex (Faber, 2010) and neurons in the basolateral amygdala (Faber *et al.*, 2005). In addition, dendritic SK channels have been shown to play a role in constraining NMDA spike-like plateau potentials in CA1 neurons (Cai *et al.*, 2004). The dampening effect of SK channel activation during EPSPs is achieved by constraining NMDAR activation in the spine head as the SK potassium conductance opposes the depolarization caused by activation of synaptic NMDA and AMPA receptors (Ngo-Ahn *et al.*, 2005). This in turn leads to a dampening of spine calcium influx during EPSPs. Dendritic SK channels are tightly coupled to their calcium source, located in nanodomains on the order of 25-50 nm in size (Ngo-Ahn *et al.*, 2005; Faber *et al.*, 2005; Faber, 2010). The identity of the calcium source for SK channels in dendrites is controversial however. Some studies suggest R-type VDCCs are the sole calcium source controlling SK activation (Bloodgood & Sabatini, 2007; Higely & Sabatini, 2010; Giessel *et al.*, 2011), while others identify NMDARs as the primary calcium source (Faber *et al.*, 2005; Ngo-Ahn *et al.*, 2005; Lin *et al.*, 2008; Wang *et al.*, 2014).

SK channels can be modulated by the phosphorylation state of calmodulin. Protein kinase CK2 and protein phosphatase 2A (PP2A) are co-localised in a protein complex with SK channels and the coupled calmodulin (Bildl *et al.*,

2004; Allen *et al.*, 2007). CK2 activity leads to a reduction in the apparent sensitivity of SK channels to calcium, while the activity of PP2A together with a reduction in CK2 activity, leads to an increase in SK channel sensitivity to calcium (Bildl *et al.*, 2004; Allen *et al.*, 2007). PKA has also been implicated in the modulation of SK channel function by phosphorylation (Buchanan *et al.*, 2010). The activity of CK2 and PKA can be regulated by the activation of M1 muscarinic receptors resulting in SK channel modulation by acetylcholine (Buchanan *et al.*, 2010; Giessel & Sabatini, 2010). In addition, a loss of SK channels from the membrane has been shown to occur during hippocampal LTP (Lin *et al.*, 2008) and following β_2 adrenergic receptor activation (Faber & Sah, 2008).

Presumably due to their impact on calcium influx during synaptic input, SK channels play a role in limiting synaptic plasticity induced by tetanic stimulation (Behnisch & Reymann, 1998; Stackman *et al.*, 2002; Faber *et al.*, 2005). In addition, a few studies have shown that changes in synaptic strength during plasticity are also associated with changes in SK channel function via internalisation from the spine membrane (Lin *et al.*, 2008; Lin *et al.*, 2009). The involvement of SK channels in plasticity induced by other types of stimuli, for example during STDP, is at present unknown.

THESIS OUTLINE

This study investigates the function of dendritic and somatic SK channels in L5 pyramidal neurons. The activation of dendritic SK channels during bAPs is studied in Chapter 3. Chapter 4 examines the calcium sources required for the activation of somatic SK channels mediating the mAHP in addition to the proximity of somatic SK channels to their calcium source(s). Chapter 5 investigates some of the physiological consequences of dendritic SK channel activation by bAPs during AP-EPSP pairing and STDP. Finally, Chapter 6 discusses the results for these different chapters in the context of micro- and nano- domain calcium signaling and STDP, in addition to commenting on the limitations of the study and the way ahead.

CHAPTER 2: GENERAL METHODS

ACUTE CORTICAL BRAIN SLICE PREPARATION

Parasaggital brain slices of the cerebral cortex were taken from Wistar rats of either sex aged between 3 and 5 weeks. All procedures with regard to the handling of animals were in accordance with guidelines approved by the Animal Experimentation Ethics Committee of the Australian National University. More conventional procedures were adopted for initial experiments in the study (outlined below), but some experimentation was subsequently undertaken to enhance slice quality.

Dissection

Rats were anaesthetized by inhalation of isofluorane and then decapitated at the level of the cervical medulla with scissors. A sagittal cut along the midline was made with a scalpel, and the skin over the skull retracted. With dissecting scissors the skull was cut along the midline from caudal to frontal beginning at the foramen magnum and ending at the level of the olfactory bulb. A single mediolateral cut was then made on either side of the midline at the level of the olfactory blubs and just frontal to the cerebellum. Using forceps the section of skull over the cortex and cerebellum of both hemispheres was removed by pulling back the skull on each side in the lateral direction, making sure any meningeal connections are cut prior to full retraction as these can damage the brain. At this point the head was quickly immersed in ice-cold cutting ACSF. The cerebellum was then removed with a single coronal cut and the

hemispheres divided using a sagittal cut through the corpus callosum. Both hemispheres were then removed from the base of the skull in the rostro-caudal direction and placed into ice-cold cutting ACSF. Saline was removed from the medial surface of each hemisphere by transferring them onto a piece of filter paper. Both hemispheres were then glued medial side down onto a angled slicing stage (15-degrees) with the pial surface of the cortex orientated towards the lower side of the incline and the cutting blade.

Slicing procedure

Approximately half the hemisphere was cut off in the first advance of the blade. Subsequently, thin slices of 250-300 µm thick were taken until the hippocampus was no longer visible. Each slice was transferred immediately after being cut to a holding chamber filled with ACSF at 35 degrees. Slices are arranged in the holding chamber in the order in which they were cut to aid identification. The best slices, with apical dendrites parallel to the surface of the slice were typically the third and forth last to be cut using this method. Slices were then incubated for 30-45 minutes at 35 degrees before being maintained at room temperature before use.

Standard ACSF (in mM): 125 NaCl, 25 $NaHCO_3$, 2.5 KCl, 1.25 $NaHPO_4$, 25 glucose, 2 $CaCl_2$, 1 $MgCl_2$. pH 7.4 oxgenated with carbogen (95% oxygen, 5% carbon dioxide).

ACUTE HIPPOCAMPAL BRAIN SLICE PREPARATION

Transverse hippocampal slices were obtained from 3-5 week old Wister rats of either sex. All procedures with regard to the handling of animals were in accordance with guidelines approved by the Animal Experimentation Ethics Committee of the Australian National University.

Dissection

The brain was removed from the skull using the same approach as that described above for the preparation of cortical slices.

Slicing procedure

Either hemisphere was placed onto a piece of 3% agar, medial side down. The dorsal part of the brain was then cut at an angle of 0 degrees to the horizontal (vertical blade), removing 10-20 % of the brain volume. The brain and agar block was then transferred onto a piece of filter paper ventral side up to remove any saline and the brain glued onto a flat slicing stage ventral side up with the cortex facing the cutting blade. 300 µm slices were then cut from the lateral to the medial side of the brain. Slices in the middle third of the cashew-like structure of the hippocampus were used. Typically five slices can be obtained from each hemisphere.

Modifications to Improve Slice Quality

There was some experimentation with the ACSF used for cutting slices as different groups have report superior slice quality using a variety of strategies. The first strategy adopted was to increase the concentration of $MgCl_2$ to 6 mM in order to increase the block of NMDA receptors during the slicing procedure. This strategy significantly increased slice quality. Further improvements were observed when the $CaCl_2$ concentration was decreased to 0.5 mM. In addition, the inclusion of ascorbic acid (5 mM) and sodium pyruvate (3 mM), chosen for their anti-oxidative stress and anti-hypoxic properties, also led to further enhancement of slice health.

Modified Cutting ACSF (in mM): 125 NaCl, 25 $NaHCO_3$, 2.5 KCl, 1.25 $NaHPO_4$, 25 glucose, 6 $MgCl_2$, 0.5 $CaCl_2$, 3 sodium pyruvate, 5 ascorbic acid, pH 7.4 oxgenated with carbogen (95% oxygen, 5% carbon dioxide).

Other modifications to the cutting solution focused on sodium replacement with either N-methyl-D-glucamine (Zhao *et al.*, 2011) and/or sucrose (Debanne *et al.*, 2008). The rationale is that the replacement of sodium removes the electrical driving force for sodium influx into neurons decreasing excitotoxicity. Both these strategies led to good slice quality but the improvement was not sufficient to warrant extensive use. In addition, the use of NMDG in the cutting solution was associated with a significant change in L5 pyramidal neuron firing patterns and the incidence of burst firing. As a consequence the use of these solutions were abandoned.

NMDG cutting solution (in mM): 93 NMDG, 93 HCl, 2.5 KCl, 1.25 $NaHPO_4$, 30 $NaHCO_3$, 25 glucose, 20 HEPES, 5 ascorbic acid, 3 sodium pyruvate, 6 $MgCl_2$, 0.5 $CaCl_2$. pH 7.4

Sucrose cutting solution (in mM): 260 sucrose, 25 NaHCO3, 2.5 KCl, 1.25 NaHPO4, 25 glucose, 6 $MgCl_2$, 5 ascorbic acid, 3 sodium pyruvate 0.5 $CaCl_2$. pH 7.4

Modifications to the incubation solution and time also lead to enhanced slice quality and longevity. In contrast to the conventional method outlined above, better results were obtained if freshly cut slices were initially incubated in the cutting solution maintained at 35 degrees for 10 minutes and then transferred to another holding chamber filled with standard ACSF at room temperature for 1 hour prior to use.

WHOLE-CELL PATCH CLAMP ELECTROPHYSIOLOGY

Slices were transferred to the recording chamber and perfused with standard ACSF continuously bubbled with carbogen. The solution in the recording chamber was maintained at 35-36 degrees using a custom-built inline heater. Perfusion was achieved using a peristaltic pump, which allowed for tight control of the perfusion rate (3-4 ml/minute). The microscope was mounted on an anti-vibration table (Physical Instruments, Germany) together with the recording chamber and the electrode micromanipulators (Luigs and Neumann, Germany). Neurons were visualized using infrared differential interference contrast optics

(DIC) on an Olympus BX51 upright microscope mounted with a CCD camera (Optronics).

Recordings were made from L5 pyramidal neurons located in the hindlimb area of somatosensory cortex. These neurons are easily identified by their large diameter soma (25-30 µm) and apical dendrite, as well as the location of their cell body from the pia. Somatic whole-cell recordings were made using BVC700A current-clamp amplifiers (Dagan Corporation, USA). Patch pipettes were made from thick walled filamented borosilicate glass using a multistep horizontal puller (Sutter Instrument Company, USA). The typical tip resistance was between 4 and 6 MΩ. Electrodes were filled with an intracellular solution containing 130 K-gluconate, 10 KCl, 10 HEPES, 4 Mg-ATP, 0.3 Na-GTP, 10 Na_2-phosphocreatine, pH 7.2 adjusted with KOH. This solution was connected via a chlorided silver wire within the electrode holder to the preamplifier headstage, which was mounted on motorized micromanipulators (Luigs and Neumann, Germany). Positive pressure was applied to the electrode in order to prevent contamination of the tip, which was located under the objective and positioned above the neuron of choice. The pipette was then navigated slowly through the slice under visual control ensuring to avoid contact with cells or debris other than the neuron of interest. The pipette offset was then set to zero in voltage clamp mode and the tip was then pushed into the cell membrane slightly until a small deformation was observed. At this point the positive pressure was quickly released and slight negative pressure applied whilst setting the amplifier to -65 mV. A gigaseal was judged to have been obtained if the current required to hold the patch of membrane beneath the pipette at the

selected voltage was less than 20 pA. Brief pulses of negative pressure were then applied through a mouthpiece to rupture the membrane beneath the pipette tip and achieve the whole-cell configuration. The amplifier was then switch and maintained in current clamp for all recordings. Short (50 ms) hyperpolarizing current pulses were injected into the neuron in order to facilitate correct adjustment of the bridge balance and capacitance compensation. This is important as it corrects for the voltage drop across the series resistance of the electrode during current injection and compensate for the filtering caused by the electrode capacitance. Series resistances were between 6 and 15 MΩ for all recordings and continuously monitored over the course of experiments.

Voltage traces were filtered at 10 kHz and digitised at 50 kHz using an analogue-digital convertor (ITC-18, Instrutech) connected to an Apple iMac computer. All electrophysiological data was acquired using Axograph X (Axograph Scientific, Australia). In most experiments the input resistance, a robust indicator of neuron health, was monitored throughout the recording period using long hyperpolarizing current steps (-20 or -50 pA, 1 second). APs were evoked using short (2-4 nA, 2ms), medium (250-450 pA, 200 ms) or long current pulses (200-300 pA, 500 ms).

In some experiments, EPSPs in the postsynaptic cell were evoked via extracellular electrical stimulation. In these experiments fluorescence microscopy was used to place the stimulating electrode in close proximity to the dendrite of interest. In other experiments whole-cell recordings were established

from synaptically connected L5 pyramidal neurons, facilitating tight control over EPSP and AP timing in the postsynaptic neuron over long time periods.

Fluorescent Calcium Imaging

Changes in intracellular calcium were monitored with a laser-scanning confocal microscope (FV300, Olympus, Japan). This technique requires the introduction of a fluorescent calcium indicator into the neuron of interest, which was achieved in our experiments via diffusion from the recording pipette. The choice of indicator and the concentration at which it is used are important considerations to make and depend on the cellular properties/mechanisms under investigation as well as the sensitivity of the microscope being used in the experimental setup.

Choice of indicator

Several studies have provided experimentally determined estimates on the change in calcium concentration in the spine head associated with bAPs and synaptic stimulation (Sabatini *et al.*, 2002; Cornelisse *et al.*, 2007). Thus, whilst trial and error can be used to optimize the selection of an appropriate dye and the concentration at which it should be used, it can also be helpful to estimate the concentration of bound indicator as a result of the kinds of stimuli the experimenter wishes to observe. Although a comprehensive explanation on performing such calculations can be found in Higley & Sabatini 2008, the pertinent issues will be briefly discussed here.

The interaction of calcium with the indicator can be represented by the following equation:

$$[Ca] + [B] \rightleftharpoons [BCa]$$

Where [Ca], [B] and [BCa] correspond to the concentrations of free calcium, free indicator and bound indicator respectively.

The dissociation constant (K_D) is defined as quotient of the rates of binding (k_{on}) and unbinding (k_{off}) and describes the affinity of the indicator for calcium.

$$K_D = \frac{k_{off}}{k_{on}}$$

The K_D can also be expressed as:

$$K_D = \frac{[Ca][B]}{[BCa]}$$

Combining the above equation with the expression for the total buffer concentration, $[B_T] = [BCa] + [B]$ produces:

$$[BCa] = [B_T]\frac{[Ca]}{[Ca]+K_D}$$

The endogenous buffer capacity of spines from L5 pyramidal neurons is thought to be ~19 and the change in free calcium concentration associated with an AP ~1 μM (Cornelisse *et al.* 2007). Using these values the total change in calcium concentration during an AP can be calculated using the equation below (Helmchen *et al.*, 1996, Higley & Sabatini, 2008):

$$\Delta[Ca_T]=[\Delta Ca_{AP}](1 + \kappa_B)$$

There ΔCa_{AP} is the change in free calcium concentration following an AP, ΔCa_T is the change in total calcium concentration and κ_B is the sum of the endogenous buffer capacities. Using $[\Delta Ca_{AP}]$ of 1 μM and a κ_B of 19 the change in total calcium concentration in the spine due to a single AP is estimated to be on the order of 20 μM. Similar predictions have been made for CA1 pyramidal neurons (Sabatini *et al.* 2002).

Combining:

$$[BCa] = B_T \frac{[Ca]}{[Ca] + K_D}$$

With an expression for total calcium concentration $[Ca_T]$, being the sum of both free [Ca] and bound [BCa] calcium:

$$[Ca_T] = [Ca] + [BCa]$$

Produces the following expression relating the concentration of bound indicator to the total calcium concentration:

$$[BCa] = \frac{1}{2}([Ca_T] + [B_T] + [K_D]) - \sqrt{([Ca]_T + [B_T] + [K_D])^2 - 4([B_T] \times [Ca_T])}$$

Using this equation it is possible to estimate of the concentration of bound indicator for dyes with different properties and at different concentrations. This calculation has been performed for the high affinity indicator Oregon Green BAPTA-1 (K_D ~0.2 μM) and the low affinity indicator Oregon Green BAPTA-6F (K_D ~3 μM), which were both used in this study (Figure 2.1).

Based on these calculations we can see that a significant concentration of the high-affinity calcium indicator OGB-1 is bound at resting calcium concentrations (Figure 2.1A), and thus can be used to visualize neuron morphology. Further, these calculations show that for the expected change in total calcium concentration during a single AP (20 μM) OGB-1 is in the linear range and does not approach saturation at any of the concentrations examined. The low affinity indicator OGB-6F (Figure 2.1B) is also expected to be in the linear range during single APs, but as there is much less bound indicator at resting calcium concentration (~100 nM; Sabatini *et al.*, 2002; Cornelisse *et al.*, 2007) morphological visualization will be limited. For this reason OGB-1 (200 μM) was used in the majority of experiments. A high concentration was used in order to make sure sufficient dye diffused to distal spines during the time course of these experiments. In some experiments OGB-6F was used to control for the possible impact of OGB-1 on SK channel function.

Microscope setup

Excitation of the indicator was achieved using a 488 nm solid-state laser (Meles Griot). Due to the large size of L5 pyramidal neurons imaging was only commenced 50-60 minutes after the establishment of the whole-cell

Figure 2.1.

Figure 2.1. – Relationships between calcium-bound indicator and free or total calcium concentration.

A-B, Relationship between bound indicator [BCa] and total calcium concentration $[Ca]_{total}$ plotted for a buffer with a K_D of 0.2 μM, simulating Oregon Green BAPTA-1 ***(A)*** or a K_D of 3 μM, simulating, Oregon Green BAPTA 6-F ***(B)***. Curves have been calculated for a total buffer concentration (sum of bound ([BCa]) and free buffer) of either 75, 100, 150 or 200 μM. The contribution of endogenous calcium buffers were ignored. Values of [BCa] that correspond to the expected [BCa] given a resting $[Ca]_{free}$ of 100 nM (squares) or [Ca] due to a series of action potentials (circles) where ΔCa_T per action potential was estimated as 20 μM. All concentrations in all plots are in μM.

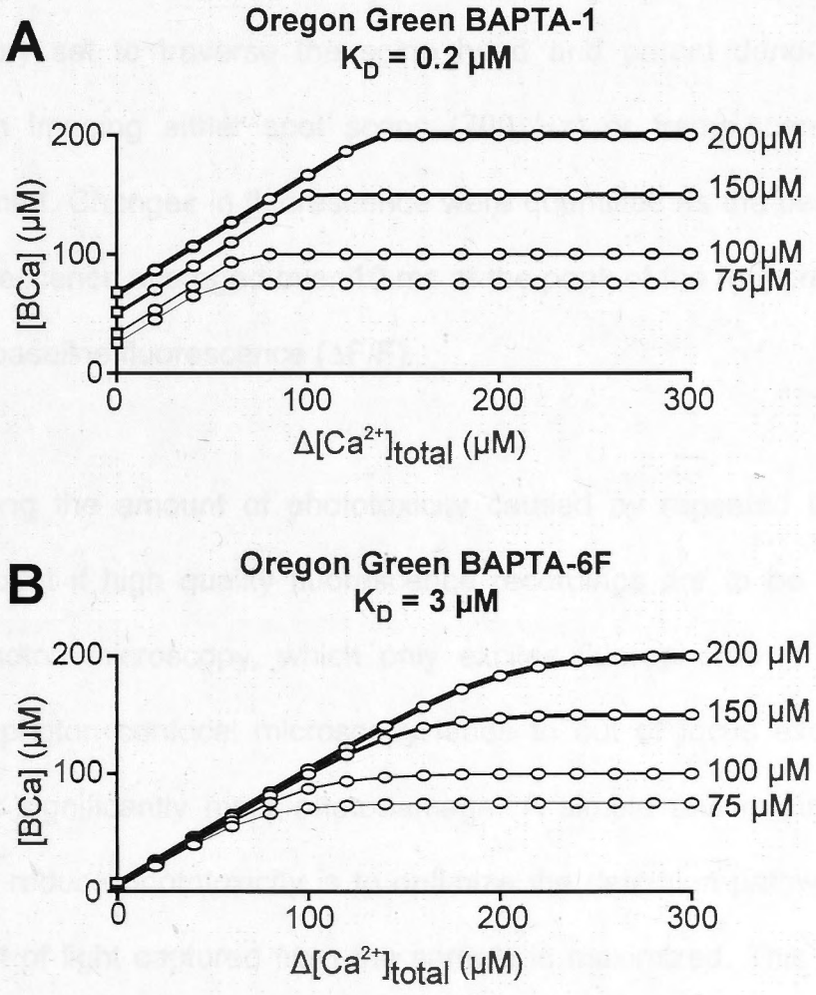
A
Oregon Green BAPTA-1
K_D = 0.2 µM
200µM
150µM
100µM
75µM
[BCa] (µM)
200
100
0
0
100
200
300
$\Delta[Ca^{2+}]_{total}$ (µM)
B
Oregon Green BAPTA-6F
K_D = 3 µM
200 µM
150 µM
100 µM
75 µM
[BCa] (µM)
200
100
0
0
100
200
300
$\Delta[Ca^{2+}]_{total}$ (µM)

configuration. Even longer filling times were required in some experiments. This is necessary in order for the indicator concentration to reach steady state, which is important for obtaining stable changes in fluorescence over time. Experiments investigating both dendritic and somatic calcium influx were performed. For dendritic and spine calcium imaging frame-scans were performed to identify the dendrite and spine of interest. Repeated line-scans were subsequently performed at 500-700 Hz during APs with the laser trajectory set to traverse the spine head and parent dendrite. For somatic calcium imaging either spot scans (700 Hz) or frame-scans (20 Hz) were performed. Changes in fluorescence were quantified as the percentage change in fluorescence averaged over 10 ms at the peak of the response relative to the mean baseline fluorescence ($\Delta F/F$).

Reducing the amount of phototoxicity caused by repeated light exposure is paramount if high quality fluorescence recordings are to be obtained. Unlike multiphoton microscopy, which only excites fluorophores in the focal plane, single photon confocal microscopy leads to out of focus excitation and thus causes significantly more photodamage. A simple and relatively inexpensive way to reduce phototoxicity is to optimize the detection pathway such that the amount of light captured from the sample is maximized. This was achieved in two ways, (1) a high power (60x) objective with a high numerical aperture was selected (1.1 NA) and (2) a high transmittance longpass emission filter (500 nm; Chroma Technology, USA) was custom fitted to the microscope. Together these measures significantly increased the sensitivity of the detection system and

substantially reduced excitation light intensities (by at least 50%) whilst still producing an acceptable signal to noise.

PHARMACOLOGY

In all experiments various antagonists were either added to the bath solution or applied locally via a large diameter patch pipette (5-10µm). The details of antagonists, concentration and method of application for each experiment are outlined in the Methods section of Chapters 3, 4 and 5.

DATA ANALYSIS

Electrophysiological data was analysed using Axograph X software (Axograph Scientific, Sydney, Australia) and fluorescence data with Image J. Both programs were run on an Apple iMac computer. All data were subjected to the D'Agostino-Pearson omnibus normality test prior to further statistical analysis. Results were evaluated using T tests in either the paired or unpaired configuration where appropriate. All statistics were performed using Prism 6 (Graphpad Software Inc.)

CHAPTER 3: THE ROLE OF SK CHANNELS IN THE REGULATION OF CALCIUM INFLUX DURING BACKPROPAGATING ACTION POTENTIALS

INTRODUCTION

In the central nervous system information is represented and transferred by fast, large amplitude voltage changes called action potentials. Although action potentials are initiated in the first tens of micrometres of the axon in an area called the axon initial segment (Stuart *et al.*, 1997; Palmer & Stuart, 2006; Kole *et al.*, 2008) and propagate orthodromically leading to neurotransmitter release, they also propagate antidromically into the dendritic tree (Stuart & Sakmann 1994). This antidromic or backpropagation of APs has been shown to lead to calcium influx into both the dendritic shaft and dendritic spines (Yuste & Denk, 1995). Such influxes of calcium are vital for modifications of synaptic strength as well as synapse preservation and elimination during synaptic plasticity (Zucker 1999; Alvarez & Sabatini, 2007).

Most studies investigating action potential backpropagation have focused on the large diameter apical dendrite of cortical and hippocampal pyramidal neurons, primarily due to their accessibility for patch clamp recordings. Even though studies employing such techniques have and continue to provide a considerable understanding of synaptic integration in neurons, most excitatory synaptic inputs onto cortical pyramidal neurons occur onto fine basal and

oblique dendrites (Larkman, 1991). Due to the small diameter of these structures, obtaining electrophysiological recordings presents significant technical challenges (although see Nevian *et al*, 2007). For the past two decades optical techniques such as calcium and voltage imaging have been used to overcome these difficulties and have proved invaluable as a tool for the investigation of the electrical events that occur in fine dendrites and spines.

In recent years there has been considerable interest in the function of small conductance calcium-activated potassium channels (SK channels) in dendrites, and particularly in dendritic spines. There is a growing body of evidence demonstrating that SK channels located in the spine head regulate calcium influx into spines during EPSPs (Ngo-Ahn *et al*, 2005; Bloodgood & Sabatini, 2007). The main consequence of SK channel activation in spines is dampening of calcium influx through NMDARs, which in turn constrains EPSP size (Ngo-Ahn *et al* 2005; Faber *et al*. 2005; Bloodgood & Sabatini, 2007). Interestingly, SK channels in spines are not activated by bulk calcium influx but rather via calcium entry from a particular source. Two different calcium sources have been identified to activate SK channels in spines during excitatory input. Some studies indicate a primary role of R-type voltage-dependent calcium channels (Bloodgood & Sabatini, 2007; Faber 2010), whereas others indicate a primary role of calcium influx through NMDARs (Ngo-Ahn *et al* 2005, Faber *et al* 2005, Lin *et al*, 2008, Wang *et al* 2014).

This chapter describes experiments investigating the role of SK channels in regulating calcium influx during bAPs and identifies the calcium source. Basal

dendrites of L5 cortical pyramidal neurons were the subject of these investigations due to their relatively high spine density and close proximity to the soma.

METHODS

Electrophysiology

Whole-cell patch-clamp electrophysiology was performed on L5 pyramidal neurons from somatosensory cortex of Wistar rats, as described in the General Methods (Chapter 2). Backpropagating APs were evoked with brief somatic current injections (2-4 nA, 2 ms).

Confocal calcium imaging

Neurons were loaded with the high affinity calcium-sensitive dye Oregon Green BAPTA-1 (OGB-1) or the low affinity dye Oregon Green BAPTA 6F (OGB-6F) via the recording pipette. The calcium indicator was added directly to the K-gluconate intracellular solution. Cells were typically loaded for 50-60 minutes after obtaining the whole-cell configuration and prior to the commencement of imaging. Longer loading periods of up to 120 minutes were used for spines located further than 150 µm away from the soma. OGB-1 was employed to detect the small calcium transients in spines and dendrites associated with single bAPs and was used in most experiments. OGB-6F was used in some experiments to control for the potential impact of the high buffer capacity of OGB-1. Frame scans were used to identify dendrites and spines of interest. Repeated line scans were subsequently performed at 500-700 Hz during APs with the laser trajectory set to traverse the spine head and parent dendrite. In experiments using OGB-6F spot scans were performed at 5 kHz. A rapid acquisition rate was necessary due to the fast kinetics of this indicator. In

experiments using cyclopiazonic acid to inhibit intracellular stores neurons were filled with OGB-6F and frame scans of the soma performed at 20 Hz.

Pharmacology

SK and VDCC antagonists were dissolved in oxygenated ACSF immediately before use. In most cases, pharmacological agents were applied locally via a patch pipette with large tip diameter (~20µm). Initial experiments indicated that mechanical movement of fine dendrites and spines often lead to an irreversible depression of calcium influx that was only prevented by using low-pressure applications (less than 10 mmHg). When using low-pressure applications, it was important to make sure the dendrite and spine of interest were located near the surface of the slice such that the slice penetration requirement of the antagonists was minimized. In some experiments one antagonist was applied in the presence of another. This was achieved by using a second local application pipette containing both antagonists. In experiments investigating the role of intracellular stores, cyclopiazonic acid (CPA) was bath applied for 15 minutes prior to the commencement of imaging and apamin was locally co-applied with CPA. ACh (100 µM) was locally applied to the soma using brief (10 ms) pulses applied with a Picospritzer III (Parker, USA) from a standard patch pipette (tip diameter 2-3 µm). Antagonists and concentrations used are indicated in the subsequent table.

Antagonists for the inhibition of SK, VDCCs and intracellular calcium stores

Target	Antagonist	Concentration	Manufacturer
SK channels	Apamin	1 µM	Sigma Aldrich
SK channels	UCL 1684	1 µM	Tocris
R-Type	SNX 482	1 µM	Alamone Labs or Japanese Peptide Institute
N/P/Q-Type	Conotoxin MVIIC	10 µM	Japanese Peptide Institute
SERCA Pump	Cyclopiazonic acid	30 µM	Tocris

RESULTS

SK channels constrain spine and dendrite calcium influx during bAPs

Basal dendrites of cortical L5 pyramidal neurons were identified by their emanation from the soma, the presence of spines and the characteristic radial projection pattern within L5 (Figure 3.1A). Calcium influx into spines at various distances from the soma (50-200 µm) was monitored with the high affinity indicator OGB-1 (Figure 3.1A). Single bAPs caused large changes in fluorescence, detected by repeated line-scans across the spine head and parent dendrite (Figure 3.1A)

The role of SK channels in regulating calcium influx into spines and dendrites during bAPs was investigated with the SK channel antagonist apamin. Local application of apamin (1 µM in ACSF) caused a significant increase in calcium influx during bAPs in both spines and dendrites (Figure 3.1B-D; n=31). Across all spines we observed an average increase in fluorescence of around 40%, which was larger than the increase in the adjacent dendrite (Figure 3.1B). The properties of APs recorded at the soma were unaffected by apamin (AP amplitude: ACSF: 100.9 ± 2.4 mV, apamin: 101.3 ± 2.1 mV, P = 0.77; half-width: ACSF: 0.62 ± 0.01 ms; apamin: 0.63 ± 0.03 ms, P = 0.82; n = 5). Importantly, the affect of apamin on bAP-evoked calcium influx into spines and dendrites was distance dependent, with apamin having the greatest impact at distal dendritic locations (Figure 3.1E,F). As OGB-1 is a high affinity calcium buffer (K_D ~200 nM), and may therefore perturb SK channel activation, the

Figure 3.1.

Figure 3.1. – SK channels constrain calcium influx into spines and dendrites during bAPs.

A1, Confocal image of a layer 5 pyramidal neuron filled with 200 μM OGB1. Scale bar 25 μm. Yellow box indicates region of interest (ROI) in a distal basal dendrite. ***A2,*** ROI at high magnification. Dashed line shows location of line-scan. Scale bar 1 μm. ***A3,*** Repeated line-scans through the spine and dendrite shown in ***A2***. A single AP evoked after 30 ms (red arrow) caused a large increase in fluorescence in both compartments. ***B,*** AP-evoked change in fluorescence in a spine *(top)* and dendrite *(bottom)* before (black) and after (red) local application of apamin (1 μM). Same spine as in ***A2***. In this and all subsequent figures the solid line and shaded regions represent the mean ±SEM. ***C,D,*** Average AP-evoked peak ΔF/F (±S.E.M) in spines in the absence and presence of apamin ***(C)*** and average change in AP-evoked fluorescence (±S.E.M) in spines and dendrites after application of apamin ***(D)***, pooled from spines located at distances between 50-200 μm from the soma (n=32). ***E,F,*** Change in AP-evoked fluorescence in spines *(E)* and dendrites *(F)* after apamin application versus distance of the ROI from the soma. Lines represent linear fits to OGB-1 data. Pearson's co-efficient 0.868 (***E***) and 0.860 (***F***). ***G-H,*** Average change in AP-evoked fluorescence (± S.E.M) in spines and dendrites after application of UCL1684 (***G***; 1 μM; n=15) and normal ACSF (***H***; n=12), pooled data from spines and parent dendrites located at distances greater than 100 μm from the soma. ** denotes $p < 0.01$, * denotes $p < 0.05$, 'ns' denotes not significant

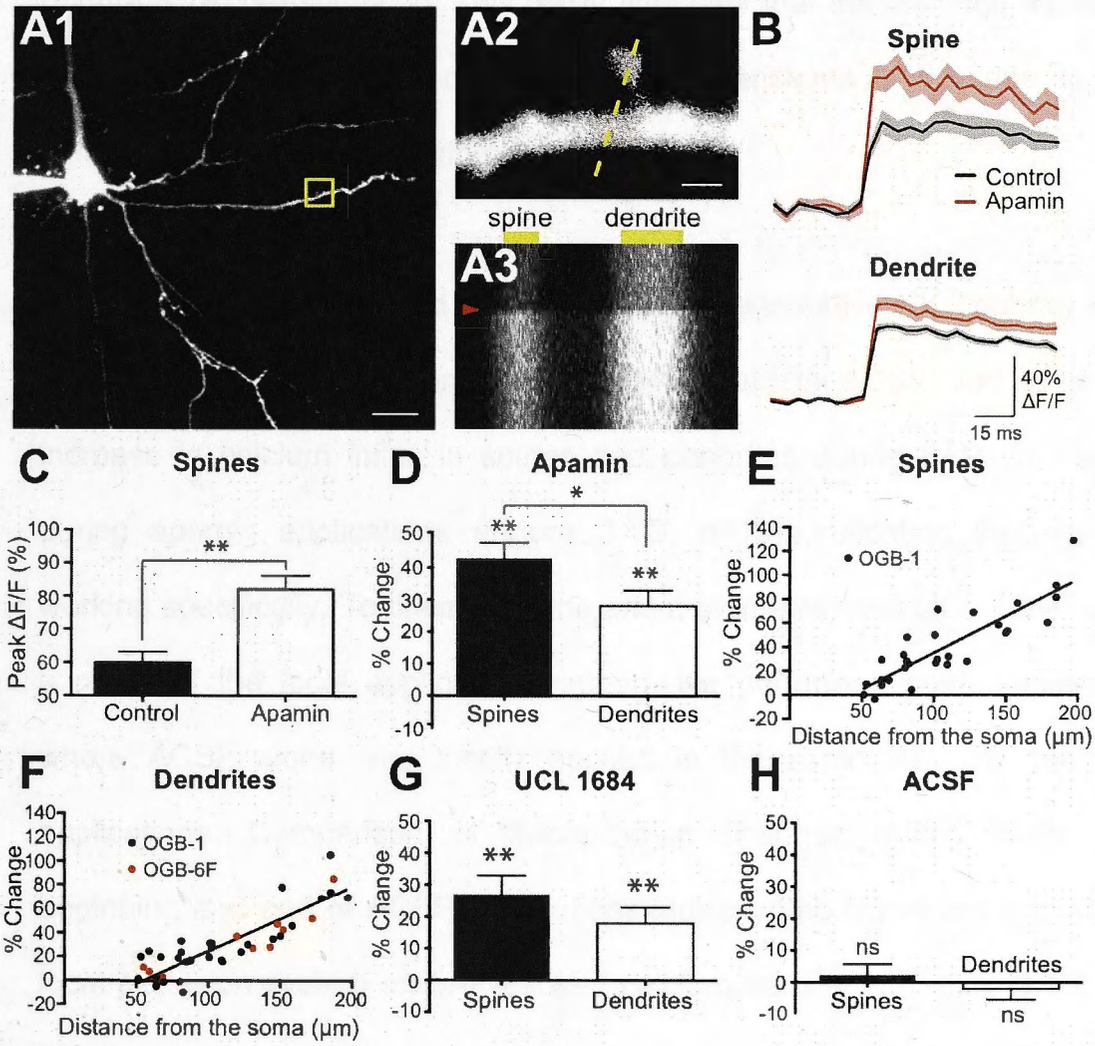
A1
A2
spine
dendrite
A3
B
Spine
Control
Apamin
Dendrite
40%
ΔF/F
15 ms
C
Spines
Peak ΔF/F (%)
Control
Apamin
D
Apamin
% Change
Spines
Dendrites
E
Spines
OGB-1
% Change
Distance from the soma (μm)
F
Dendrites
OGB-1
OGB-6F
% Change
Distance from the soma (μm)
G
UCL 1684
% Change
Spines
Dendrites
H
ACSF
% Change
ns
Spines
Dendrites
ns

observed distance dependence could be due to a higher concentration of calcium indicator at proximal compared to distal locations. To investigate this possibility, we repeated these experiments with the low affinity indicator OGB-6F (K_D ~3 μM). While we did not have the sensitivity to resolve calcium transients in spines in these experiments, using OGB-6F apamin caused a similar distance-dependent increase in dendritic calcium transients during bAPs (Figure 3.1F, red symbols). This result suggests that the distance dependence of the impact of apamin on bAP calcium transients is not due to spatial differences in calcium buffering.

In addition, we investigated the impact of the alternative SK channel inhibitor UCL1684. Local application of UCL1684 (1 μM in ACSF) led to a similar increase in calcium influx in spines and dendrites during bAPs to that seen during apamin applications (Figure 3.1G, n=15), indicating that apamin is working specifically. To check that the affect of apamin and UCL 1684 were not a result of the local application method, we performed control experiments where ACSF alone was locally applied in the same way as during drug applications. Comparison of fluorescence changes during bAPs at the beginning and end of ACSF applications indicated no significant impact of our local perfusion system on bAP-evoked calcium transients (Figure 3.1H; n=12). Finally, the impact of apamin on spines in apical oblique dendrites was also investigated. While apamin led to a significant increase bAP evoked calcium transients in apical oblique spines (24.3 ± 6.4 % change; $p < 0.01$), similar to spines on basal dendrites, there was no significant effect on adjacent oblique dendrites (4.7 ± 2.5 %; $p = 0.1$; n=10). Together, these data indicate that SK

channels in L5 cortical pyramidal neurons play an important role in regulating calcium influx into spines and basal dendrites during bAPs, particularly at distal dendritic locations.

R-type calcium channels control SK channel activation during bAPs

We next investigated the calcium source(s) controlling activation of SK channels in spines and dendrites during bAPs. Other groups have shown that SK channels in spines during synaptic input are activated by calcium influx through R-type VDCCs (Bloodgood and Sabatini, 2007; Faber, 2010) and/or NMDARs (Faber *et al.*, 2005; Ngo-Anh *et al.*, 2005; Wang *et al.*, 2014). Given that NMDAR activation during bAPs is negligible (Koester and Sakmann, 2000; Sabatini and Svoboda, 2000; Bloodgood and Sabatini, 2007), we examined whether SK channel activation during bAPs requires calcium influx through R-type VDCCs using the antagonist SNX 482. Local application of SNX 482 (1 μM) caused a significant decease in bAP-evoked calcium transients in dendrites but not in spines (Figure 3.2A-C; spines: $P = 0.561$, dendrites: $P = 0.0182$, n=12). There are two possible explanations for this result. The first is that R-type VDCCs are not present in spines or not activated by bAPs. The second is that R-type VDCCs contribute both to calcium influx into spines and provide the calcium necessary for SK channel activation. If the second explanation is correct, during the application of SNX 482 the contribution of R-type VDCCs to calcium influx is expected to decrease but the perturbation of SK channel function and its impact on the activation of other VDCC subtypes present in the spine head could compensate. This could in principle lead to no net impact of blocking R-type VDCCs on spine calcium influx during bAPs. To isolate the

Figure 3.2.

Figure 3.2. – R-type VDCCs control SK channel activation during bAPs.

A, AP-evoked change in fluorescence in a spine (top) and dendrite (bottom) in control (black) and after local application of SNX482 (1 μM; blue). ***B,*** Average AP-evoked peak ΔF/F for spines before and after local application of SNX482 (±S.E.M; n=15). ***C,*** Average % change in AP-evoked fluorescence in SNX482 compared to control in spines and dendrites (±S.E.M; n=15). ***D,*** AP-evoked change in fluorescence in a spine (top) and dendrite (bottom) in the presence of apamin (1 μM; red) and after local application of SNX482 in apamin (blue). ***E,*** Average AP-evoked peak ΔF/F for spines before and after application of SNX482 in the continued presence of apamin (±S.E.M; n=19). ***F,*** Average % change in AP-evoked fluorescence in SNX 482 plus apamin compared to apamin alone in spines and dendrites (±S.E.M; n=19). ***G,*** AP-evoked change in fluorescence in a spine (top) and dendrite (bottom) in the presence of SNX482 (blue) and after local application of apamin in SNX482 (red). ***H,*** Average AP-evoked peak ΔF/F for spines before and after application of apamin in the continued presence of SNX482 (±S.E.M; n=21). ***I,*** Average % change in AP-evoked fluorescence in apamin plus SNX482 compared to SNX482 alone in spines and dendrites (±S.E.M; n=21). * denotes $p < 0.05$, ** denotes $p < 0.01$, ns denotes not significant.

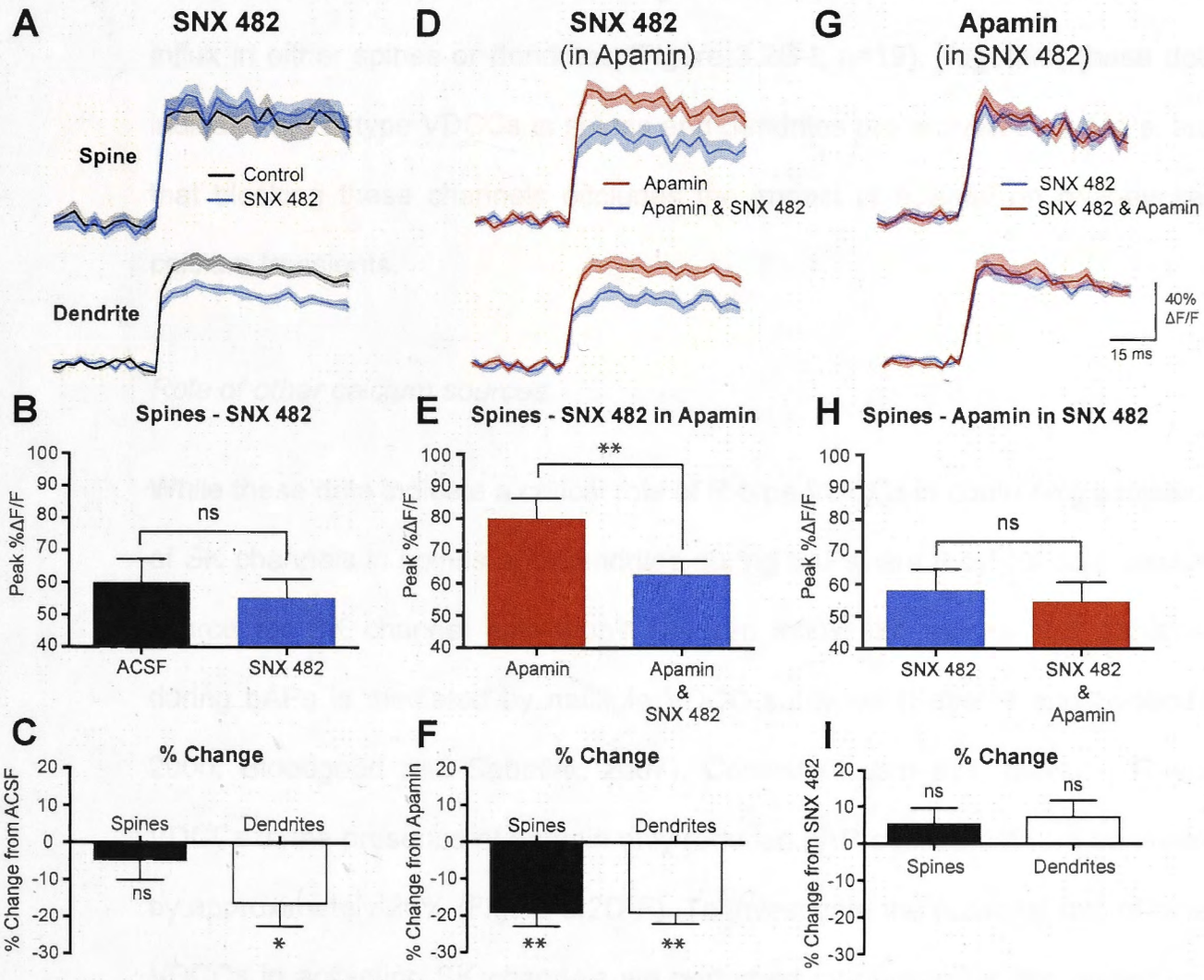
A
SNX 482
Spine
Control
SNX 482
Dendrite
D
SNX 482
(in Apamin)
Apamin
Apamin & SNX 482
G
Apamin
(in SNX 482)
SNX 482
SNX 482 & Apamin
40%
ΔF/F
15 ms
B
Spines - SNX 482
Peak %ΔF/F
ns
ACSF
SNX 482
E
Spines - SNX 482 in Apamin
**
Apamin
Apamin & SNX 482
H
Spines - Apamin in SNX 482
ns
SNX 482
SNX 482 & Apamin
C
% Change
% Change from ACSF
Spines
Dendrites
ns
*
F
% Change
% Change from Apamin
Spines
Dendrites
**
**
I
% Change
% Change from SNX 482
ns
ns
Spines
Dendrites

impact of R-type VDCC block on calcium influx from its potential impact on SK channel activation, SNX 482 was applied in the presence of apamin. Under these conditions SNX 482 caused a significant decrease in bAP-evoked calcium transients in both dendrites and spines (Figure 3.2D-F; n=19). These findings indicate that R-type VDCCs are present in both spines and dendrites. To test if calcium influx through R-type VDCCs channels is required for SK channel activation, apamin was applied in the presence of SNX 482. Under these conditions, apamin had no significant impact on bAP-evoked calcium influx in either spines or dendrites (Figure 3.2G-I; n=19). Together, these data indicate that R-type VDCCs in spines and dendrites are activated by bAPs, and that blocking these channels occludes the impact of apamin on bAP-evoked calcium transients.

Role of other calcium sources

While these data indicate a critical role of R-type VDCCs in controlling activation of SK channels in spines and dendrites during bAPs, are they the sole calcium source for SK channel activation? Calcium influx into spines and dendrites during bAPs is mediated by multiple VDCC subtypes (Sabatini and Svoboda, 2000; Bloodgood and Sabatini, 2007). Consistent with this, blocking R-type VDCCs in the presence of apamin only reduced bAP-evoked calcium transients by approximately 20% (Figure 3.2D-F). To investigate the potential role of other VDCCs in activating SK channels we perturbed calcium influx into spines and dendrites by inhibiting N and P/Q type VDCCs using local applications of conotoxin MVIIC (10 μM). Blocking N and P/Q VDCCs significantly reduced bAP-evoked calcium influx into spines and dendrites by approximately 20%

(Figure 3.3A-C; spines: n=10), indicating that N and P/Q type VDCCs are present in basal spines and dendrites of L5 pyramidal neurons and activated by bAPs. In contrast to SNX 482, however, the application of apamin in the presence of conotoxin MVIIC still lead to a significant (~30%) increase in bAP-evoked calcium transients in both spines and dendrites (Figure 3.3D-F; n=10). These data show that calcium influx through N- and/or P/Q-type VDCCs in spines and dendrites during bAPs is not required for SK channel activation. Furthermore, they indicate that despite multiple VDCCs contributing to calcium influx in spines and dendrites during bAPs, SK channel activation is triggered solely by calcium influx through R-type VDCCs.

A recent study showed that SK channel activation during EPSPs can be abolished by blocking calcium release from intracellular stores, suggesting a role of calcium-induced calcium release in SK channel activation (Faber, 2010). To investigate the potential impact of calcium release from intracellular stores on SK channel activation during bAPs we depleted intracellular calcium stores with the calcium-ATPase inhibitor cyclopiazonic acid (CPA; 30 µM in the bath) (Seidler *et al.*, 1989). Local application of apamin in the presence of CPA caused a similar enhancement of bAP-evoked calcium transients in basal spines and dendrites to that seen under control conditions (Figure 3.4A-C; n=10; compare with Figure 3.1D). This data suggests that intracellular calcium stores are unlikely to be involved in controlling SK channel activation during bAPs. To confirm that CPA had emptied intracellular calcium stores we locally applied acetylcholine (ACh) to the soma, which is known to cause intracellular calcium release leading to a large increase in somatic calcium (Gulledge and

Figure 3.3.

Figure 3.3. – Block of N and P/Q type VDCCs does not affect SK channel activation

A, AP-evoked change in fluorescence in a spine (top) and dendrite (bottom) before (black) and after application of conotoxin MVIIC (10 μM; green) to block N and P/Q type VDCCs. ***B,*** Average AP-evoked peak ΔF/F in spines before and after the application of contoxin MVIIC. ***C,*** Average % change in AP-evoked fluorescence in spines and dendrites after application of conotoxin MVIIC (±S.E.M; n=10). ***D,*** AP-evoked change in fluorescence in a spine (top) and dendrite (bottom) in conotoxin MVIIC (green) and after application of apamin (1 μM) in the presence of conotoxin MVIIC (red). ***E***, Average AP-evoked peak ΔF/F in spines before and after application of apamin in the continued presence of conotoxin MVIIC (±S.E.M; n=10). ***F,*** Average % change in AP-evoked fluorescence after application of apamin in the presence of conotoxin MVIIC (±S.E.M; n=10). * denotes $p < 0.05$, ** denotes $p < 0.01$.

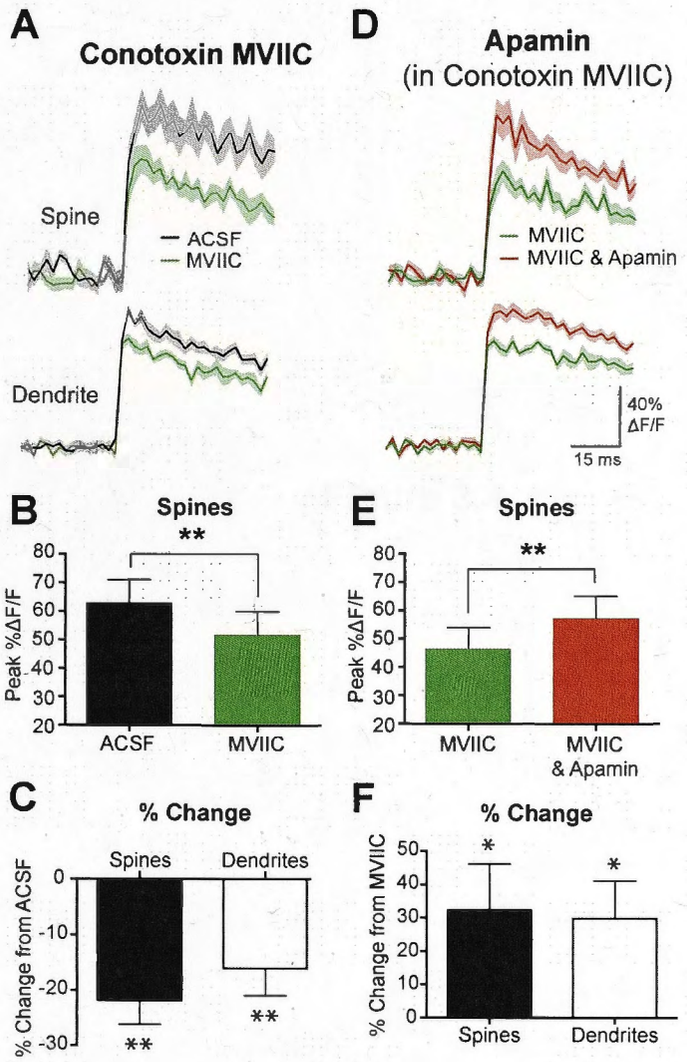
A
Conotoxin MVIIC
Spine
ACSF
MVIIC
Dendrite
D
Apamin
(in Conotoxin MVIIC)
MVIIC
MVIIC & Apamin
40%
ΔF/F
15 ms
B
Spines
**
Peak %ΔF/F
80
70
60
50
40
30
20
ACSF
MVIIC
E
Spines
**
Peak %ΔF/F
MVIIC
MVIIC
& Apamin
C
% Change
Spines
Dendrites
% Change from ACSF
0
-10
-20
-30
**
**
F
% Change
% Change from MVIIC
50
40
30
20
10
0
*
*
Spines
Dendrites

Figure 3.4.

Figure 3.4. – Inhibition of intracellular calcium stores does not affect SK channel activation.

A, AP-evoked change in fluorescence in a spine (left) and dendrite (right) in the presence of CPA to deplete intracellular calcium stores (30 μM; black) and after application of apamin (1 μM) in the present of CPA (red). ***B,*** Average AP-evoked peak ΔF/F in spines before and after application of apamin in the continued presence of CPA (±S.E.M; n=10). ***C,*** Average % change in AP-evoked fluorescence after application of apamin in the presence of CPA (±S.E.M; n=10). ***D,*** Change in fluorescence at the soma in response to a 10 ms local application of 100 μM acetylcholine to the soma in normal ACSF (black) and in the presence of CPA (blue). ***E,*** Average change in fluorescence during somatic acetylcholine applications in ACSF and CPA (n=4). ** denotes $p < 0.01$, ns denotes not significant.

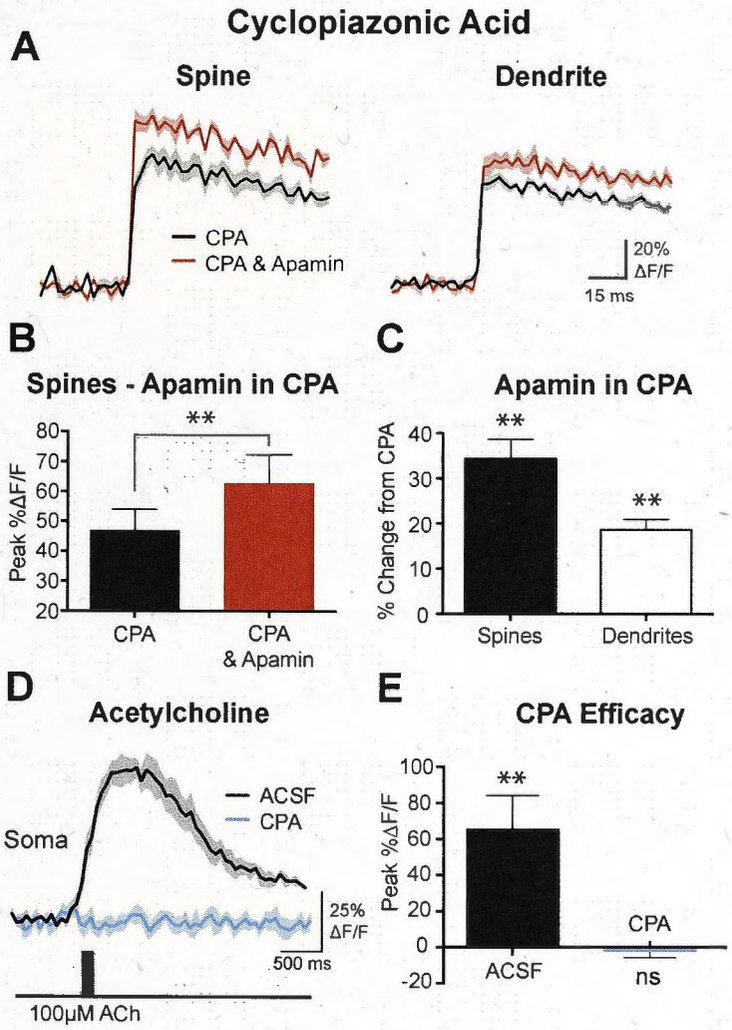
Cyclopiazonic Acid
A
Spine
Dendrite
CPA
CPA & Apamin
20%
ΔF/F
15 ms
B
Spines - Apamin in CPA
**
Peak %ΔF/F
80
70
60
50
40
30
20
CPA
CPA
& Apamin
C
Apamin in CPA
**
**
% Change from CPA
40
30
20
10
0
Spines
Dendrites
D
Acetylcholine
ACSF
CPA
Soma
25%
ΔF/F
500 ms
100μM ACh
E
CPA Efficacy
**
Peak %ΔF/F
100
80
60
40
20
0
-20
CPA
ACSF
ns

Stuart, 2005; Gulledge *et al.*, 2007). The low affinity calcium indicator OGB-6F (200 μM) was included in the recording pipette and calcium transients in these experiments were evoked by brief (10 ms) applications of ACh (100 μM) in the absence and presence of CPA. As expected, the presence of CPA abolished ACh-induced calcium transients (Figure 3.4D-E; n=4), indicating that CPA was effective in emptying intracellular calcium stores under our experimental conditions.

Discussion

This chapter has provides evidence for SK channels playing a role in regulating calcium influx in dendrites and spines during bAPs, and shows that the sole calcium source for SK channel activation by bAPs is via R-type VDCCs.

SK channel activation in dendrites and spines during action potentials

The observed increase in bAP-evoked calcium influx during SK channel block is presumably due to enhanced activation of VDCCs in spines and dendrites following an increase in amplitude or broadening of bAPs. Consistent with this idea, it has recently been observed that SK channels can control bAP amplitude in cerebellar Purkinje neurons (Ohtsuki *et al.*, 2012). The observation that dendritic SK channels can influence bAPs is surprising given that apamin had no impact on the somatic AP waveform. Previous studies indicate that SK channels can activate within a millisecond during rapid changes in intracellular calcium at room temperature (Xia *et al.*, 1998), and would be expected to activate even faster at physiological temperatures. In addition, one might expect SK channels to have a greater impact on bAPs due to their increased duration compared to somatic APs (Stuart *et al.*, 1997; Nevian *et al.*, 2007). Consistent with this idea, the impact of SK channels on bAP-evoked calcium transients was greatest at distal locations where bAP duration in basal dendrites is longest (Kampa and Stuart, 2006; Nevian *et al.*, 2007) (although see Antic, 2003). The distance-dependent impact of apamin on bAP-evoked calcium transients may also be explained by a higher expression of SK or R-type calcium channels at distal dendritic locations. Finally, we observed that blocking SK channels

caused a greater increase in bAP-evoked calcium influx in spines compared to dendrites, particularly in oblique dendrites. While this effect may also be due to differences in channel expression in spines versus dendrites, the larger surface to volume ratio of spines compared to dendrites would be expected to contribute (Sabatini *et al.*, 2002).

Calcium sources for SK channel activation in dendritic spines

While there is evidence that R-type VDCCs control SK channel activation in spines during EPSP-like events evoked by glutamate-uncaging (Bloodgood and Sabatini, 2007), other studies have suggested that calcium influx through NMDA receptors is critical for SK channel activation during EPSPs (Faber *et al.*, 2005; Ngo-Anh *et al.*, 2005; Faber, 2010; Wang *et al.*, 2014). Consistent with this latter idea, NMDA receptors and SK channels are co-localised within the postsynaptic density in CA1 pyramidal neurons (Lin *et al.*, 2008). Because SK channels in spines modulate NMDA receptor activation (Faber *et al.*, 2005; Ngo-Anh *et al.*, 2005; Faber, 2010), which provides the main calcium source during synaptic activation (Kovalchuk *et al.*, 2000; Sabatini *et al.*, 2002), identifying the calcium source driving SK channel activation in spines during EPSPs is complex. This complication does not exist in our experiments, as NMDA receptor activation during bAPs is negligible (Koester and Sakmann, 2000; Sabatini and Svoboda, 2000; Bloodgood and Sabatini, 2007). During bAPs we find that inhibition of solely R-type VDCCs is sufficient to block SK channel activation. Moreover, inhibition of N and P/Q type VDCCs, which are expressed in spines along with R-type VDCCs and led to similar calcium influx during bAPs, did not influence SK channel activation. This indicates tight and

specific coupling between R-type VDCCs and SK channels within the spine head. This conclusion is similar to that made previously during EPSP-like events evoked by glutamate-uncaging in spines from CA1 pyramidal neurons (Bloodgood and Sabatini, 2007). These data suggest that R-type VDCCs and SK channels in the spine head are coupled in nanodomains, consistent with previous observations showing that only high concentrations of the fast, high affinity calcium buffer BAPTA are able to interfere with SK channel activation in spines during EPSPs (Ngo-Anh *et al.*, 2005)

Possible physiological significance

As SK channels play an important role in regulating dendritic calcium dynamics, modulation of these channels would be expected to modify neuronal excitability and synaptic plasticity. Consistent with this idea, down regulation of SK channels following activation of M_1 muscarinic or β adrenergic receptors in CA1 pyramidal (Buchanan *et al.*, 2010; Giessel and Sabatini, 2010) and lateral amygdala neurons (Faber *et al.*, 2008), respectively, increases synaptic strength. Conversely, changes in synaptic strength during synaptic plasticity have been shown to be associated with changes in SK channel function (Lin *et al.*, 2008; Ohtsuki *et al.*, 2012). Given the specific coupling of R-type VDCCs to SK channels in spines, as shown here and elsewhere (Bloodgood and Sabatini, 2007), modulation of R-type VDCCs following activation of D_2 dopamine receptors (Higley and Sabatini, 2010) may provide another mechanism in which SK channel activation in spines can be regulated. Recent evidence indicates that GABAergic inhibition can modulate calcium influx onto individual dendritic spines during bAPs in a selective manner (Chiu *et al.*, 2013). These data

suggest that spine-specific SK channel modulation could act to influence calcium influx into only those spines during bAPs.

What possible function might SK channels in spines and dendrites serve when activated by bAPs? The capacity of SK channels in spines and dendrites to constrain the amplitude and/or width of bAPs would be expected to influence NMDA receptor activation during EPSP-AP pairing. This effect would be greatest at distal dendritic locations, where NMDA receptor activation during synaptic events is most pronounced (Branco and Hausser, 2011). Given that changes in synaptic strength during spike-timing dependent plasticity (STDP) are dependent on NMDA receptor activation (Markram *et al.*, 1997), the impact of SK channels on the bAP time course may play a role in setting the STDP time window (Froemke *et al.*, 2005; Letzkus *et al.*, 2006), possibly increasing the fidelity of co-incidence detection during STDP.

CHAPTER 4: ON THE FUNCTION OF SOMATIC CALCIUM-ACTIVATED POTASSIUM CHANNELS DURING ACTION POTENTIALS.

INTRODUCTION

SK channels have long been known to mediate the medium afterhyperpolarisation (mAHP) in many types of neurons, including cortical pyramidal neurons (Schwindt *et al*, 1988), neurons in the lateral amygdala (Faber & Sah, 2002) vagal motorneurons (Sah & McLachlan, 1991) and cerebellar Purkinje neurons (Womack & Khodakhah, 2003; Womack *et al*, 2004). The involvement of SK channels in the mAHP in CA1 pyramidal neurons is more controversial. While it was initially thought that SK channels were involved in generation of the mAHP in these neurons more recent work suggests this is not the case (Stocker *et al*., 1999; Gu *et al*., 2005; Gu *et al*., 2008). Because it generates a hyperpolarization after APs the mAHP plays a key role in regulating action potential accommodation, output gain and in some cases burst firing (Schwindt *et al*., 1988; Faber & Sah, 2002; Womack & Khoakhah, 2003; Womack *et al*., 2004).

The source of calcium for somatic SK channel activation seems to be largely dependent on neuronal cell type. For example, in midbrain dopaminergic neurons activation of SK channels during the mAHP is solely dependent on T-type VDCCs (Wolfart & Roeper, 2002), whereas only L-type channels are coupled to somatic SK channels in hippocampal pyramidal neurons (Marrion &

Travalin, 1998). Given the expression of multiple VDCC subtypes at the soma of these neurons and the specificity of SK-VDCC coupling, these findings suggest that somatic SK channels, like those in spines, are not activated by bulk calcium influx but exist in a nanodomain with their calcium source (Fakler & Adelman, 2008).

This chapter describes experiments investigating the activation of somatic SK channels in layer 5 pyramidal neurons. The aim was to investigate the strength of coupling of somatic SK channels to their calcium source, as well as identify the calcium source(s).

METHODS

Electrophysiology

Whole-cell patch-clamp recording were made from large L5 pyramidal neurons, as described in the General Methods (Chapter 2). Single APs were elicited by 200 ms current pulses just above rheobase. 50-100 APs were aligned and averaged to reveal the AP waveform and mAHP under the different conditions. Input-output relationships were performed using a series of 500 ms long current pulses ascending in 100 pA steps from 0 to 1600 pA. Oregon Green BAPTA-1 at 200 μM or ethylene glycol tetraacetic acid (EGTA) at 200 μM or 1 mM were added to the intracellular solution to evaluate the affect of calcium chelators on somatic SK channel activation.

Data was only analyzed from cells with stable resting membrane potentials (defined as a less than 2 mV change) more negative than -60 mV. Neuron input resistance was measured throughout each experiment using repeated current injections of -20 pA with a duration of 1 second (60-100 sweeps were typically averaged). Rheobase was determined using 200 ms somatic current injections and denoted as the lowest current amplitude that evoked an action potential.

Confocal calcium imaging

In some experiments neurons were loaded with 200μM Oregon Green BAPTA-1 via the recording pipette and spot calcium imaging was performed on the soma and basal dendrites using a rate of 700 Hz, as described in the General Methods (Chapter 2).

Pharmacology

Antagonists for VDCCs, SK and BK channels were applied in the bath at the concentrations listed in the table below.

Antagonists used to inhibit SK, BK and VDCCs

Target	Antagonist	Concentration	Manufacturer
SK channels	Apamin	100 nM	Sigma Aldrich
BK channels	Paxilline	1 µM	Tocris Bioscience
R-type VDCC	SNX-482	300 nM	Alamone Labs
N type VDCC	Conotoxin GVIA	1 µM	Alamone Labs
L-type VDCC	Nifedipine	15 µM	Sigma Aldrich
T-type VDCC	NNC-	20 µM	Sigma Aldrich
P/Q-Type VDCC	Agatoxin IVA	300 nM	Alamone Labs

RESULTS

Somatic SK channels are not tightly coupled to their source of calcium

SK channels have long been known to contribute to the generation of the mAHP in L5 pyramidal neurons (Schwindt *et al.*, 1988). Hence we were It was surprised to find that applications of apamin did not affect the mAHP in our calcium imaging experiments. We hypothesized that this may be the case because OGB-1, which is related to the fast calcium buffer BAPTA, perturbs SK channel activation at the soma through calcium chelation. To test this hypothesis, changes in the amplitude of the mAHP were quantified in the absence and presence of OGB-1 in the pipette internal solution. Single APs in these experiments were elicited at depolarized membrane potentials by 200 ms long positive current pulses instead of brief (2 ms), high amplitude, pulses from the resting membrane potential. APs evoked in this way had larger mAHPs as the membrane potential after the AP is more depolarization, increasing the driving force for the SK current. The strength of current pulses was set to be just above rheobase.

In the absence of OGB-1 in the internal solution, bath application of apamin (100 nM) lead to a significant reduction in the amplitude of the mAHP (Figure 4.1A,D; n=5). Inclusion of OGB-1 (200 μM) in the internal solution, however, lead to a time-dependent decrease in the mAHP, with the impact of apamin on the mAHP occluded 30 minutes after break in (Figure 4.1B,D; n=5). The observation that low concentrations of the calcium-sensitive dye OGB-1 blocked the mAHP suggests that the coupling of somatic SK channels to their calcium

Figure 4.1.

Figure 4.1. – Impact of calcium chelators on the mAHP.

A-C, Truncated somatic action potentials evoked by 200 ms somatic current pulses showing the mAHP in control just after initiation of recording (black, solid line), 30 minutes after recording (black, dashed line) and/or in the presence of apamin (red, solid line). Recordings were made with no internal calcium indicator in the pipette solution (***A***), with OGB-1 (***B***; 200 μM) or with EGTA in the pipette solution (***C***; 1 mM). The mAHP amplitude was measured 30 ms after AP onset (dashed vertical line in ***A***). ***D***,***E***, Average change in mAHP amplitude in the absence (black) and presence (red) of apamin in cells with and without OGB-1 in the pipette solution (***D***) and in cells dialyzed with 200 μM or 1 mM EGTA (***E***; n=6 for each). * denotes $p < 0.05$, ns denotes not significant.

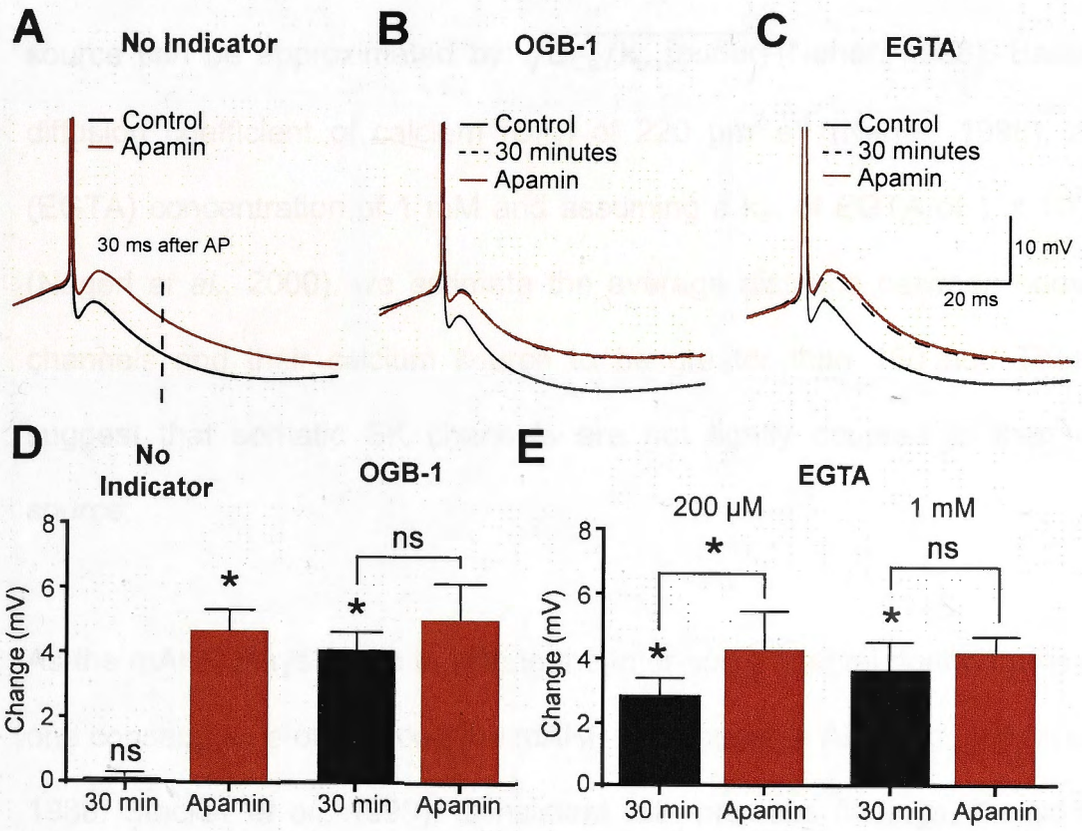
A
No Indicator
Control
Apamin
30 ms after AP
B
OGB-1
Control
30 minutes
Apamin
C
EGTA
Control
30 minutes
Apamin
10 mV
20 ms
D
No Indicator
OGB-1
Change (mV)
ns
*
*
ns
30 min
Apamin
30 min
Apamin
E
EGTA
200 µM
1 mM
Change (mV)
*
*
ns
*
30 min
Apamin
30 min
Apamin

source is weak. To investigate this further we tested the impact of EGTA on the mAHP. EGTA is a calcium buffer that has a binding rate ~40 times slower than BAPTA (Nagerl *et al.*, 2000), and thus can only interfere with calcium dependent processes where the source and effector are within a microdomain (Neher, 1998). Using the same concentration of EGTA (200 μM) a partial perturbation of the mAHP was observed (n=6), with full inhibition of the mAHP occurring when the EGTA concentration was increased to 1 mM (Figure 4,1C,E; n=6). The diffusional distance between somatic SK channels and their calcium source can be approximated by: $\sqrt{D_{Ca}/k_{on}[buffer]}$ (Neher, 1998). Based on a diffusion coefficient of calcium (D_{Ca}) of 220 $\mu m^2\ s^{-1}$ (Neher, 1998), a buffer (EGTA) concentration of 1 mM and assuming a k_{on} of EGTA of $1 \times 10^7\ M^{-1} s^{-1}$ (Nagerl *et al.*, 2000), we estimate the average distance between somatic SK channels and their calcium source to be greater than 150 nm. These data suggest that somatic SK channels are not tightly coupled to their calcium source.

As the mAHP plays a role in setting the inter-spike interval during trains of APs, one consequence of blocking the mAHP is to increase AP firing (Schwindt *et al.*, 1988; Stocker *et al.*, 1999). Consistent with previous findings, the addition of apamin to the extracellular solution caused a significant increase in AP firing frequency during long somatic current steps (500 ms) and led to burst firing in 7 out of 10 neurons during shorter current steps (200 ms) just above rheobase (Figure 4.2A,B,E). We next investigated whether dialysis of OGB-1 also leads to similar changes in AP firing frequency and the propensity for burst firing. So as to obtain conditions in the absence of OGB-1 pipettes in these experiments

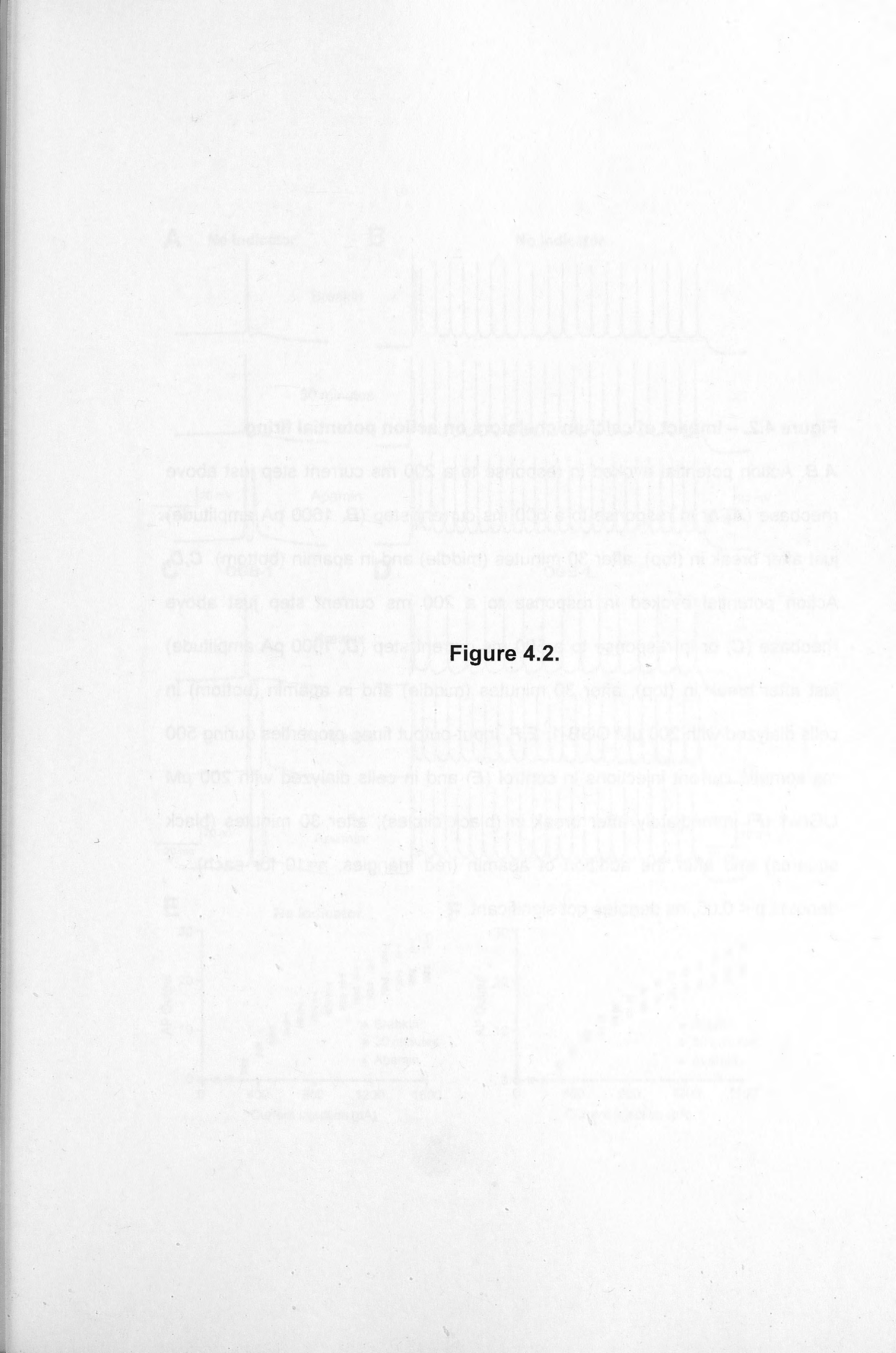

Figure 4.2.

Figure 4.2. – Impact of calcium chelators on action potential firing.

A,***B***, Action potential evoked in response to a 200 ms current step just above rheobase (***A***) or in response to a 500 ms current step (***B***, 1600 pA amplitude) just after break in (top), after 30 minutes (middle) and in apamin (bottom). ***C,D,*** Action potential evoked in response to a 200 ms current step just above rheobase (***C***) or in response to a 500 ms current step (***D***, 1600 pA amplitude) just after break in (top), after 30 minutes (middle) and in apamin (bottom) in cells dialyzed with 200 μM OGB-1. ***E,F,*** Input-output firing properties during 500 ms somatic current injections in control (***E***) and in cells dialyzed with 200 μM OGB-1 (***F***) immediately after break in (black circles), after 30 minutes (black squares) and after the addition of apamin (red triangles; n=10 for each). * denotes $p < 0.05$, ns denotes not significant.

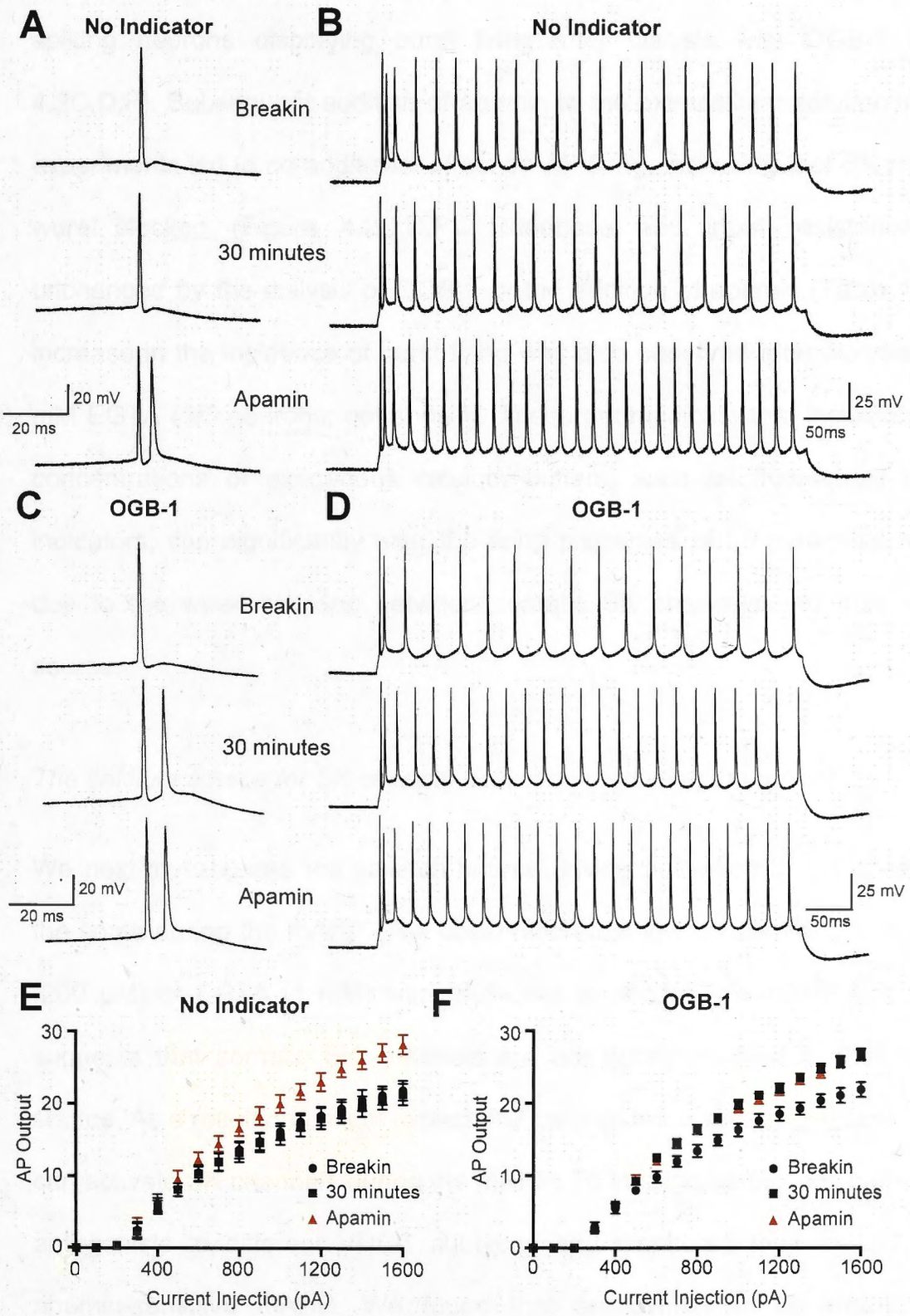
A
No Indicator
Breakin
30 minutes
Apamin
20 mV
20 ms
B
No Indicator
25 mV
50ms
C
OGB-1
Breakin
30 minutes
Apamin
20 mV
20 ms
D
OGB-1
25 mV
50ms
E
No Indicator
AP Output
Current Injection (pA)
Breakin
30 minutes
Apamin
F
OGB-1
AP Output
Current Injection (pA)
Breakin
30 minutes
Apamin

were tip filled with intracellular solution without the indicator and then back filled with solution containing the dye. Over the first 30 minutes of the recording there was a significant change in the F-I relationship, with many (8 out of 10) regular spiking neurons displaying burst firing after dialysis with OGB-1 (Figure 4.2C,D,F). Subsequent addition of apamin to the extracellular solution in these experiments led to no additional effect on AP firing, indicating that SK channels were blocked (Figure 4.2C,D,F). Rheobase and input resistance were unchanged by the dialysis of OGB-1 or the addition of apamin (Table 4.1). An increase in the incidence of burst firing was also observed after dialysis with 1 mM EGTA (3/6 neurons; not shown). These data indicate that inclusion of low concentrations of exogenous calcium buffers, such as fluorescent calcium indicators, can significantly alter the firing properties of L5 pyramidal neurons due to the weak coupling between somatic SK channels and their calcium source.

The calcium source for SK channel activation mediating the mAHP

We next investigated the calcium source driving activation of SK channels at the soma during the mAHP. The observation that low concentrations of OGB-1 (200 μM) or EGTA (1 mM) were sufficient to abolish the mAHP (Figure 4.1) suggests that somatic SK channels are not tightly coupled to their calcium source. As a result one might expect that calcium influx through multiple VDCCs can activate SK channels during the mAHP. To investigate this, we bath applied antagonists to different VDCC subtypes and monitored their impact on the apamin-sensitive mAHP. We found that antagonists to all known VDCC subtypes except R-type VDCCs caused a reduction in the amplitude of the

Table 4.1. – Impact of apamin and OGB-1 on rheobase and input resistance (R_N)

No Indicator				
	Breakin	**30min**	**Apamin**	**N**
Rheobase (pA)	324 ± 32.31	323 ± 35.30	319 ± 35.51	10
R_N (MΩ)	27 ± 1.71	27± 1.63	26± 1.60	10
OGB-1				
	Breakin	**30min**	**Apamin**	**N**
Rheobase (pA)	269 ±12.69	265 ± 16.20	265 ± 14.92	10
R_N (MΩ)	29 ± 1.37	28 ± 1.51	27 ± 2.13	10

mAHP (Figure 4.3). To determine whether an additional calcium source other than N, P/Q, L and T-type VDCCs contributes to SK channel activation during the mAHP we applied a cocktail of antagonists to these VDCCs. Under these conditions the addition of apamin had no significant affect on the mAHP (Figure 4.3F,G; n=6), indicating that the activation of SK channels during the mAHP can be completely perturbed by blocking N, P/Q, L and T-type VDCCs. The effect of the VDCC antagonist cocktail was occluded by the presence of apamin (Figure 4.3G; n=4), indicating that inhibition of VDCCs modulates the mAHP solely by blocking SK channels and not via perturbing a different calcium-dependent conductance active at the same time after an AP.

One likely explanation for the absence of a contribution of R-type VDCCs to the amplitude of the mAHP is that R-type VDCCs aren't expressed at the soma of L5 pyramidal neurons. To investigate this, somatic and dendritic calcium imaging was performed in the absence and presence of SNX482. There was no difference in calcium influx at the soma in the two conditions, whereas a ~20% decrease in calcium influx was observed in basal dendrites ~100μm from the soma in the presence of SNX482 (Figure 4.4; n=5). This data suggests that R-type VDCCs are not expressed at the soma, but are expressed in basal dendrites as observed in Chapter 3. These data indicate that the absence of a role of R-type VDCCs in the generation of the mAHP (Figure 4.3A,G) is due to the lack of expression of these channels at the soma.

Together, these findings demonstrate that SK channels mediating the apamin-sensitive component of the mAHP can be activated by calcium influx through a

Figure 4.3.

Figure 4.3. – The calcium source for the mAHP in cortical pyramidal neurons.

A-F, Truncated somatic action potentials evoked by 200 ms somatic current pulses showing the mAHP in control (black, solid line), after bath application of VDCC blockers (colored dashed line) and in the presence of apamin (red, solid line). ***A,*** Impact of the R-type VDCC blocker SNX 482 (300 nM; n=5). ***B,*** Impact of the N-type VDCC blocker conotoxin GVIA (1 μM; n=6). ***C,*** Impact of the L-type VDCC blocker nifedipine (15 μM; n=6). ***D,*** Impact of the T-type VDCC blocker NNC 55-0396 (20 μM, n=5). ***E,*** Impact of the P/Q-type VDCC blocker agatoxin IVA (300 nM; n=6). ***F,*** Impact of a cocktail of N, L, T and P/Q type VDCC blockers (n=4). ***G,*** Average change in mAHP amplitude (±S.E.M) relative to control under the indicated recording conditions (measured 30 ms after AP onset). * denotes $p < 0.05$, ** denotes $p < 0.01$, ns denotes not significant.

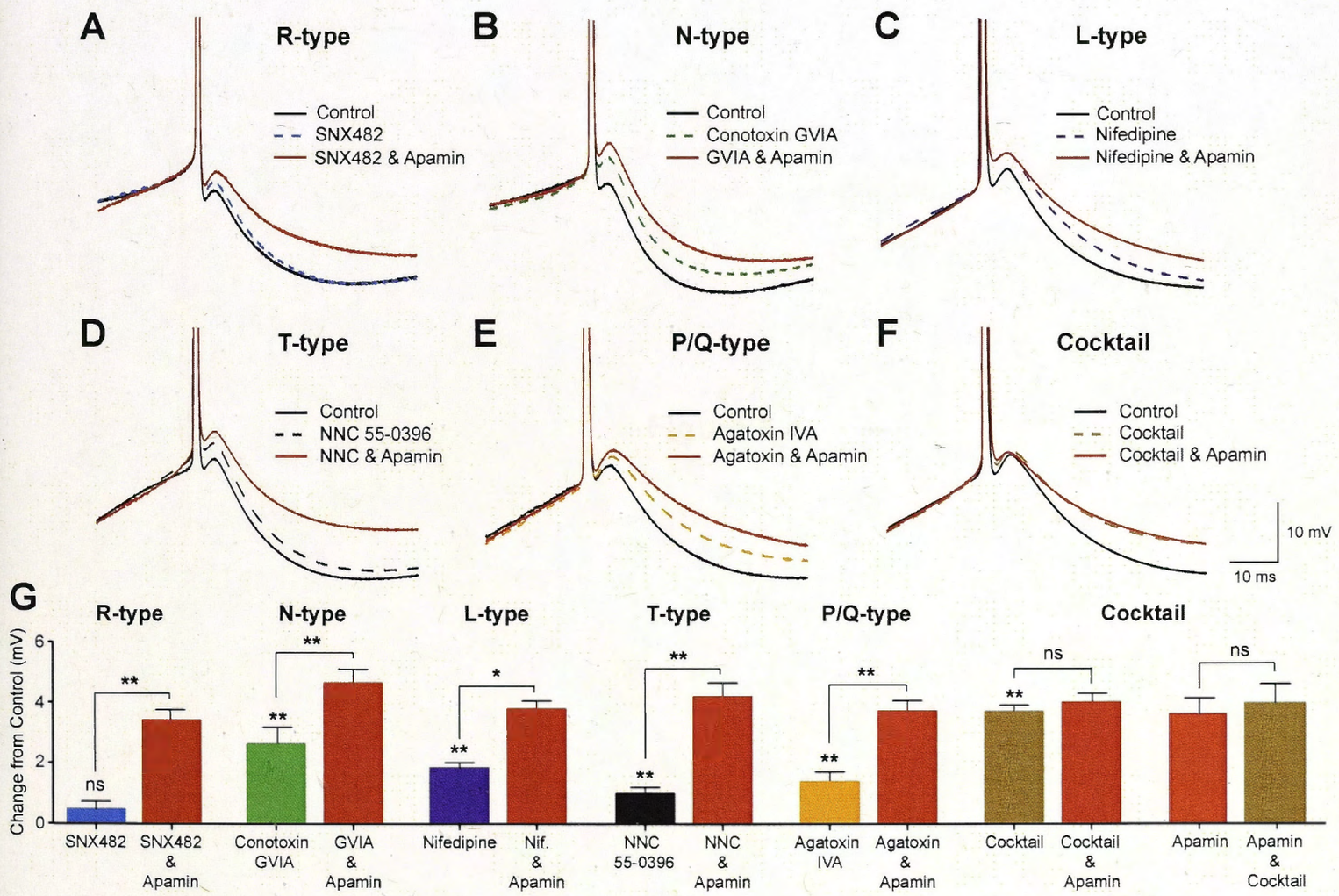
A
R-type
Control
SNX482
SNX482 & Apamin
B
N-type
Control
Conotoxin GVIA
GVIA & Apamin
C
L-type
Control
Nifedipine
Nifedipine & Apamin
D
T-type
Control
NNC 55-0396
NNC & Apamin
E
P/Q-type
Control
Agatoxin IVA
Agatoxin & Apamin
F
Cocktail
Control
Cocktail
Cocktail & Apamin
10 mV
10 ms
G
R-type
N-type
L-type
T-type
P/Q-type
Cocktail
Change from Control (mV)
0
2
4
6
ns
**
*
SNX482
SNX482 & Apamin
Conotoxin GVIA
GVIA & Apamin
Nifedipine
Nif. & Apamin
NNC 55-0396
NNC & Apamin
Agatoxin IVA
Agatoxin & Apamin
Cocktail
Cocktail & Apamin
Apamin
Apamin & Cocktail

Figure 4.4.

Figure 4.4. – R-type VDCCs are not expressed at the soma of L5 pyramidal neurons.

A, L5 pyramidal neuron filled with OGB-1. The black and yellow boxes indicate somatic and dendritic regions of interest (ROIs) during point scans. ***B,*** Point-scans of the ROIs shown in ***A*** during a single AP before and after wash in of SNX482. Solid line and shaded regions represent the mean ± SEM. ***C,*** Average peak $\Delta F/F$ at somatic and dendritic ROI before and after wash in of SNX482 (±S.E.M; n=5). ***D,*** Average % change in fluorescence after wash in of SNX482 at somatic and dendritic ROIs (±S.E.M; n=5).

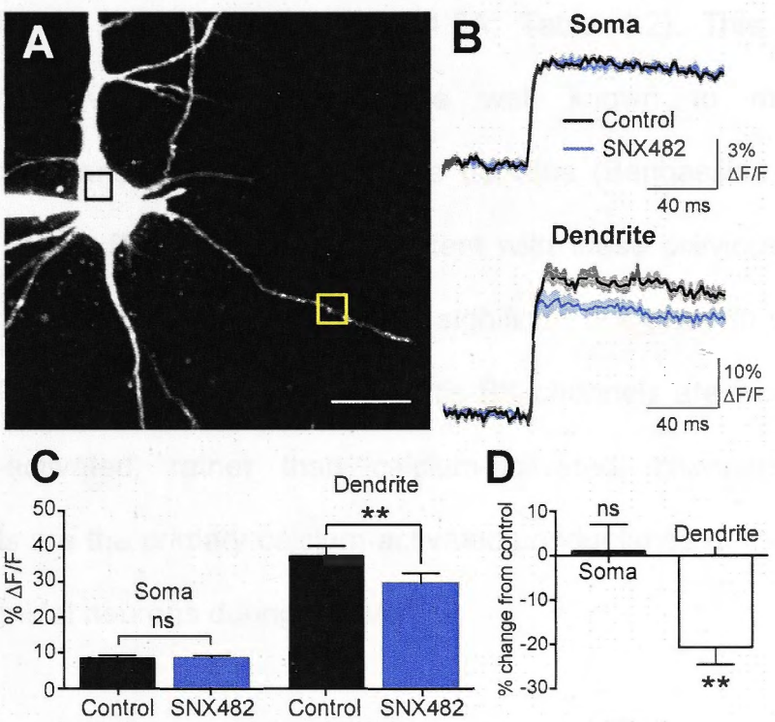
A
B
Soma
Control
SNX482
3%
ΔF/F
40 ms
Dendrite
10%
ΔF/F
40 ms
C
Dendrite
**
% ΔF/F
50
40
30
20
10
0
Soma
ns
Control
SNX482
Control
SNX482
D
ns
Dendrite
Soma
% change from control
10
0
-10
-20
-30
**

variety of VDCC subtypes, consistent with the idea that they are not tightly coupled to their calcium source. Furthermore, in contrast to SK channels in spines and dendrites, which are coupled solely to R-type VDCCs, SK channels mediating the mAHP at the soma of cortical L5 pyramidal neurons are activated by all known VDCCs sub-types except R-type.

Somatic BK channels do not require calcium influx for activation

Blocking R, N, L, T and P/Q type VDCCs did not lead to a significant increase in the width of somatic APs (Figure 4.5A; Table 4.2). This observation was surprising given BK channels are well known to mediate the fast afterhyperpolarisation (fAHP) in these neurons (Benhassine & Berger, 2005; Benhassine & Berger, 2009). Consistent with these previous studies, the BK antagonist paxilline (1 μM) led to a significant increase in AP width (Figure 4.5B). These data suggest that somatic BK channels are working primarily as voltage-activated, rather than calcium-activated, channels, and that SK channels are the primary calcium-activated conductance at the soma of cortical L5 pyramidal neurons during single APs.

Figure 4.5.

Figure 4.5. – Impact of VDCC antagonists and BK channel block on somatic APs.

A, Top, Somatic APs elicited by 200 ms positive current pulses in control (black) and a VDCC antagonist cocktail including antagonists for N, P/Q, T and L-type VDCCs (yellow). Bottom, Average half width of somatic APs in control (black) and the VDCC antagonist cocktail (yellow, n=6). ***B,*** Top, Somatic APs elicited by 200 ms positive current pulses in control (black) and the BK channel antagonist paxilline (green). Bottom, Average half width of somatic APs in control (black) and paxilline (green, n=5). ** denotes $p < 0.01$.

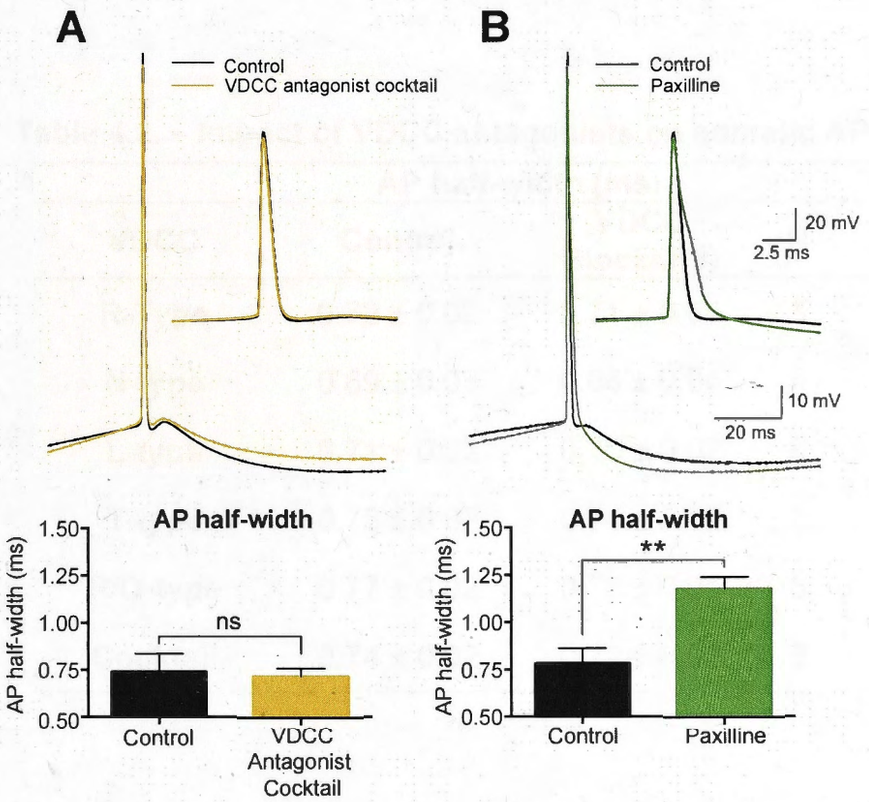
A
Control
VDCC antagonist cocktail
B
Control
Paxilline
20 mV
2.5 ms
10 mV
20 ms
AP half-width
AP half-width (ms)
1.50
1.25
1.00
0.75
0.50
ns
Control
VDCC Antagonist Cocktail
AP half-width
**
Control
Paxilline

Table 4.2. – Impact of VDCC antagonists on somatic AP half-width

	AP half-width (ms)			
VDCC	**Control**	**VDCC Blocker(s)**	**N**	**P-value**
R-Type	0.72 ± 0.02	0.71 ± 0.02	5	0.596
N-type	0.69 ± 0.05	0.66 ± 0.04	5	0.349
L-type	0.71 ± 0.02	0.70 ± 0.02	6	0.202
T-type	0.76 ± 0.02	0.74 ± 0.02	6	0.232
P/Q-type	0.77 ± 0.02	0.76 ± 0.01	6	0.319
Cocktail	0.74 ± 0.02	0.72 ± 0.02	6	0.403

Discussion

SK channel function during the somatic medium afterhyperpolarisation

SK channels contribute to the mAHP in many neuronal cell types, including L5 pyramidal neurons (Schwindt *et al.*, 1988; Faber & Sah, 2002; Womack & Khodakhah, 2003; Womack *et al.*, 2004), although this is controversial in CA1 pyramidal neurons (Stocker *et al.*, 1999; Gu *et al.*, 2008). The ability of low concentrations of both fast (OGB-1) and slow (EGTA) calcium buffers to inhibit the mAHP in L5 cortical pyramidal neurons suggests that the calcium influx driving activation of somatic SK channels is working within a microdomain rather than a nanodomain (Neher, 1998; Augustine *et al.*, 2003; Eggerman *et al.*, 2012), with a coupling distance greater than ~150 nm. Consistent with this idea we show that the SK-dependent component of the mAHP in L5 neurons is controlled by all known VDCC sub-types except R-type VDCCs, which aren't expressed at the soma.

The coupling between somatic SK channels and their calcium source in L5 neurons differs from that in other cell types, where the calcium source for SK channel activation during the mAHP has been linked to specific VDCC sub-types. For example, in midbrain dopaminergic neurons activation of SK channels during the mAHP is solely dependent on T-type VDCCs (Wolfart & Roepar, 2002), whereas only L-type channels are coupled to somatic SK channels in hippocampal pyramidal neurons (Marrion and Tavalin, 1998). The reason(s) for this difference between neuronal cell types, and why it is that SK

channels are weakly coupled to multiple calcium sources in L5 neurons, is unclear.

Finally, it is worth noting that our observation that low concentrations of the calcium indicator OGB-1 blocks the mAHP, increasing firing rate and promoting burst firing, raises the concern that the use of high-affinity calcium indicators to investigate network activity (Garaschuk *et al.*, 2006) may inadvertently influence neuronal excitability and thereby network dynamics.

BK channel function at the soma during the fast afterhyperpolarisation

None of the VDCC antagonists nor the VDCC antagonist cocktail had any impact on somatic APs, despite the finding that blocking BK channels increased AP width and abolished the fast AHP (Figure 4.4). BK channels, unlike SK channels, are both calcium and voltage dependent. Increases in intracellular calcium shift the activation curve of BK channels to more hyperpolarised, physiologically relevant, membrane potentials (Marty *et al.*, 1981, Latorre *et al.*, 1982; Cui *et al.*, 1997). The insensitivity of BK channels to VDCC antagonists is surprising given that strong activation of BK channels has previously been shown to require intracellular calcium concentrations in excess of 10 µM (Brenner *et al.*, 2000). Such changes in calcium concentration are only observed at sites very close to calcium sources such as VDCCs (Eilers *et al* 1995, Naraghi & Neher 1997, Tadross *et al* 2013). The absence of an effect of VDCC antagonists on AP width therefore suggests that BK channels in L5 pyramidal neurons are not tightly coupled to their calcium source. Furthermore, these observations suggest that voltage gating of BK channels at resting

calcium concentrations is sufficient to subserve the role BK channels play in controlling AP width in L5 pyramidal neurons. Such a conclusion, however, assumes the complete inhibition of calcium influx by the VDCC cocktail. While the observation that this cocktail could completely perturb somatic SK channel activation is consistent with this idea, a small percentage of active VDCCs channels could, in principle, be sufficient to preserve the activation of BK channels if they were coupled in nanodomains. While we think this is unlikely, at present this possibility cannot be ruled out.

In this chapter it has been shown that SK channels are loosely coupled to their calcium source, and controlled by calcium microdomains rather than nanodomains. This result is contrary to SK channel function in many other neuronal types. We also provide evidence that BK channels are also loosely coupled to their calcium source, also contrary to observations in other cells. The reason for these differences between L5 pyramidal neurons and other neuronal cell types is unclear.

CHAPTER 5: ON THE FUNCTION OF DENDRITIC SK CHANNELS DURING SPIKE-TIMING DEPENDENT PLASTICITY

INTRODUCTION

In the last decade there have been numerous demonstrations of SK channel activation in dendritic spines of cortical and hippocampal pyramidal neurons during EPSPs (Ngo-Anh *et al.*, 2005; Faber *et al.*, 2005; Bloodgood & Sabatini, 2007; Wang *et al.*, 2014). These studies have shown that excitatory synaptic input and consequential calcium influx into spines leads to SK channel activation, which acts to repolarizes the spine membrane potential reducing NMDAR activation by promoting magnesium block of NMDARs (Mayer *et al*, 1984; Nowak *et al.*, 1984). As a consequence, SK channels in spines constrain calcium influx through NMDARs, and thereby form part of a negative feedback loop controlling EPSP size and calcium influx during synaptic events (Ngo-Ahn *et al.*, 2005). As described in Chapter 3 of this thesis SK channels are also activated in spines and dendrites during bAPs, controlling calcium influx into these structures through VDCCs.

The capacity of SK channels to limit calcium influx during both EPSPs and bAPs is likely to have has consequences for the induction of synaptic plasticity, given the central role of calcium in this phenomenon (Yang *et al.*, 1999). Consistent with this idea, blocking SK channel activation, and thereby the impact of SK channels on NMDAR function, can promote and enhance LTP evoked by tetanic stimulation in hippocampal pyramidal (Behnisch & Reymann,

1998; Stackman *et al.*, 2002) and amygdala neurons (Faber *et al* 2005). As SK channels also influence calcium influx during bAPs, presumably by modulating AP width and/or amplitude in spines, it seems likely that SK channels will also influence the induction of spike-timing dependent synaptic plasticity (STDP). The influence of SK channels on STDP induction may not be limited to times when EPSPs and AP overlap. Sustained activation of dendritic SK channels by bAPs may suppress EPSPs evoked after APs, and thereby influence the timing window for induction of LTD.

This chapter investigates whether SK channel activation by bAPs can influence subsequently evoked EPSPs. We also investigate the influence of SK channel activation during bAPs on NMDAR activation and the impact this has on the induction of STDP.

METHODS

The function of dendritic SK channels during EPSPs was investigated with somatic whole-cell electrophysiology in cortical or hippocampal brain slices as outlined in Chapter 2.

Synaptic stimulation

In the majority of experiments EPSPs were evoked during recordings from synaptically coupled pairs of L5 pyramidal neurons. Paired recording was used principally because it offers the capacity to activate known inputs to L5 neurons from a homogeneous population. In addition, this experimental approach allowed stable recording of EPSPs for periods longer than an hour. Extracellular stimulation was used to evoke EPSPs in L2/3 and CA1 pyramidal neurons as paired recordings in these cells were either less stable (in layer 2/3 neurons) or difficult to establish (in hippocampal CA1 neurons). Due to the anatomy of the hippocampus extracellular stimulation is likely to predominately activate a homogenous set of inputs.

Neuronal selection was important for regularly obtaining recordings from connected L5 neurons. The highest success rate was during recordings from pairs of neurons that are within the same cortical column, separated by less than 50 µm in distance and greater than 50 µm deep in the slice. The chance of finding a synaptically connected pair was increased by making recordings from three or four neurons at the same time. To evaluate whether there was a connection between two given neurons, single APs were evoked in the putative

presynaptic neuron whilst monitoring the membrane potential in the putative postsynaptic neuron. An average of many repetitions was often needed to resolve unitary EPSPs due to their small size as well as the high proportion of failures.

During paired recording presynaptic APs were generated at a frequency of either 0.2 or 0.3 Hz. EPSPs were recorded for 15-30 minutes to confirm stability prior to the introduction of pharmacological compounds to the bathing solution or the induction of synaptic plasticity. Only recordings that were stable (less than 10% change in EPSP size) during the final 10 minutes of this baseline period were analysed. In addition, recordings were rejected if the input resistance of pre- or postsynaptic neurons, measured from the voltage response to 700 ms current steps of -50 pA amplitude, changed more than 10% during the course of the experiment.

For extracellular stimulation a custom-built theta glass bipolar extracellular stimulating electrode was used to evoke EPSPs in layer 2/3 and hippocampal CA1 pyramidal neurons. In these experiments Alexa Fluor 488 (Invitrogen) was dialysed into the neuron and Alexa 555 (Invitrogen) was added to the stimulating electrode solution. This allowed both the dendritic tree of the neuron and the tip of the stimulating electrode to be visualized using fluorescence microscopy. The tip of the stimulating electrode was placed within 10-15 µm of the dendrite (L2/3: basal; CA1: oblique) of the neuron of interest. EPSPs were generated at 0.1 Hz using a short negative current pulse (10-20 µA, 0.2 ms) from an isolated stimulator (World Precision Instruments). The stimulating

electrode was filled with 1M NaCl as this was found to significantly reduce the current required to evoke the desired postsynaptic response and thus reduced the stimulus artifact. The stimulus current was set to produce an EPSP of between 1 and 2 mV.

Artificial EPSPs

In some experiments current injection via the somatic whole-cell recording pipette was used to mimicking EPSP waveforms. These current injections had an exponential rise with a time constant of 0.3 ms and exponential decay with a time constant of 3 ms. These parameters were chosen to mimic spontaneous EPSCs measured at the soma of L5 neurons (Stuart & Sakmann, 1995).

AP-EPSP pairing & STDP induction protocols

To investigate the impact of APs on EPSPs, EPSPs were evoked alone or paired with postsynaptic APs evoked at different times before EPSP onset. Two different pairing protocols were used. Either APs were evoked 10 ms before EPSPs ("-10 ms" timing) in experiments on layer 2/3 or CA1 pyramidal neurons, or a range of AP timings was investigated (-10 ms, -20 ms, -50 ms and -100 ms) in paired recordings from L5 neurons. As a result, AP-EPSP pairing at -10 ms occurred every 20 seconds in experiments on L2/3 or CA1 pyramidal neurons, or every 16.7 or 25 seconds in paired recordings from L5 neurons. Postsynaptic APs alone were interleaved midway between EPSPs and digitally subtracted from the AP-EPSP waveform to reveal the paired EPSP (see below). For experiments on STDP, STDP was induced by 60 repetitions of single pre

and postsynaptic APs at 0.2 Hz (every 5 seconds) paired at a time interval of +10 or -10 ms.

Pharmacology

SK channels were blocked by apamin (100 nM; Sigma Aldrich) and NMDARs blocked by D(-)-2-amino-5-phosphono-pentanoic acid (D-AP5; 100 µM; Tocris Bioscience). Both agents were bath applied. Solution flow rate was 3-4 ml/min, leading to steady-state concentrations in the recording chamber within 5 minutes from the commencement of wash in.

Data analysis

For pairing experiments, the EPSP during AP-EPSP pairing, called the "paired EPSP", was isolated by digitally subtracting an AP evoked on its own from the AP-EPSP response. AP-EPSP pairing protocols were designed such that each EPSP, whether evoked alone or paired with a postsynaptic AP, was interleaved with a postsynaptic AP evoked on its own. The impact of pharmacological compounds or STDP induction was evaluated after 20-30 minutes. All data was analysed using Axograph X. Statistical significance between groups was evaluated with T-tests in either the paired or unpaired configuration as appropriate. Statistics were performed in Graphpad Prism 6. EPSPs were binned into five-minute periods, unless otherwise specified, and each period was averaged and expressed as the mean ± SEM.

RESULTS

Unitary EPSPs between synaptically connected pairs of L5 pyramidal neurons.

Somatic whole-cell patch-clamp recordings were performed from synaptically connected L5 pyramidal neurons. The probability of finding a connection in these experiments was ~0.2, similar to reports in other studies (Markram *et al.*, 1997a; Markram *et al.*, 1997b). Connection probability in brain slice preparations is likely to be an underestimate due to removal of inputs during the slicing procedure. In addition, the success rate is also experimenter dependent, as the depth from the slice surface and proximity of selected neurons to each other are key determinants in finding a synaptic connection; generally the deeper the selected neurons, the greater the probability of finding a connected pair. Synaptic responses usually displayed significant 'run up' or 'run down' immediately after obtaining a connection. Ten to twenty minutes were typically required before stable responses were observed, and recordings were only continued if stable responses were maintained throughout the entire time period of an experiment (usually 1-1.5 hours).

Effect of SK channel activation on EPSPs paired with bAPs

To investigate the impact of SK channel activation by bAPs on synaptic responses, unitary EPSPs in L5 neurons were evoked with and without preceding postsynaptic APs. In order to determine the impact of preceding postsynaptic APs on EPSPs, postsynaptic APs generated on their own were subtracted from the AP-EPSP waveform (see Methods). APs evoked 10 ms before EPSPs (-10 ms timing) were found to suppress EPSPs (Figure 5.1A-C).

Figure 5.1.

Figure 5.1. – SK channels suppress EPSPs during AP-EPSP pairing.

A, Schematic of the experimental approach and recording setup showing simultaneous whole-cell patch-clamp recording from synaptically connected L5 pyramidal neurons. APs in both neurons were paired in the postsynaptic (orange) before presynaptic (purple) configuration with -10 ms timing. ***B,*** Unpaired (black) and paired (blue) EPSPs in the postsynaptic neuron in the absence (top) and presence (bottom) of apamin at a timing of -10ms. ***C,*** Plot of the unpaired (black) and paired (blue) EPSPs over time. Each point represents the average of responses over 2.5 minutes (12 responses) ± SEM. ***D-F,*** Top: Pre- and postsynaptic APs during AP-EPSP pairing at -20 ms (***D***), -50 ms (***E***) and -100 ms (***F***). Bottom: Unpaired (black) and paired (blue) EPSPs in the absence (top) and presence (bottom) of apamin during AP-EPSP pairing at -20 ms (***D***), -50 ms (***E***) and -100 ms (***F***). ***G-I,*** Percentage change in the paired EPSP peak amplitude (***G***), integral (***H***), width at 25% (***I***) relative to the unpaired EPSP in control (black) and apamin (red) at the indicated AP-EPSP timings (n=6). * denotes $p < 0.05$, ** denotes $p < 0.01$, 'ns' not statistically significant.

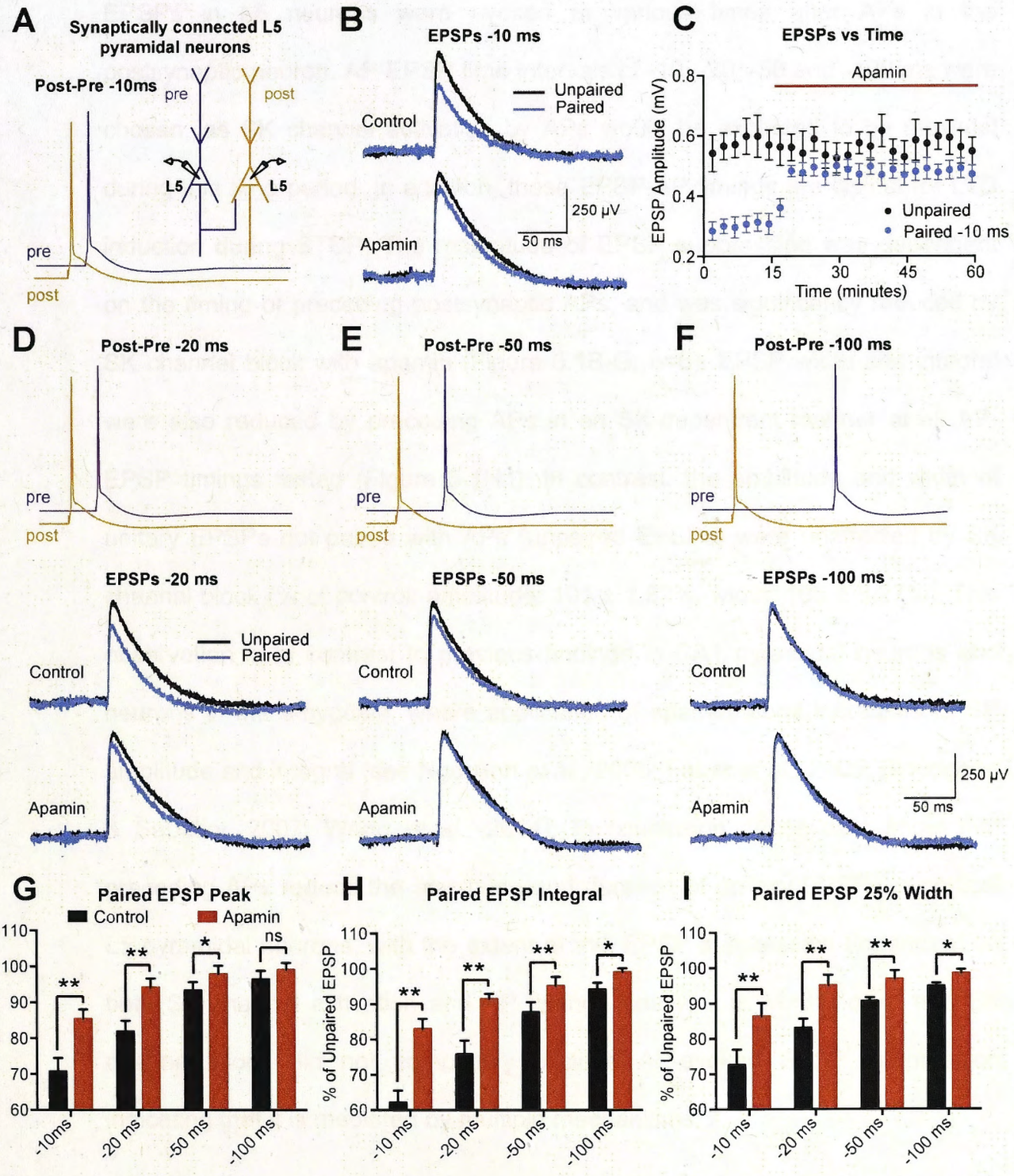
A
Synaptically connected L5 pyramidal neurons
Post-Pre -10ms
pre
post
L5
L5
pre
post
B
EPSPs -10 ms
Unpaired
Paired
Control
Apamin
250 µV
50 ms
C
EPSPs vs Time
Apamin
EPSP Amplitude (mV)
0.8
0.6
0.4
0.2
Unpaired
Paired -10 ms
0
15
30
45
60
Time (minutes)
D
Post-Pre -20 ms
pre
post
E
Post-Pre -50 ms
pre
post
F
Post-Pre -100 ms
pre
post
EPSPs -20 ms
Unpaired
Paired
Control
Apamin
EPSPs -50 ms
Control
Apamin
EPSPs -100 ms
Control
Apamin
250 µV
50 ms
G
Paired EPSP Peak
Control
Apamin
% of Unpaired EPSP
110
100
90
80
70
60
**
**
*
ns
-10ms
-20 ms
-50 ms
-100 ms
H
Paired EPSP Integral
% of Unpaired EPSP
**
**
**
*
-10 ms
-20 ms
-50 ms
-100 ms
I
Paired EPSP 25% Width
% of Unpaired EPSP
**
**
**
*
-10 ms
-20 ms
-50 ms
-100 ms

This EPSP suppression by APs required SK channel activation as it was largely occluded by introduction of apamin to the bath (Figure 5.1B,C). To investigate the dependence of AP-induced EPSP suppression on AP-EPSP timing unitary EPSPs in L5 neurons were evoked at various times after APs in the postsynaptic neuron. AP-EPSP time intervals of -10, -20, -50 and -100 ms were chosen, as SK channel activation by APs would be expected to be maximal during this time period. In addition, these EPSP-AP timings are typical for LTD induction during STDP. The magnitude of EPSP suppression was dependent on the timing of preceding postsynaptic APs, and was significantly reduced by SK channel block with apamin (Figure 5.1B-G; n=6). EPSP width and integral were also reduced by preceding APs in an SK-dependent manner at all AP-EPSP timings tested (Figure 5.1H,I). In contrast, the amplitude and width of unitary EPSPs not paired with APs (unpaired EPSPs) were unaffected by SK channel block (% of control; amplitude: 101 ± 1.82%, width: 105 ± 3.27%). This observation is in contrast to previous findings in CA1 pyramidal neurons and neurons in the amygdala, where application of apamin alone increases EPSP amplitude and integral (see Ngo-Anh *et al.*, 2005; Faber *et al.*, 2005; Bloodgood & Sabatini, 2007; Wang *et al.*, 2014). In conclusion, these data show that preceding APs reduce the amplitude and duration of unitary EPSPs in cortical L5 pyramidal neurons, with the extent of this EPSP suppression dependent on both SK channel activation and AP timing. Finally, it is worth noting that SK channel block did not completely occlude AP-evoked EPSP suppression indicating that it is mediated by multiple mechanisms.

SK channels in AP-evoked EPSP suppression in other neurons

In order to investigate whether SK mediated suppression of EPSPs by APs occurs in other types of neurons, we performed similar AP-EPSP pairing experiments on L2/3 and hippocampal CA1 pyramidal neurons. For these experiments a timing interval of -10 ms was chosen, as this timing had the greatest effect in L5 pyramidal neurons. For technical reasons (see Methods) EPSPs in these experiments were evoked by extracellular stimulation.

Consistent with our observations in L5 pyramidal neurons, preceding APs led to suppression of EPSPs in both L2/3 and CA1 pyramidal neurons (Figure 5.2). In both neuronal cell types suppression of EPSPs by preceding postsynaptic APs was significantly reduced by apamin, indicating a central role of SK channels (Figure 5.2; n=7 each). These observations show that AP evoked suppression of EPSPs by SK channels occurs in a range of neuronal cell types. Furthermore, as observed in L5 pyramidal neurons, EPSPs evoked on their own in L2/3 neurons were unaffected by SK channel block by apamin (Figure 5.2B). In contrast, unpaired EPSPs in CA1 pyramidal neurons were increased by blocking SK channels with apamin (Figure 5.2B), consistent with earlier work in this cell type (Ngo-Ahn *et al.*, 2005; Bloodgood & Sabatini, 2007). These data indicate that preceding APs suppressed EPSPs via a SK channel-dependent mechanism in a range of neuronal cell types, irrespective of whether SK channels influence the amplitude of EPSPs evoked on their own or not.

Figure 5.2.

Figure 5.2. – Impact of SK channel activation during AP-EPSP pairing in L2/3 and CA1 pyramidal neurons.

A, Unpaired (black) and paired (blue) EPSPs in the absence (left) and presence (right) of apamin using a timing of -10ms in L2/3 pyramidal (top) and CA1 pyramidal neurons (bottom). ***B,*** Average unpaired EPSP amplitude in the absence (black) and presence (red) of apamin in L2/3 pyramidal (top) and CA1 pyramidal neurons (bottom). ***C,*** Percentage change in the paired EPSP amplitude relative to the unpaired EPSP in the absence (black) and presence (red) of apamin in L2/3 pyramidal (top) and CA1 pyramidal neurons (bottom; n=7 for each). * denotes $p < 0.05$. 'ns' not statistically significant.

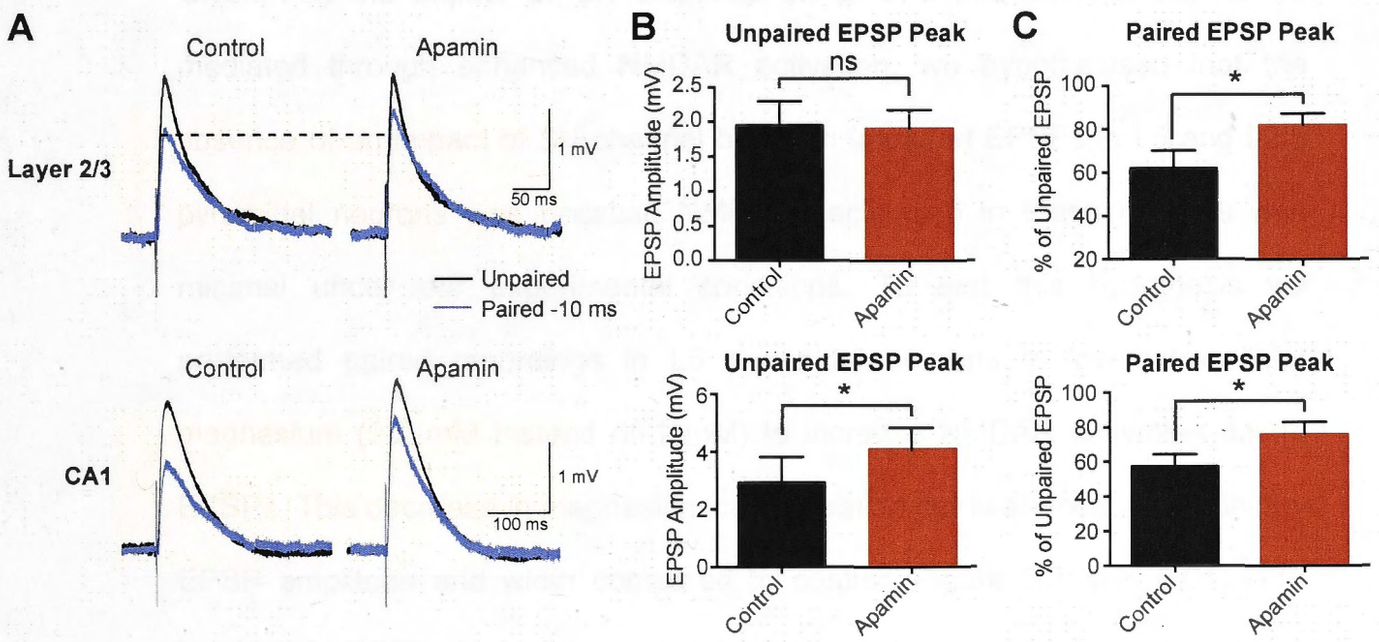
A
Control
Apamin
Layer 2/3
1 mV
50 ms
Unpaired
Paired -10 ms
Control
Apamin
CA1
1 mV
100 ms
B
Unpaired EPSP Peak
ns
EPSP Amplitude (mV)
2.5
2.0
1.5
1.0
0.5
0.0
Control
Apamin
Unpaired EPSP Peak
*
EPSP Amplitude (mV)
6
4
2
0
Control
Apamin
C
Paired EPSP Peak
*
% of Unpaired EPSP
100
80
60
40
20
Control
Apamin
Paired EPSP Peak
*
% of Unpaired EPSP
100
80
60
40
20
0
Control
Apamin

SK channel impact on unpaired EPSPs in L5 neurons

As indicated above, in both L5 and L2/3 pyramidal neurons there was no impact of SK channel block on unpaired EPSPs. This result is surprising given that SK channels are present in spines of L5 pyramidal neurons, and can be activated by bAPs (Chapter 3). In addition, previous work indicates that SK channels can influence EPSP amplitude in other cell types (Faber *et al* 2005; Ngo-Ahn *et al.*, 2005), consistent with our observation that SK channel block increased the amplitude of EPSP evoked on their own in CA1 neurons (Figure 5.2B, bottom). Given that the impact of SK channels on EPSPs has been shown to be mediated through enhanced NMDAR activation, we hypothesised that the absence of an impact of SK channel block on unpaired EPSPs in L5 and L2/3 pyramidal neurons was because NMDARs activation in these neurons was minimal under our experimental conditions. To test this hypothesis we performed paired recordings in L5 pyramidal neurons in low extracellular magnesium (0.2 mM instead of 1 mM) to increase NMDAR activation during EPSPs. This decrease in magnesium concentration led to an increase in unitary EPSP amplitude and width compared to control (Figure 5.3; $p < 0.01$). The increase in EPSP size was presumably due to a decrease in magnesium block of NMDARs, increasing their probability for activation (Mayer *et al.*, 1984; Nowak *et al.*, 1984). SK channel block by apamin under these conditions led to a further increase in EPSP amplitude (Figure 5.3; $p < 0.01$), and subsequent wash in of the NMDAR antagonist AP5 caused the EPSP amplitude to return to that observed in the presence of 1 mM magnesium (Figure 5.3; $p = 0.576$ compared to control; n=7). These data indicate that SK channel activation can

Figure 5.3.

Figure 5.3. – SK channels suppress EPSPs in L5 neurons under conditions of increased NMDAR activation.

A, Unpaired unitary EPSPs in L5 neurons recorded in control (1 mM magnesium, black), 0.2 mM magnesium (blue), subsequent addition of apamin (red) and then AP5 (green). ***B,*** Unpaired EPSP amplitude plotted over time in control (black), 0.2 mM magnesium (blue), after addition of apamin (red) and finally AP5 (green). Large symbols represent the 5-minute average, small dots individual data points. ***C,*** Percentage change in the unpaired EPSP relative to control under the indicated conditions (n=7). ** denotes $p < 0.01$, 'ns' denotes not significant.

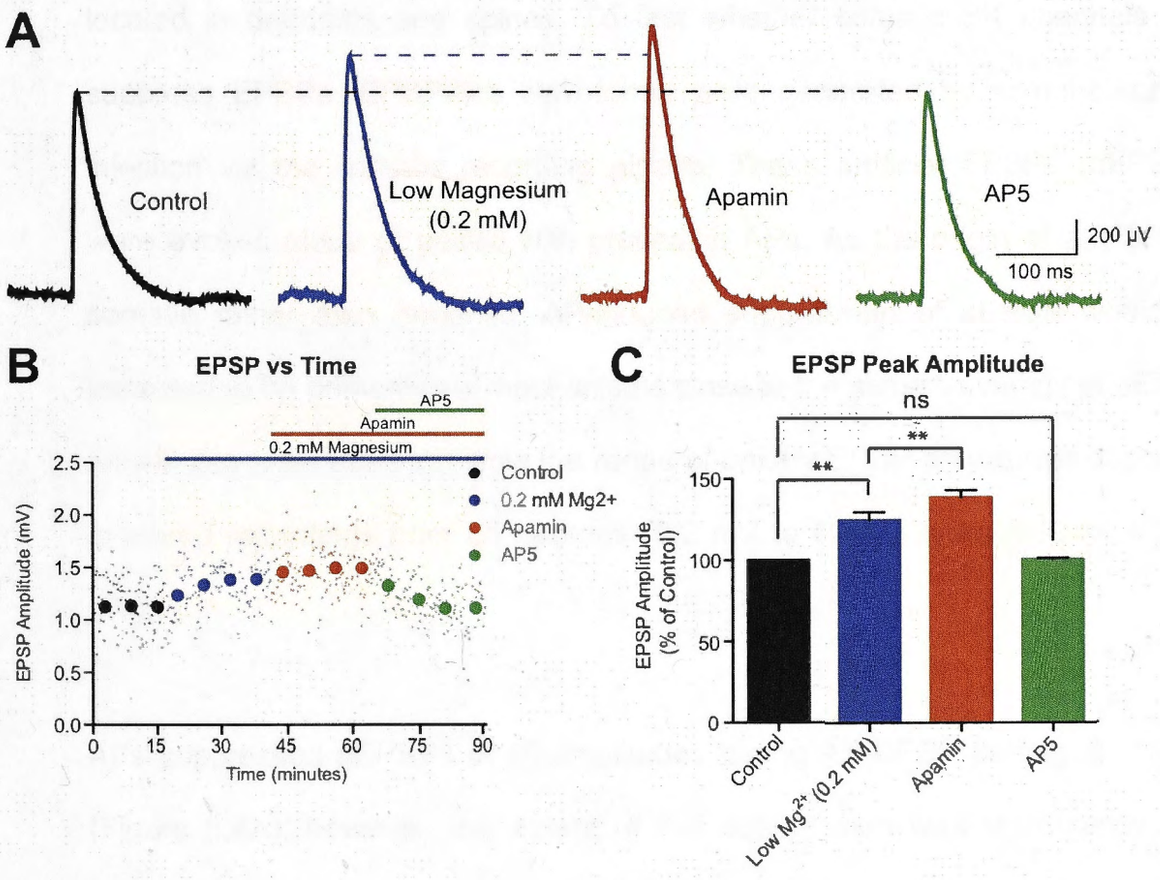
A
Control
Low Magnesium
(0.2 mM)
Apamin
AP5
200 µV
100 ms
B
EPSP vs Time
AP5
Apamin
0.2 mM Magnesium
Control
0.2 mM Mg2+
Apamin
AP5
EPSP Amplitude (mV)
Time (minutes)
C
EPSP Peak Amplitude
ns
**
**
EPSP Amplitude
(% of Control)
Control
Low Mg2+ (0.2 mM)
Apamin
AP5

constrain the amplitude of unitary EPSPs in L5 pyramidal neurons, but only under conditions where NMDAR activation is enhanced.

Involvement of somatic SK channels in EPSP suppression

Somatic SK channels play a role in generation of the mAHP in L5 neurons (Chapter 4) and thus may contribute to AP evoked EPSP suppression. Alternatively, suppression of EPSPs by APs may be mediated by SK channels located in dendrites and spines. To test whether somatic SK channels can suppress EPSPs, EPSP-like waveforms were generated by somatic current injection via the somatic recording pipette. These artificial EPSPs (aEPSPs) were evoked alone or paired with preceding APs. As the origin of aEPSPs is somatic rather than dendritic, AP-induced suppression of aEPSP would be expected to be primarily via mechanisms close to the soma. A variety of aEPSP amplitudes were used to mimic the range of unitary EPSP amplitudes observed in paired recordings from L5 neurons (0.2 mV to 5 mV; average: 0.84 ± 0.09 mV).

APs suppressed aEPSPs of all amplitudes during AP-EPSP pairing at -10 ms (Figure 5.4A), however, the extent of this suppression was significantly less than that observed during unitary EPSPs (aEPSP peak reduced to 86.2 ± 2.1% of control compared to 70.7 ± 3.8% for unitary EPSPs; n=6; $p < 0.01$; aEPSP amplitude 1 mV). Furthermore, the magnitude of AP-induced suppression of aEPSPs was similar to that observed during unitary EPSPs in the presence of apamin (unitary EPSP peak reduced to 85.5% ± 2.6 at -10 ms in apamin; n=6; $p = 0.77$). These data suggest that the SK-insensitive component of AP-induced

Figure 5.4.

Figure 5.4. – Amplitude dependence of AP-evoked suppression of somatic EPSPs by SK channels.

A, Unpaired (black) and paired (blue) artificial EPSPs (aEPSPs) generated by somatic current injection with amplitude of 0.2 mV (left), 1 mV (middle) and 2 mV (right) in the absence (top) and presence (bottom) of apamin for an AP timing of -10ms. Unpaired aEPSPs scaled to the same size to aid comparison. ***B-D,*** Percentage change in peak amplitude (***B***), integral (***C***) and width at 25% (***D***) of paired EPSPs relative to the unpaired EPSP in control (black) and apamin (red) for the indicated AP timings for 0.2 mV aEPSPs (left), 1 mV aEPSPs (middle) and 2 mV aEPSPs (right; n=6). * denotes $p < 0.05$, ** denotes $p < 0.01$, 'ns' denotes not significant.

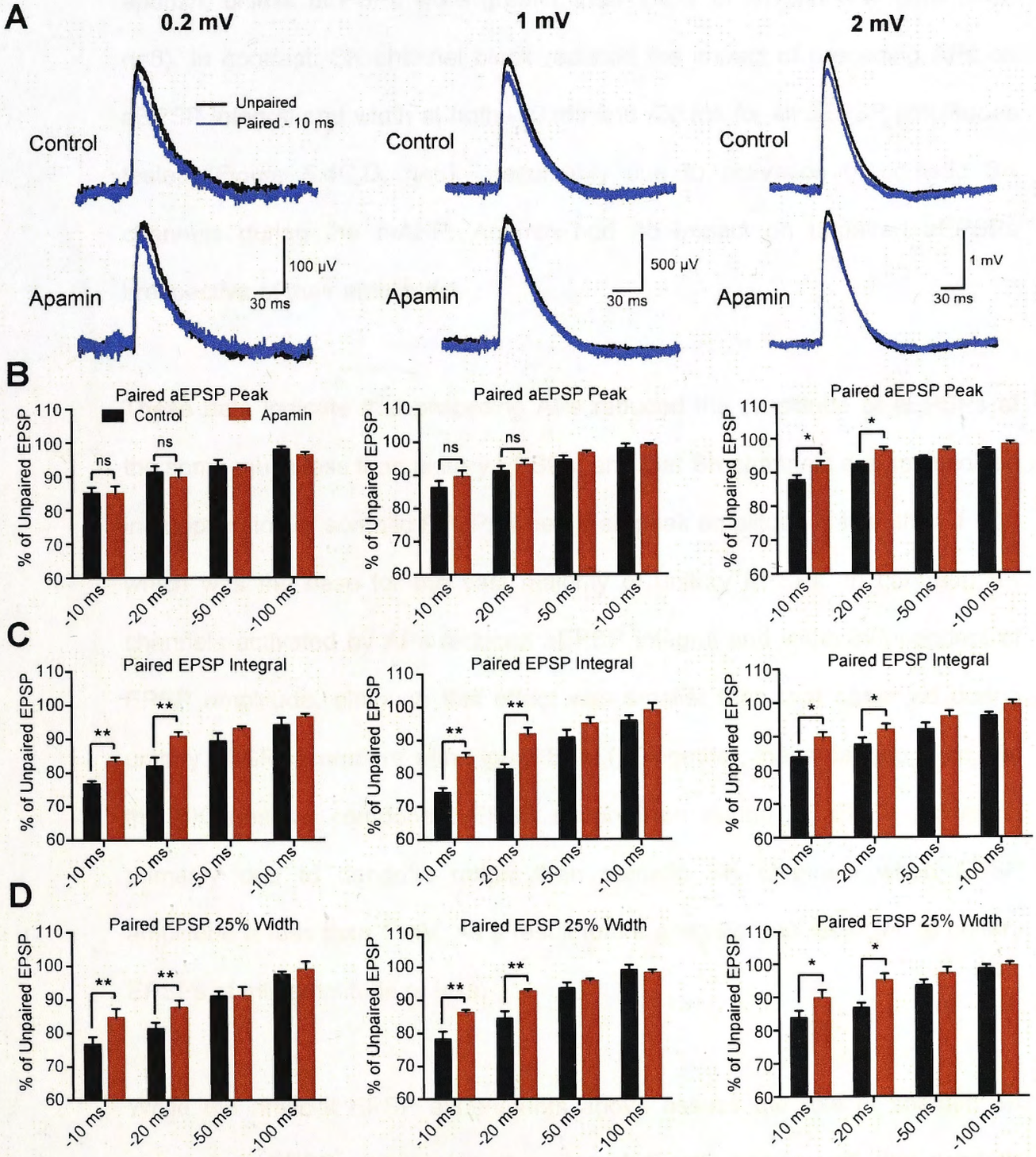
A
0.2 mV
1 mV
2 mV
Unpaired
Paired - 10 ms
Control
Apamin
100 µV
30 ms
500 µV
1 mV
B
Paired aEPSP Peak
Control
Apamin
% of Unpaired EPSP
ns
*
C
Paired EPSP Integral
**
*
D
Paired EPSP 25% Width
-10 ms
-20 ms
-50 ms
-100 ms

suppression is somatic in origin, and likely involves conductances other than SK channels that contribute to the mAHP in L5 pyramidal neurons. Consistent with this idea, the suppression of aEPSP peak by preceding APs was insensitive to apamin, unless aEPSPs were greater than 1 mV in amplitude (Figure 5.4B; n=6). In contrast, SK channel block reduced the impact of preceding APs on aEPSP integral and width at both -10 ms and -20 ms for all aEPSP amplitudes tested (Figure 5.4C,D, n=6), presumably due to activation of somatic SK channels during the mAHP. Apamin had no impact on unpaired aEPSPs irrespective of their amplitude.

These data indicate that preceding APs reduced the amplitude of aEPSPs at the soma much less than unitary EPSPs, and that SK channels are not involved in suppression of somatic EPSPs when their peak amplitude is less than 1 mV, which was the case for the vast majority of unitary EPSPs. In contrast, SK channels activated by APs reduced aEPSP integral and width independent of EPSP amplitude, although this effect was smaller than that observed during unitary EPSPs (compare with Figure 5.1H,I). Together, these data suggest that the SK-sensitive component EPSP suppression during AP-EPSP pairing is primarily due to dendritic rather than somatic SK channels when EPSP amplitude is less than 1 mV. As a result future analysis was restricted to unitary EPSPs of this amplitude or less.

While the artificial EPSP experiments above assess the role of somatic SK channels in EPSP suppression, they do not directly address whether dendritic SK channels suppress EPSPs. In order to isolate the impact of dendritic SK

channels on EPSP suppression, a low concentration (300 μM) of the fast calcium chelator BAPTA was added to the pipette solution. As shown in previous chapters, this concentration of BAPTA will perturb somatic SK channels (Chapter 4) whilst preserving the function of SK channels in dendrites (Chapter 3). Consistent with these earlier observations, low concentrations of BAPTA completely abolished the SK-mediated component of the mAHP (Figure 5.5A). Under these conditions preceding APs suppressed unitary EPSPs to a similar extent to that observed in the absence of BAPTA (Figure 5.5, compare with Figure 5.1). These data further support the idea that dendritic, rather than somatic, SK channels are critical for suppression of EPSP amplitude during AP-EPSP pairing in L5 pyramidal neurons.

NMDA receptors in SK channel dependent EPSP suppression

We investigated the role of NMDARs in AP-induced suppression of EPSPs in L5 pyramidal neurons (Figure 5.6). Consistent with a critical role of NMDARs, the presence of the NMDAR antagonist AP5 occluded the impact of SK channel block on the amplitude of the paired EPSP (Figure 5.6C; $p = 0.567$; n=5). SK channel block, however, still led to a reduction in AP-mediated suppression of EPSP integral and width under these conditions, consistent with this effect being mediated via somatic SK channels (Figure 5.6D,E; $p < 0.01$; n=5). Interestingly, block of NMDARs with AP5 enhanced AP-mediated suppression of EPSPs (Figure 5.7C-E; $p < 0.01$; n=5), suggesting that activation of NMDARs by preceding APs limits EPSP suppression. These data indicate that SK channel-dependent suppression during AP-EPSP pairing is primarily mediated though a reduction in NMDAR activation.

Figure 5.5.

Figure 5.5. – Block of somatic SK channels does not alter apamin-sensitive suppression of EPSPs during AP-EPSP pairing.

A, Postsynaptic AP evoked by a short positive current pulse (2 ms, 3 nA) in a L5 neuron with 300 µM BAPTA in the pipette solution (dashed) and after wash in of apamin (red), showing block of the SK-component of the mAHP at the soma by intracellular BAPTA. ***B,*** Unpaired (black) and paired (blue) EPSPs in L5 neurons in the absence (top) and presence (bottom) of apamin during AP-EPSP pairing at -10 ms in the presence of intracellular BAPTA. ***C,*** Plot of unpaired (black) and paired (blue) EPSP amplitude over time in the presence of intracellular BAPTA. Each point represents the 2.5 minute average (12 responses) ± SEM. ***D-F,*** Percentage change in the paired EPSP peak amplitude (***D***), integral (***E***), and width at 25% (***F***) relative to the unpaired EPSP in control (black) and apamin (red) for the indicated AP-EPSP timings in the presence of intracellular BAPTA (n=6). denotes $p < 0.05$, ** denotes $p < 0.01$.

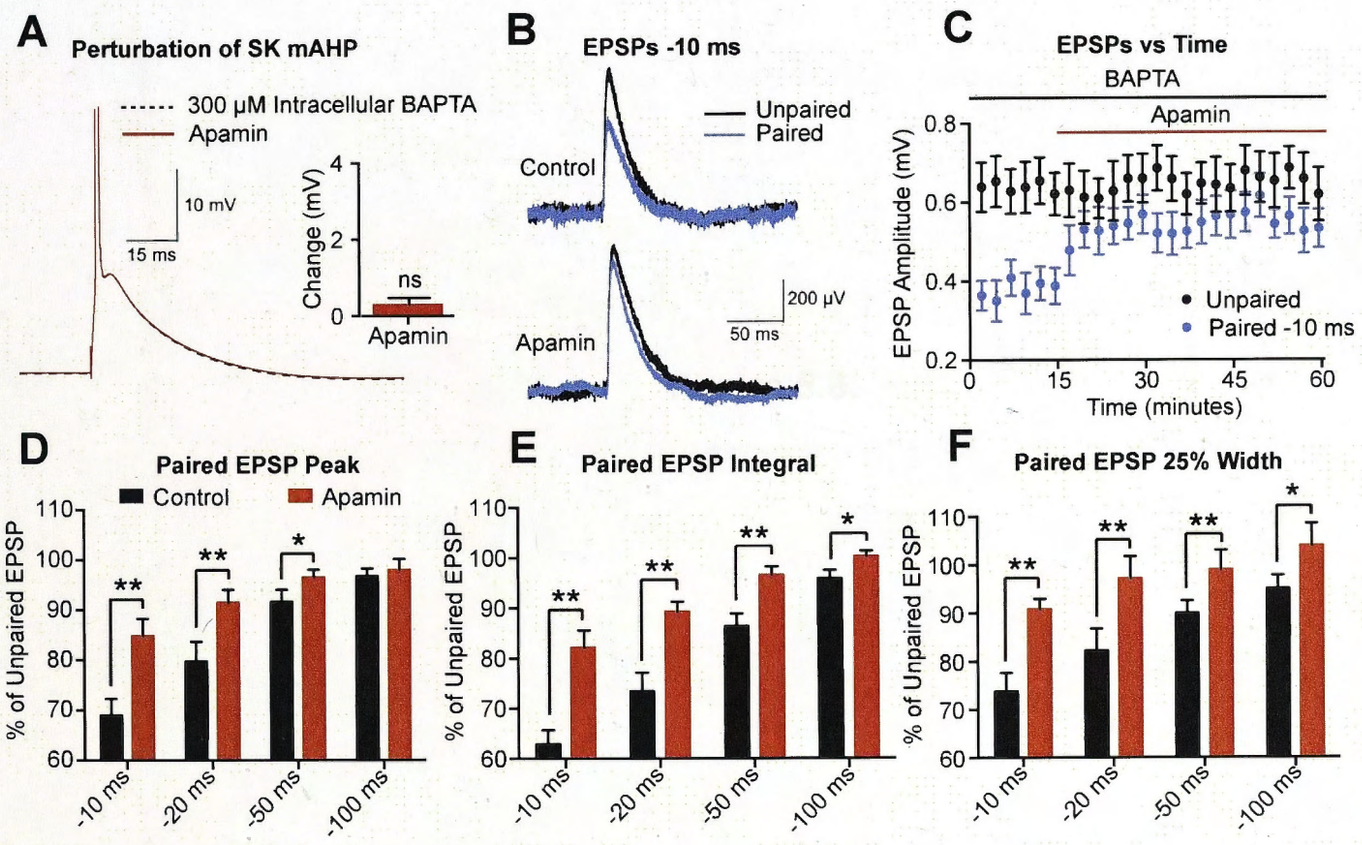
A
Perturbation of SK mAHP
300 µM Intracellular BAPTA
Apamin
10 mV
15 ms
Change (mV)
ns
Apamin
B
EPSPs -10 ms
Unpaired
Paired
Control
Apamin
200 µV
50 ms
C
EPSPs vs Time
BAPTA
Apamin
EPSP Amplitude (mV)
Unpaired
Paired -10 ms
Time (minutes)
D
Paired EPSP Peak
Control
Apamin
% of Unpaired EPSP
-10 ms
-20 ms
-50 ms
-100 ms
E
Paired EPSP Integral
F
Paired EPSP 25% Width

Figure 5.6.

Figure 5.6. – SK mediated suppression requires NMDARs.

A, Unpaired (black) and paired EPSPs in control conditions (left; blue), AP5 (middle; green), and apamin (right; red) for an AP-EPSP timing of -10 ms. **B,** Plot of unpaired (black) and paired EPSP amplitude (blue, green and red representing control, AP5 and apamin, respectively) over time for a representative neuron. Each point represents the 2.5 minute average (12 responses) ± SEM. ***C-E,*** Percentage change in the paired EPSP peak amplitude (***C***), integral (***D***) and width at 25% (***E***) relative to the unpaired EPSP in control (black), AP5 (green) and apamin (red; n=5). ** denotes $p < 0.01$, 'ns' denotes not significant.

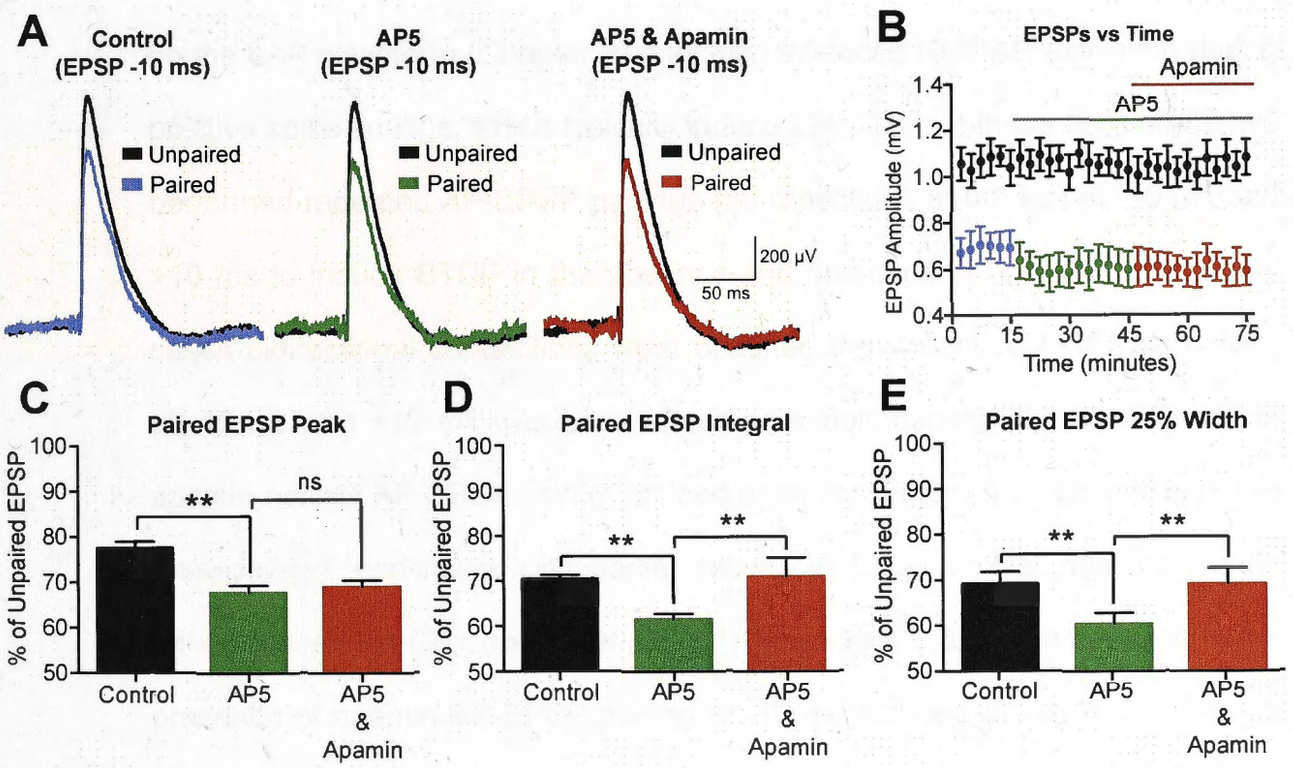
A
Control
(EPSP -10 ms)
AP5
(EPSP -10 ms)
AP5 & Apamin
(EPSP -10 ms)
Unpaired
Paired
Unpaired
Paired
Unpaired
Paired
200 µV
50 ms
B
EPSPs vs Time
Apamin
AP5
EPSP Amplitude (mV)
1.4
1.2
1.0
0.8
0.6
0.4
0
15
30
45
60
75
Time (minutes)
C
Paired EPSP Peak
% of Unpaired EPSP
100
90
80
70
60
50
**
ns
Control
AP5
AP5
&
Apamin
D
Paired EPSP Integral
% of Unpaired EPSP
**
**
Control
AP5
AP5
&
Apamin
E
Paired EPSP 25% Width
% of Unpaired EPSP
**
**
Control
AP5
AP5
&
Apamin

SK channels regulate spike timing-dependent synaptic plasticity

The extent of NMDAR activation is crucial for determining the threshold, magnitude and sign of STDP (Markram *et al.*, 1997; Bi & Poo, 1998; Sjostrom *et al.*, 2001; Kampa *et al.*, 2006). It has been shown previously that AP-EPSP pairing at negative spike timings can lead to LTD in many cell types. Given that our data is consistent with the idea that SK channels in L5 pyramidal neurons constrain NMDAR activation during AP-EPSP pairing, it seems likely this will influence the induction of LTD. In addition, the possible impact of SK channels on the bAP waveform (Chapter 3) may also influence NMDAR activation during positive spike timings, which typically induce LTP. To test these possibilities we performed repeated AP-EPSP pairings (60 repetitions at 0.2 Hz) at -10 ms and +10 ms to induce STDP in the absence and presence of apamin. As in many cases bidirectional connections were obtained the impact of AP-EPSP pairing at -10 ms and +10 ms was often observed simultaneously. In the absence of apamin neither AP-EPSP timing induced plasticity (Figure 5.7A,D; n=7 and n=5 respectively), consistent with earlier results in L5 pyramidal neurons during paired recordings (Sjostrom *et al.*, 2001; Kampa *et al.*, 2006). In contrast, in the presence of apamin AP-EPSP pairing at -10 ms induced robust LTD, whereas pairing at +10 ms induced robust LTP (Figure 5.7B,C,E,F; $p < 0.05$; n=6 and n=5 respectively). These data indicate that dendritic SK channels play a key role in regulating the induction of STDP in L5 pyramidal neurons during single AP-EPSP pairing, presumably through their capacity to limit NMDAR activation.

Figure 5.7.

Figure 5.7. – Impact of SK channels on spike timing dependent plasticity.

A-B, EPSPs before and after AP-EPSP pairing (left) in the absence (***A***) and presence (***B***) of apamin for AP-EPSP timing of - 10 ms. Right, EPSP amplitude over time. ***C,*** Average EPSP amplitude 20-30 minutes after pairing relative to that prior to pairing at -10 ms in the absence (black) and presence (red) of apamin (n=7). ***D-E,*** EPSPs before and after AP-EPSP pairing (left) in the absence (**D**) and presence (**E**) of apamin for AP-EPSP timing of +10 ms. Right, EPSP amplitude over time. ***F,*** Average EPSP amplitude (20-30 minutes after pairing) relative to that prior to AP-EPSP pairing at +10 ms in the absence (black) and presence (red) of apamin (n=5).

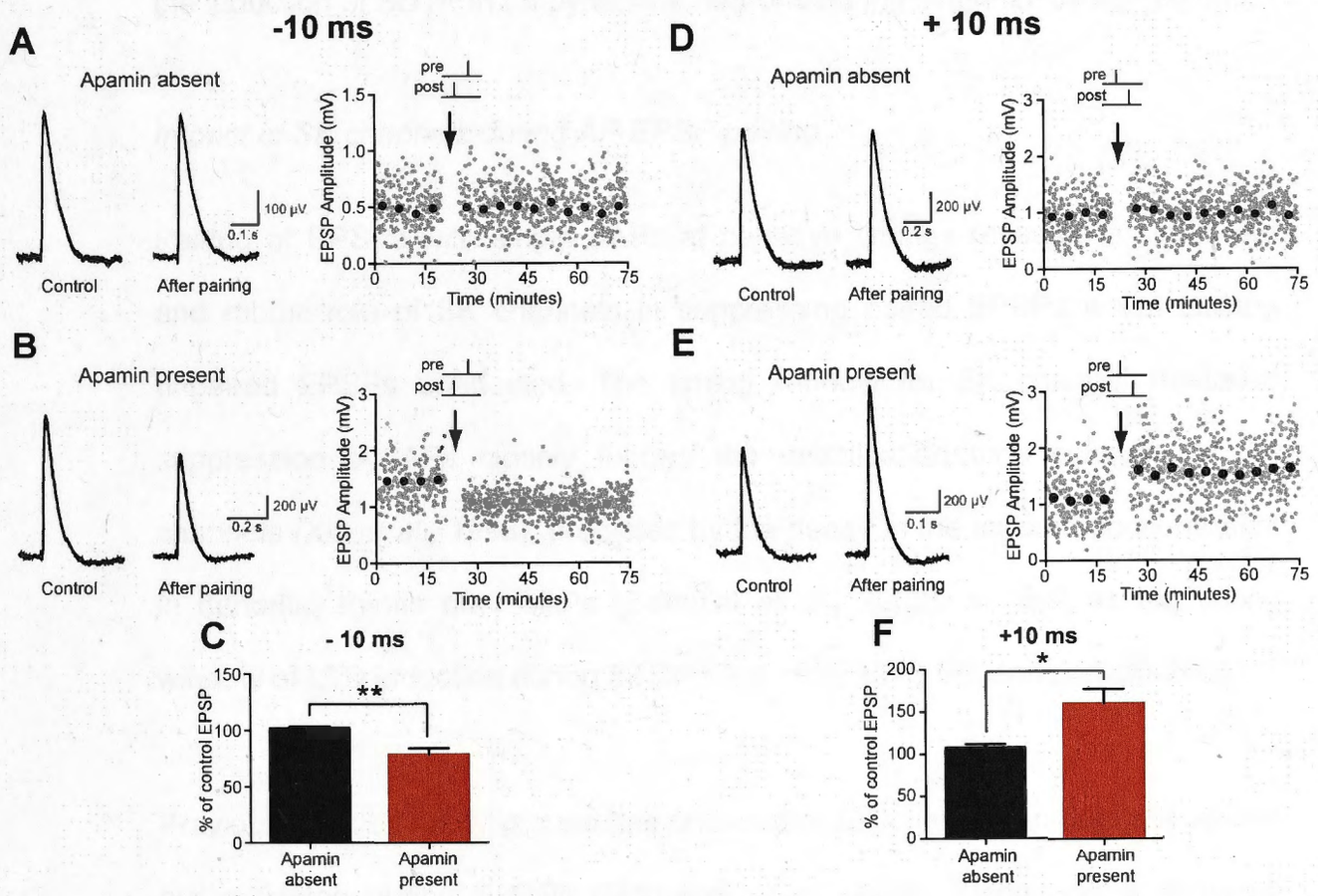
A
-10 ms
Apamin absent
100 µV
0.1 s
Control
After pairing
pre
post
EPSP Amplitude (mV)
Time (minutes)
B
Apamin present
200 µV
0.2 s
C
- 10 ms
**
% of control EPSP
Apamin absent
Apamin present
D
+ 10 ms
E
F
*

DISCUSSION

The data described in this chapter indicates that dendritic SK channels activated by preceding bAPs in L5 pyramidal neurons can reduce the amplitude, integral and duration of EPSPs. Similar observations were made in L2/3 cortical and CA1 hippocampal pyramidal neurons. This SK mediated effect was dependent on NMDAR activation and found to play a critical role in limiting the induction of SDTP in L5 pyramidal neurons during single EPSP-AP pairing.

Impact of SK channels during AP-EPSP pairing

Pairing of EPSPs with single bAPs at negative timings revealed a significant and robust role of SK channels in suppressing paired EPSPs whilst leaving unpaired EPSPs unaffected. The timing window for SK channel mediated suppression by APs closely follows the deactivation time constant of SK channels (Xia *et al.*, 1998), predicted by the decay in the calcium concentration in dendritic spines after bAPs (Sabatini *et al.*, 2002), as well as the timing window of LTD induction during STDP (Bi & Poo, 1998; Froemke *et al.*, 2005).

Previous work by many groups has shown that SK channels in dendritic spines are activated during EPSPs (Ngo-Ahn *et al.*, 2005; Bloodgood & Sabatini, 2007). This potassium current opposes the depolarization of the spine membrane, which in turn limits EPSP size and calcium influx by constraining activation of NMDARs (Faber *et al.*, 2005; Ngo-Anh *et al.*, 2005, Bloodgood & Sabatini, 2007). The lack of affect of SK channel blockade on unpaired EPSPs in L5 pyramidal neurons under control conditions was unexpected given the

results of Chapter 3, indicating that SKs are present in spines of these neurons, and previous studies showing an impact of SK channels on EPSPs in other cell types (Faber *et al* 2005; Ngo-Ahn *et al* 2005; Bloodgood & Sabatini, 2007). SK channel block also had no effect on the amplitude of unpaired EPSPs in L2/3 pyramidal neurons. Our observation that apamin could increase the amplitude of EPSPs in L5 pyramidal neurons when recorded in low extracellular magnesium suggests that significant NMDAR activation is required to observe an impact of SK channels on unpaired EPSPs in these neurons. The reason(s) for the difference in the ability of SK channels to control the amplitude of EPSPs in L5 and L2/3 pyramidal neurons in somatosensory cortex compared to other neuronal types is unclear, but presumably involves differences in NMDAR activation between cells types. NMDAR activation in L5 pyramidal neurons during unitary EPSPs is known to be very low, having no impact on EPSP amplitude or width (Figure 5.6; Markram *et al.*, 1997), which explains the lack of an impact of SK channel block on unpaired EPSPs in these cells.

Limited recruitment of NMDARs during unitary EPSPs in L5 neurons may be due to a number of factors. L5-L5 synaptic connections are dispersed onto many branches of the basal dendritic tree (Markram *et al.*, 1997). In contrast synapses recruited by extracellular stimulation may cluster on only a few branches, leading to a more localised dendritic depolarisation causing enhanced NMDAR activation. In addition, the low impedance of L5 dendrites will cause EPSPs to decay rapidly, limiting NMDAR recruitment; an affect augmented by conductances such as I_h. Although the expression of I_h is substantially lower in basal compared to distal apical dendrites (Lorincz *et al.*,

2002; Kole *et al.*, 2006; Nevian *et al.*, 2007), it still might be sufficient to significantly affect L5-L5 synaptic responses. Furthermore, some of the previous studies in CA1 pyramidal neurons have investigated SK channel effects on EPSPs at room temperature (Ngo-Ahn *et al.*, 2005; Lin *et al.*, 2008; Wang *et al.*, 2014). One would expect NMDAR activation to be greater at lower temperatures as EPSP duration is increased due to a higher R_m leading to a longer membrane time constant (Thompson *et al.*, 1985). It is also possible that SK channel densities are substantially higher, or their properties different, in other cell types compared to L5 and L2/3 pyramidal neurons.

While block of somatic SK channels using low concentrations of BAPTA confirmed that dendritic SK channels are involved in the suppression of EPSPs during AP-EPSP pairing, SK channels are also present at the soma where they contribute to generation of the mAHP. Using somatic current injections to mimic the voltage waveform of EPSPs at the soma (aEPSPs), an impact of somatic SK channels on the integral and width of paired aEPSPs was observed, confirming that the SK channels underlying the mAHP can influence evoked EPSPs. This effect on aEPSP integral and width, but not peak for EPSPs less than 1 mV in amplitude, was presumably mediated by the impact of somatic SK channels on the somatic membrane resistance. The absence of a significant impact on EPSP peak for small aEPSPs can be explained as EPSP peak is primarily determined by the local membrane capacitance and is relatively insensitive to changes in resting conductance, in contrast to EPSP integral and duration (Lev-Tov *et al.*, 1983; Thurbon *et al.*, 1998).

In contrast, the impact of somatic SK channels on the peak amplitude of paired aEPSPs greater than 1 mV is most likely due to recruitment of the persistent sodium current, I_{NaP} during the mAHP. During AP-EPSP pairing, the EPSP is generated during the afterdepolarisation (ADP) following the somatic AP. This slow voltage waveform maintains the depolarization of the soma above the resting membrane potential for ~30-40 ms after the AP, and is influenced by the SK-mediated component of the mAHP. During AP-EPSP pairing the somatic membrane potential is significantly depolarized above rest by 10-15 mV during pairing at -10 ms and 5-8 mV during pairing at -20 ms. Block of somatic SK channels will increase the depolarization during the ADP further. This would be expected to enhance recruitment of I_{NaP} during large EPSPs, boosting these events (Stuart & Sakmann, 1995; Carter *et al.*, 2012), and thereby reducing the suppression by APs in the presence of apamin. Although we have not directly tested this hypothesis, we think it a likely explanation of the data. Due to this putative effect of I_{NaP} on large EPSPs, evaluation of EPSP suppression during AP-EPSP pairing was restricted to synaptic responses that had amplitudes of 1 mV or less at the soma.

The influence of SK channels on NMDAR activation

The SK channel-mediated suppression of EPSPs by preceding APs was absent when NMDAR activation was blocked, indicating a role of NMDARs in this process. In addition, NMDAR block significantly increased suppression of EPSPs by APs (Figure 5.6), suggesting that AP-EPSP pairing increases NMDAR activation. Why does this happen? As discussed above, the ADP following the AP keeps the somatic membrane potential depolarized above rest.

This somatic depolarization would be expected to propagate with minimal attenuation into basal dendrites (Nevian *et al.*, 2007), the predominant location of L5-L5 connections (Markram *et al.*, 1997), and depolarise the postsynaptic membrane of activated synapses. As a result the ADP is likely to reduce the voltage-dependent magnesium block of NMDARs (Mayer *et al.*, 1984; Nowak *et al.*, 1984), enhancing their activation. Under these conditions it seems likely that SK channel activation by APs can constrain NMDAR activation, which presumably underlies their role in EPSP suppression.

Based on these data we envisage the following scenario during AP-EPSP pairing. Preceding APs reduce EPSPs evoked within a brief time window due to a reduction in driving force during the ADP as well as activation of SK channels. In addition, other, as yet unidentified, conductances suppressed EPSPs at the soma by approximately 15% (Figure 5.4). Enhanced NMDA activation of EPSPs evoked after APs reduces the extent of EPSP suppression, but is kept in check by SK channels. As a result, blocking dendritic SK channels increases NMDAR activation, reducing AP-induced EPSP suppression. This scenario indicates that the extent of NMDAR activation during AP-EPSP pairing is finely tuned and kept in balance by SK channels, consistent with their critical role in regulating the induction of STDP.

SK channels and spike-timing dependent plasticity

Spike timing-dependent plasticity, or STDP, is an important form of synaptic plasticity whereby the strength of synaptic connections is modified by the precise timing of synaptic input and postsynaptic APs or dendritic spikes (Markram *et al.*, 1997; Bi & Poo, 1998; Song *et al.*, 2000; Sjostrom *et al.*, 2001; Hardie & Spruston, 2009). The postsynaptic depolarization provided by postsynaptic APs or dendritic spikes enhances calcium influx both directly through VDCCs (Markram *et al.*, 1995; Larkum *et al.*, 1999; Kampa *et al.*, 2006; Nevian & Sakmann, 2006), and by reducing the magnesium block on NMDARs (Koester *et al.*, 1998; Schiller *et al.*, 1998; Kampa *et al.*, 2004; Kampa *et al.*, 2006). This enhanced calcium influx is crucial for the induction of STDP (Bi & Poo, 1998; Song *et al.*, 2000; Kampa *et al.*, 2006; Nevian & Sakmann, 2006). In pyramidal neurons, positive spike timings, where the postsynaptic AP occurs after the presynaptic AP, lead to LTP, whereas negative spike timings, where the postsynaptic AP occurs before the presynaptic AP, induce LTD (Markram *et al.*, 1997; Bi & Poo, 1998; Debanne *et al.*, 1998; Froemke *et al.* 2005). As shown in this chapter, negative spike timings in L5 pyramidal neurons suppress EPSPs largely due to activation of dendritic SK channels, which act to reduce NMDAR activation. Consistent with this idea, negative spike timings, causing LTD, are associated with calcium influx that is less than or equal to the sum of the calcium influx that occurs during the EPSP and AP alone (Koester & Sakmann 1998; Nevian & Sakmann, 2004, Nevian & Sakmann, 2006). On the other hand, positive spike timings are associated with calcium influx that is greater than the sum of the calcium influx during the EPSP and AP alone (Koester & Sakmann 1998; Nevian & Sakmann, 2004, Kampa & Stuart, 2006;

Nevian & Sakmann, 2006, Holbro *et al.*, 2010). This supralinear calcium increase presumably occurs because during positive spike timings the bAP depolarises active synapses, enhancing NMDAR activation by removal of magnesium block (Schiller *et al.*, 1998; Kampa *et al.*, 2004).

There have been numerous demonstrations of STDP induction using repeated low frequency (0.1-0.2 Hz) pairings of single pre and postsynaptic APs (Dan & Poo, 1998; Froemke *et al.*, 2005; Nevian *et al.*, 2006), where LTD and LTP are induced via negative or positive spike timings, respectively. In contrast, L5 pyramidal neurons generally require much more intense stimuli for plasticity to be induced. Whilst LTD can be induced between L2/3-L5 connections with single APs at positive timings at distal dendritic locations (Letzkus *et al.*, 2006), L5-L5 connections do not display plasticity using single APs regardless of the timing used (Sjostrom *et al.*, 2001; Kampa *et al.*, 2006). In contrast, multiple pre and postsynaptic AP pairings must be performed at high frequencies (20-40 Hz) in order to induce STDP (Markram *et al.*, 1997; Sjostrom & Hausser, 2006). In addition, STDP can also be induced at L5-L5 connections using postsynaptic AP bursts at a frequency that leads to generation of dendritic calcium spike (Kampa *et al*, 2006). Such strong stimuli are presumably required to provide sufficient postsynaptic depolarization and calcium influx, via either NMDARs and/or dendritic VDCCs (Kampa *et al.*, 2006, Letzkus *et al.*, 2006).

We show here that SK channels limit the induction of STDP presumably via their capacity to limit NMDAR activation and associated calcium influx during AP-EPSP pairing. As shown in Chapter 3, SK channels reduce calcium influx

via VDCCs into spines during bAPs, presumably by constraining the bAP waveform. In addition, as we show in this chapter, SK channel activation by preceding APs also reduces the amplitude of EPSPs, presumably due to reduced activation of NMDARs. The net effect is that SK channels limit calcium influx during single AP-EPSP pairing at both positive and negative times. This acts to constrain the induction of both LTP and LTD, which can only be observed after SK channel block (Figure 5.7).

Despite differences in the mechanisms involved in the induction of LTD and LTP during STDP, a threshold level of dendritic calcium influx is thought to be required for STDP induction (Yang *et al.*, 1999; Zucker *et al.*, 1999, Sjostrom *et al.*, 2004). As we show here, SK channels, by constraining calcium influx, play a key role in regulating the induction of STDP in L5 pyramidal neurons. To what extent SK channels also influence the STDP threshold and/or timing window during dendritic regenerative events, such as NMDA or dendritic calcium spikes, is yet to be determined.

CHAPTER 6: GENERAL DISCUSSION

Cortical neurons receive thousands of excitatory inputs, typically onto dendritic spines. Through a variety of dendritic mechanisms these inputs are integrated to generate an action potential. The action potential not only propagates orthodromically, to release neurotransmitter, but also antidromically into the dendritic tree. Antidromic or backpropagating APs (bAPs) provide an important retrograde electrical signal to the synapses about the output of the neuron. The properties of bAPs are of interest as they are key determinants of dendritic excitability and also critical for the induction of some forms of synaptic plasticity. In Chapter 3, we illustrated that small conductance calcium-activated potassium channels (SK channels) constrain calcium influx into dendrites and spines, presumably through regulation of the amplitude and/or width of the bAP waveform. We also identified that dendritic SK channels are tightly coupled to R-type VDCCs, which are the sole calcium source for SK channel activation by bAPs. In contrast, Chapter 4 demonstrated that somatic SK channels are loosely coupled to all known VDCC subtypes, except R-type VDCCs. This loose coupling means that the impact of SK channels on the firing properties of L5 neurons is easily perturbed by exogenous calcium buffers, and may represent a means by which the firing properties of these cells are manipulated under different physiological (or pathological) conditions. Chapter 5 shows that dendritic SK channels activated by preceding bAPs can suppress EPSPs and thereby constrain spike timing-dependent plasticity, presumably through regulation of NMDAR and possibly VDCC activation. In this final chapter we discuss some of the questions and issues that arise from these results, such as

the consequences of differential coupling of somatic and dendritic SK channels with their calcium sources, the role of SK channels in STDP and dendritic regenerative events, the influence of spine compartmentalisation, and future questions resulting from this research.

Dendritic versus somatic SK channels and coupling to calcium sources

There is a clear difference between how somatic and dendritic SK channels interact with their calcium source(s). SK channels in dendrites are tightly coupled in calcium nanodomains and are estimated to be within 25 and 50 nm from their calcium source (Chapter 3; Faber *et al.*, 2005; Ngo-Ahn *et al.*, 2005). In contrast, somatic SK channels display loose coupling (Chapter 4), where the calcium influx driving SK channel activation works within a microdomain greater than 150 nm. Such loose coupling at the soma is important to consider when introducing exogenous calcium buffers into L5 pyramidal neurons given that perturbation of the mAHP can have significant effects on firing properties (Chapter 4).

The differential coupling distances of dendritic and somatic SK channels to their respective calcium sources may give insights into their sensitivity for calcium. In both calcium nanodomains and microdomains, the magnitude and speed of the calcium signal is inversely related to the distance between the calcium source and the calcium-dependent effector (Neher, 1986). The peak calcium concentration in nanodomains is at least 10 times higher than in microdomains, with the rise and decay of the calcium signal taking nanoseconds in nanodomains and milliseconds for microdomains (Neher, 1986; Neher, 1998).

For an effector to be sensitive to a single calcium source within a nanodomain, particularly in the presence of other calcium sources located only 100-200 nm away, it must have a low affinity. In contrast, effectors located further from their calcium source must have a high affinity, as they need to bind calcium after the concentration has decreased due to diffusion and equilibration within the cellular compartment. These data suggest that the affinity of somatic and dendritic SK channels for calcium is likely to be different.

The calcium sensitivity of SK channels can be regulated by phosphorylation and dephosphorylation of calmodulin by the kinase CK2 and phosphatase PP2A, respectively (Bildl *et al.*, 2004; Allen *et al.*, 2007). There has also been a recent report suggesting that PKC can also lead to modulation of SK (Buchanan *et al.*, 2010), but the site of action is unknown. When calmodulin is fully dephosphorylated, SK channel affinity is high (EC_{50} ~0.3 μM). Conversely, fully phosphorylated calmodulin confers much lower calcium affinity (EC_{50} ~2 μM) (Bildl *et al.*, 2004; Allen *et al.*, 2007). Based on these observations it seems likely that dendritic SK-linked calmodulin is phosphorylated, giving dendritic and spine SK channels low affinity for calcium and thereby forcing them to work in nanodomains. In contrast, somatic SK-linked calmodulin is likely to be dephosphorylated, and as a result SK channels at the soma would have a high affinity for calcium allowing them to work in microdomains. While the phosphorylation state of calmodulin at different locations in neurons is unknown, our data predicts that it is likely to be different at the soma and dendrites of L5 neurons, which would be expected to impact other processes known to depend on calmodulin and could be tested experimentally.

The activation of M1 receptors and the subsequent activation of CK2 or PKC has been shown to perturb SK channel function in CA1 pyramidal neurons, indicating that SK-linked calmodulin at dendritic locations is not fully phosphorylated in these neurons (Buchanan *et al.*, 2010; Giessel & Sabatini, 2010). This suggests that a proportion of SK channels in spines in these cells are in a high affinity state. Differences in the phosphorylation state of SK channels may involve modulation by neurotransmitters such as acetylcholine (Buchanan *et al.*, 2010; Giessel & Sabatini, 2010) and noradrenaline (Maingret *et al.*, 2008). Nanodomain control of dendritic SK channels also allows modulation to occur at the site of the calcium source. In striatal MSNs, activation of dopaminergic D_2 receptors leads to modulation of R-type VDCCs, the likely calcium source for SK channels in these neurons, in a PKA dependent manner (Higley & Sabatini, 2010). SK modulation at the soma via modulation of their calcium source is yet to be demonstrated, but is less likely given the range of different VDCCs involved.

Dendritic SK channels and synaptic plasticity

The impact of dendritic SK channels on STDP in L5 pyramidal neurons (Chapter 5) is presumably via regulation of calcium influx for both LTP and LTD. As a result, dendritic SK channels set a threshold for the induction of STDP in these neurons, similar to neurons in the amygdala (Faber *et al.*, 2005) and CA1 pyramidal neurons (Behnisch & Reymann 1997; Stackman *et al.*, 2002). In addition to their role in plasticity induction, dendritic SK channels in CA1 pyramidal neurons are also thought to be involved in plasticity "expression", with changes in synaptic strength associated with SK channel internalisation

(Lin *et al.*, 2008; Lin *et al.*, 2010). It is unclear whether dendritic SK channels are modified in a similar way during STDP expression in L5 pyramidal neurons.

SK channels and dendritic regenerative events

The work in this thesis has used relatively weak activity and stimuli to activate SK channels, as occurs during single APs and EPSPs. Physiological activity in cortical neurons is often more intense leading to the generation of a variety of non-linear regenerative events such as dendritic calcium and NMDA spikes both *in vitro* (Larkum *et al.* 1999; Schiller *et al.*, 2000; Kampa *et al.*, 2006b; Larkum *et al.*, 2009) and *in vivo* (Lavzin *et al.*, 2012; Smith *et al.*, 2013). The large depolarisations associated with these events, caused by calcium influx in some cases, often facilitate high frequency (200-300 Hz) bursts of APs at the soma leading to a large increase in intracellular calcium (Palmer *et al.*, 2012; Smith *et al.*, 2013), and potentially the induction of plasticity (Kampa *et al.*, 2006; Hardie & Spruston, 2009). The capacity of SK channels to influence active dendritic events has largely not been investigated, although it has been shown that they can influence dendritic plateau potentials in CA1 pyramidal neurons (Cai *et al.*, 2004). Wider functional roles of SK channels are anticipated given the large increases in calcium triggered as a consequence of regenerative dendritic activity.

Spine compartmentalization and dendritic SK channel function

Even though there is no direct evidence presented here, it is likely the SK-mediated EPSP suppression by APs (Chapter 5) occurs in dendritic spines,

probably within the spine head. This idea is supported by evidence from immunohistochemistry showing that dendritic SK channels in pyramidal neurons are mainly localised to dendritic spines (Ngo-Ahn *et al.*, 2005; Lin *et al.*, 2008; Lin *et al.*, 2010). In addition, there is functional evidence supporting tight co-localisation between SK channels and their calcium source during synaptic events (Faber *et al.*, 2005; Ngo-Ahn *et al.*, 2005; Wang *et al.*, 2014).

A recent study provides evidence for compartmentalization of GABAergic inhibition in individual spines, which not only affected excitatory synaptic responses but also calcium influx during bAPs (Chiu *et al.*, 2013). These results suggest that modulation of SK channels at the level of individual spines may work in a similar way. SK channels can be modulated directly by the activation of multiple intracellular pathways controlled by M1 muscarinic (Buchannan *et al* 2010; Giessel and Sabatini 2010), and noradrenergic receptors (Maingret *et al.*, 2008), as well as indirectly through modulation of R-type VDCCs via D_2 dopaminergic receptors (Higely & Sabatini, 2012) and internalised from the plasma membrane via the activation of β_2 adrenergic receptors (Faber & Sah, 2008). Given the critical role of SK channels in regulating the induction of STDP (Chapter 5), the modulation of SK channel function in individual spines by any of the above mechanisms could in principle modulate STDP with single synapse specificity.

Future Investigations

There are three major results presented in this thesis. One, that bAP-evoked calcium transients are influenced by dendritic SK channels, possibly by

modulation of the bAP waveform (Chapter 3). Two, that dendritic and somatic SK channels are differentially coupled to their calcium sources (Chapter 4). Three, that dendritic SK channels supress EPSPs during AP-EPSP pairing and thereby influence the induction of spike timing-dependent plasticity (Chapter 5). These findings highlight the diverse functions of SK channels in neurons and prompt further investigations.

The influence of SK channels on bAP-evoked calcium influx is likely to occur through modification of the bAP waveform. It is unclear whether this is due to an effect on bAP width and/or amplitude. In addition, it is unclear whether such an effect can occur in individual spines or whether the observed effect on bAPs is distributed along an entire dendritic branch. As changes in calcium influx do not give direct information on changes in the underlying voltage response, future experiments could investigate this using voltage imaging with voltage-sensitive dyes. In addition, it would be of interest to investigate the impact of modulation of SK channels in individual spines on bAPs and STDP. This could be achieved through the use of caged neuromodulators known to modulate SK channel function, such as caged carbachol to activate M1 receptors.

In our experiments showing that dendritic SK channel activation causes suppression of EPSPs during AP-EPSP pairing (Chapter 5), the absolute requirement for bAPs is unclear. While there is good reason to believe that bAPs are crucial, the afterdepolarisation (ADP) following somatic APs and its influence on NMDAR activation complicates the interpretation of these data. To determine the relative importance of bAPs versus the somatic ADP in these

experiments, somatic current injections could be used to produce ADP-like voltage waveforms at the soma without eliciting an AP. These artificial ADPs could be paired with EPSPs to investigate their impact on NMDAR activation and SK channel effects. This experiment can be used to determine whether SK channel activation during bAPs, versus activation purely during the EPSP itself, is critical for AP-induced EPSP suppression during AP-EPSP pairing. Furthermore, the precise location of SK channel activation in this phenomenon is unclear. Although this effect is likely to occur in the spine head rather than the main dendrite, direct interrogation of calcium influx in spines and dendrites could be used to investigate this issue.

The impact of SK channels on bAP-evoked calcium influx was greatest at more distal dendritic locations (Chapter 3). Furthermore, it is known that NMDAR activation during EPSPs is also greatest at more distal locations due to an impedance gradient present in fine dendrites (Branco & Hausser, 2011). Taken together, these observations suggest that the effects of dendritic SK channel activation on STDP are likely to be dependent on the distance of active synapses from the soma. Given that the L5-L5 connections studied here synapse between 80-130 µm from the soma (Markram *et al.*, 1997b), the influence of SK channels on STDP induction may be greater for more distal synapses versus more proximal synapses. Multiphoton photolysis of caged glutamate could be utilised to test this prediction as it allows the experimenter complete control over the location of the active synapse being studied. Alternatively, distance dependent differences could also be investigated by seeing whether there is a correlation between the amount of STDP induced

(with both positive and negative timings) and somatic EPSP kinetics. A sample size larger than the one present in this study would be required for this type of analysis.

Conclusions

It is clear the SK channel function is both complex and diverse in L5 pyramidal neurons. Although initially thought to activate relatively slowly, results in this thesis have demonstrated that SK channels activate fast enough to influence fast electrical events such as bAPs. In addition, the investigations into SK channel function during unitary EPSPs have revealed important differences between L5 pyramidal neurons and other neuronal cell types where SK channel function has been investigated previously. Finally, the observations presented in this thesis point to a critical role of SK channels in modulating synaptic function and plasticity, potentially at the level of individual spines. The next step will be to determine to what extent these observations can be extended to the intact brain *in vivo*, and how SK channel activation regulates brain function in the awake behaving animal.

REFERENCES

Abbott LF & Nelson SB. (2000). Synaptic plasticity: taming the beast. *Nat Neurosci* **3 Suppl,** 1178-1183.

Acker CD, Yan P & Loew LM. (2011). Single-voxel recording of voltage transients in dendritic spines. *Biophysical Journal* **101,** L11-13.

Aiba A, Kano M, Chen C, Stanton ME, Fox GD, Herrup K, Zwingman TA & Tonegawa S. (1994). Deficient cerebellar long-term depression and impaired motor learning in mGluR1 mutant mice. *Cell* **79,** 377-388.

Allen D, Fakler B, Maylie J & Adelman JP. (2007). Organization and regulation of small conductance Ca2+-activated K+ channel multiprotein complexes. *J Neurosci* **27,** 2369-2376.

Alvarez VA & Sabatini BL. (2007). Anatomical and physiological plasticity of dendritic spines. *Annu Rev Neurosci* **30,** 79-97.

Antic SD. (2003). Action potentials in basal and oblique dendrites of rat neocortical pyramidal neurons. *J Physiol* **550,** 35-50.

Araya R, Jiang J, Eisenthal KB & Yuste R. (2006). The spine neck filters membrane potentials. *Proceedings of the National Academy of Sciences of the United States of America* **103,** 17961-17966.

Araya R, Nikolenko V, Eisenthal KB & Yuste R. (2007). Sodium channels amplify spine potentials. *Proceedings of the National Academy of Sciences of the United States of America* **104,** 12347-12352.

Augustine GJ, Santamaria F & Tanaka K. (2003). Local calcium signaling in neurons. *Neuron* **40,** 331-346.

Ballesteros-Merino C, Watanabe M, Shigemoto R, Fukazawa Y, Adelman JP & Lujan R. (2014). Differential subcellular localization of SK3-containing channels in the hippocampus. *The European Journal of Neuroscience* **39,** 883-892.

Ballesteros-Yanez I, Benavides-Piccione R, Elston GN, Yuste R & DeFelipe J. (2006). Density and morphology of dendritic spines in mouse neocortex. *Neuroscience* **138,** 403-409.

Barria A & Malinow R. (2005). NMDA receptor subunit composition controls synaptic plasticity by regulating binding to CaMKII. *Neuron* **48,** 289-301.

Bartlett TE, Bannister NJ, Collett VJ, Dargan SL, Massey PV, Bortolotto ZA, Fitzjohn SM, Bashir ZI, Collingridge GL & Lodge D. (2007). Differential roles of NR2A and NR2B-containing NMDA receptors in LTP and LTD in the CA1 region of two-week old rat hippocampus. *Neuropharmacology* **52,** 60-70.

Behnisch T & Reymann KG. (1998). Inhibition of apamin-sensitive calcium dependent potassium channels facilitate the induction of long-term potentiation in the CA1 region of rat hippocampus in vitro. *Neuroscience letters* **253,** 91-94.

Bekkers JM. (2000). Distribution and activation of voltage-gated potassium channels in cell-attached and outside-out patches from large layer 5 cortical pyramidal neurons of the rat. *J Physiol* **525 Pt 3,** 611-620.

Bekkers JM, Richerson GB & Stevens CF. (1990). Origin of variability in quantal size in cultured hippocampal neurons and hippocampal slices. *Proceedings of the National Academy of Sciences of the United States of America* **87,** 5359-5362.

Bender VA, Bender KJ, Brasier DJ & Feldman DE. (2006). Two coincidence detectors for spike timing-dependent plasticity in somatosensory cortex. *J Neurosci* **26,** 4166-4177.

Benhassine N & Berger T. (2005). Homogeneous distribution of large-conductance calcium-dependent potassium channels on soma and apical dendrite of rat neocortical layer 5 pyramidal neurons. *The European Journal of Neuroscience* **21,** 914-926.

Benhassine N & Berger T. (2009). Large-conductance calcium-dependent potassium channels prevent dendritic excitability in neocortical pyramidal neurons. *Pflugers Arch* **457,** 1133-1145.

Berger T, Larkum ME & Luscher HR. (2001). High I(h) channel density in the distal apical dendrite of layer V pyramidal cells increases bidirectional attenuation of EPSPs. *J Neurophysiol* **85,** 855-868.

Bi GQ & Poo MM. (1998). Synaptic modifications in cultured hippocampal neurons: dependence on spike timing, synaptic strength, and postsynaptic cell type. *J Neurosci* **18,** 10464-10472.

Bildl W, Strassmaier T, Thurm H, Andersen J, Eble S, Oliver D, Knipper M, Mann M, Schulte U, Adelman JP & Fakler B. (2004). Protein kinase CK2 is coassembled with small conductance Ca(2+)-activated K+ channels and regulates channel gating. *Neuron* **43,** 847-858.

Birtoli B & Ulrich D. (2004). Firing mode-dependent synaptic plasticity in rat neocortical pyramidal neurons. *J Neurosci* **24,** 4935-4940.

Bliss TV & Collingridge GL. (1993). A synaptic model of memory: long-term potentiation in the hippocampus. *Nature* **361,** 31-39.

Bliss TV & Lomo T. (1973). Long-lasting potentiation of synaptic transmission in the dentate area of the anaesthetized rabbit following stimulation of the perforant path. *J Physiol* **232,** 331-356.

Bloedel JR & Llinas R. (1969). Neuronal interactions in frog cerebellum. *J Neurophysiol* **32,** 871-880.

Bloodgood BL, Giessel AJ & Sabatini BL. (2009). Biphasic synaptic Ca influx arising from compartmentalized electrical signals in dendritic spines. *PLoS Biol* **7,** e1000190.

Bloodgood BL & Sabatini BL. (2005). Neuronal activity regulates diffusion across the neck of dendritic spines. *Science* **310,** 866-869.

Bloodgood BL & Sabatini BL. (2007). Nonlinear regulation of unitary synaptic signals by CaV(2.3) voltage-sensitive calcium channels located in dendritic spines. *Neuron* **53,** 249-260.

Bonhoeffer T & Yuste R. (2002). Spine motility. Phenomenology, mechanisms, and function. *Neuron* **35,** 1019-1027.

Bradley J, Luo R, Otis TS & DiGregorio DA. (2009). Submillisecond optical reporting of membrane potential in situ using a neuronal tracer dye. *J Neurosci* **29,** 9197-9209.

Branco T & Hausser M. (2011). Synaptic Integration Gradients in Single Cortical Pyramidal Cell Dendrites. *Neuron* **69,** 885-892.

Brenner R, Jegla TJ, Wickenden A, Liu Y & Aldrich RW. (2000). Cloning and functional characterization of novel large conductance calcium-activated potassium channel beta subunits, hKCNMB3 and hKCNMB4. *The Journal of Biological Chemistry* **275,** 6453-6461.

Buchanan KA, Petrovic MM, Chamberlain SEL, Marrion NV & Mellor JR. (2010). Facilitation of Long-Term Potentiation by Muscarinic M1 Receptors Is Mediated by Inhibition of SK Channels. *Neuron* **68,** 948-963.

Cai X, Liang CW, Muralidharan S, Kao JP, Tang CM & Thompson SM. (2004). Unique roles of SK and Kv4.2 potassium channels in dendritic integration. *Neuron* **44,** 351-364.

Cajal SR. (1911). *Histologie du systeme nerveux de l'homme et des vertebres.* Paris: Maloine.

Carter AG & Sabatini BL. (2004). State-dependent calcium signaling in dendritic spines of striatal medium spiny neurons. *Neuron* **44,** 483-493.

Carter BC, Giessel AJ, Sabatini BL & Bean BP. (2012). Transient Sodium Current at Subthreshold Voltages: Activation by EPSP Waveforms. *Neuron* **75,** 1081-1093.

Chang HT. (1952). Cortical neurons with particular reference to the apical dendrites. *Cold Spring Harbor symposia on quantitative biology* **17,** 189-202.

Chiu CQ, Lur G, Morse TM, Carnevale NT, Ellis-Davies GC & Higley MJ. (2013). Compartmentalization of GABAergic inhibition by dendritic spines. *Science* **340,** 759-762.

Christie BR, Magee JC & Johnston D. (1996). The role of dendritic action potentials and Ca2+ influx in the induction of homosynaptic long-term depression in hippocampal CA1 pyramidal neurons. *Learn Mem* **3,** 160-169.

Coetzee WA, Amarillo Y, Chiu J, Chow A, Lau D, McCormack T, Moreno H, Nadal MS, Ozaita A, Pountney D, Saganich M, Vega-Saenz de Miera E & Rudy B. (1999). Molecular diversity of K+ channels. *Annals of the New York Academy of Sciences* **868,** 233-285.

Colbert CM & Johnston D. (1996). Axonal action-potential initiation and Na+ channel densities in the soma and axon initial segment of subicular pyramidal neurons. *J Neurosci* **16,** 6676-6686.

Collingridge GL, Kehl SJ & McLennan H. (1983). Excitatory amino acids in synaptic transmission in the Schaffer collateral-commissural pathway of the rat hippocampus. *J Physiol* **334,** 33-46.

Cornelisse LN, van Elburg RA, Meredith RM, Yuste R & Mansvelder HD. (2007). High speed two-photon imaging of calcium dynamics in dendritic spines: consequences for spine calcium kinetics and buffer capacity. *PLoS One* **2,** e1073.

Coss RG & Perkel DH. (1985). The function of dendritic spines: a review of theoretical issues. *Behavioral and Neural Biology* **44,** 151-185.

Crick F. (1982). Do spines twitch? *Trends Neurosci* **5,** 44-46.

Cui J, Cox DH & Aldrich RW. (1997). Intrinsic voltage dependence and Ca2+ regulation of mslo large conductance Ca-activated K+ channels. *The Journal of General Physiology* **109,** 647-673.

Cull-Candy S, Kelly L & Farrant M. (2006). Regulation of Ca2+-permeable AMPA receptors: synaptic plasticity and beyond. *Current Opinion in Neurobiology* **16,** 288-297.

Dan Y & Poo MM. (2004). Spike timing-dependent plasticity of neural circuits. *Neuron* **44,** 23-30.

Debanne D, Boudkkazi S, Campanac E, Cudmore RH, Giraud P, Fronzaroli-Molinieres L, Carlier E & Caillard O. (2008). Paired-recordings from synaptically coupled cortical and hippocampal neurons in acute and cultured brain slices. *Nature Protocols* **3,** 1559-1568.

Debanne D, Gahwiler BH & Thompson SM. (1994). Asynchronous pre- and postsynaptic activity induces associative long-term depression in area

CA1 of the rat hippocampus in vitro. *Proceedings of the National Academy of Sciences of the United States of America* **91,** 1148-1152.

Debanne D, Gahwiler BH & Thompson SM. (1998). Long-term synaptic plasticity between pairs of individual CA3 pyramidal cells in rat hippocampal slice cultures. *J Physiol* **507 (Pt 1),** 237-247.

Edgerton JR & Reinhart PH. (2003). Distinct contributions of small and large conductance Ca2+-activated K+ channels to rat Purkinje neuron function. *J Physiol* **548,** 53-69.

Egger V, Svoboda K & Mainen ZF. (2005). Dendrodendritic synaptic signals in olfactory bulb granule cells: local spine boost and global low-threshold spike. *J Neurosci* **25,** 3521-3530.

Eggermann E, Bucurenciu I, Goswami SP & Jonas P. (2012). Nanodomain coupling between Ca(2) channels and sensors of exocytosis at fast mammalian synapses. *Nat Rev Neurosci* **13,** 7-21.

Eilers J, Callewaert G, Armstrong C & Konnerth A. (1995). Calcium signaling in a narrow somatic submembrane shell during synaptic activity in cerebellar Purkinje neurons. *Proceedings of the National Academy of Sciences of the United States of America* **92,** 10272-10276.

Elston GN & DeFelipe J. (2002). Spine distribution in cortical pyramidal cells: a common organizational principle across species. *Progress in Brain Research* **136,** 109-133.

Emptage N, Bliss TV & Fine A. (1999). Single synaptic events evoke NMDA receptor-mediated release of calcium from internal stores in hippocampal dendritic spines. *Neuron* **22,** 115-124.

Engbers JD, Anderson D, Asmara H, Rehak R, Mehaffey WH, Hameed S, McKay BE, Kruskic M, Zamponi GW & Turner RW. (2012). Intermediate conductance calcium-activated potassium channels modulate summation of parallel fiber input in cerebellar Purkinje cells. *Proceedings of the National Academy of Sciences of the United States of America* **109,** 2601-2606.

Engert F & Bonhoeffer T. (1999). Dendritic spine changes associated with hippocampal long-term synaptic plasticity. *Nature* **399,** 66-70.

Faber ES. (2010). Functional interplay between NMDA receptors, SK channels and voltage-gated Ca2+ channels regulates synaptic excitability in the medial prefrontal cortex. *J Physiol* **588,** 1281-1292.

Faber ES, Delaney AJ, Power JM, Sedlak PL, Crane JW & Sah P. (2008). Modulation of SK channel trafficking by beta adrenoceptors enhances excitatory synaptic transmission and plasticity in the amygdala. *J Neurosci* **28,** 10803-10813.

Faber ES, Delaney AJ & Sah P. (2005). SK channels regulate excitatory synaptic transmission and plasticity in the lateral amygdala. *Nat Neurosci* **8,** 635-641.

Faber ES & Sah P. (2002). Physiological role of calcium-activated potassium currents in the rat lateral amygdala. *J Neurosci* **22,** 1618-1628.

Faber ES & Sah P. (2003). Ca2+-activated K+ (BK) channel inactivation contributes to spike broadening during repetitive firing in the rat lateral amygdala. *J Physiol* **552,** 483-497.

Fakler B & Adelman JP. (2008). Control of K(Ca) channels by calcium nano/microdomains. *Neuron* **59,** 873-881.

Fiala FC, Harris, K. M. (1999). *Dendrite Structure*, vol. 1. Oxford University Press, New York.

Finch EA & Augustine GJ. (1998). Local calcium signalling by inositol-1,4,5-trisphosphate in Purkinje cell dendrites. *Nature* **396,** 753-756.

Froemke RC, Poo MM & Dan Y. (2005). Spike-timing-dependent synaptic plasticity depends on dendritic location. *Nature* **434,** 221-225.

Gainey MA, Hurvitz-Wolff JR, Lambo ME & Turrigiano GG. (2009). Synaptic scaling requires the GluR2 subunit of the AMPA receptor. *J Neurosci* **29,** 6479-6489.

Garaschuk O, Milos RI & Konnerth A. (2006). Targeted bulk-loading of fluorescent indicators for two-photon brain imaging in vivo. *Nature Protocols* **1,** 380-386.

George MS, Abbott LF & Siegelbaum SA. (2009). HCN hyperpolarization-activated cation channels inhibit EPSPs by interactions with M-type K(+) channels. *Nat Neurosci* **12,** 577-584.

Gerdeman GL, Ronesi J & Lovinger DM. (2002). Postsynaptic endocannabinoid release is critical to long-term depression in the striatum. *Nat Neurosci* **5,** 446-451.

Giessel AJ & Sabatini BL. (2011). Boosting of Synaptic Potentials and Spine Ca Transients by the Peptide Toxin SNX-482 Requires Alpha-1E-Encoded Voltage-Gated Ca Channels. *PLoS One* **6,** e20939.

Golding NL, Jung HY, Mickus T & Spruston N. (1999). Dendritic calcium spike initiation and repolarization are controlled by distinct potassium channel subtypes in CA1 pyramidal neurons. *J Neurosci* **19,** 8789-8798.

Golding NL & Spruston N. (1998). Dendritic sodium spikes are variable triggers of axonal action potentials in hippocampal CA1 pyramidal neurons. *Neuron* **21,** 1189-1200.

Gu N, Hu H, Vervaeke K & Storm JF. (2008). SK (KCa2) channels do not control somatic excitability in CA1 pyramidal neurons but can be activated by dendritic excitatory synapses and regulate their impact. *J Neurophysiol* **100,** 2589-2604.

Gu N, Vervaeke K, Hu H & Storm JF. (2005). Kv7/KCNQ/M and HCN/h, but not KCa2/SK channels, contribute to the somatic medium after-hyperpolarization and excitability control in CA1 hippocampal pyramidal cells. *J Physiol* **566,** 689-715.

Gulledge AT, Carnevale NT & Stuart GJ. (2012). Electrical advantages of dendritic spines. *PLoS One* **7,** e36007.

Gulledge AT, Park SB, Kawaguchi Y & Stuart GJ. (2007). Heterogeneity of phasic cholinergic signaling in neocortical neurons. *J Neurophysiol* **97,** 2215-2229.

Gulledge AT & Stuart GJ. (2005). Cholinergic inhibition of neocortical pyramidal neurons. *J Neurosci* **25,** 10308-10320.

Grunditz A, Holbro N, Tian L, Zuo Y & Oertner TG. (2008). Spine neck plasticity controls postsynaptic calcium signals through electrical compartmentalization. *J Neurosci* **28,** 13457-13466.

Hardie J & Spruston N. (2009). Synaptic depolarization is more effective than back-propagating action potentials during induction of associative long-term potentiation in hippocampal pyramidal neurons. *J Neurosci* **29,** 3233-3241.

Harnett MT, Xu NL, Magee JC & Williams SR. (2013). Potassium channels control the interaction between active dendritic integration compartments in layer 5 cortical pyramidal neurons. *Neuron* **79,** 516-529.

Harris KM & Stevens JK. (1988). Dendritic spines of rat cerebellar Purkinje cells: serial electron microscopy with reference to their biophysical characteristics. *J Neurosci* **8,** 4455-4469.

Harris KM & Stevens JK. (1989). Dendritic spines of CA 1 pyramidal cells in the rat hippocampus: serial electron microscopy with reference to their biophysical characteristics. *J Neurosci* **9,** 2982-2997.

Hausser M, Stuart G, Racca C & Sakmann B. (1995). Axonal initiation and active dendritic propagation of action potentials in substantia nigra neurons. *Neuron* **15,** 637-647.

Hebb DO. (1949). *The Organisation of Behaviour*. Wiley.

Helmchen F, Imoto K & Sakmann B. (1996). Ca2+ buffering and action potential-evoked Ca2+ signaling in dendrites of pyramidal neurons. *Biophysical Journal* **70,** 1069-1081.

Higley MJ & Sabatini BL. (2008). Calcium signaling in dendrites and spines: practical and functional considerations. *Neuron* **59,** 902-913.

Higley MJ & Sabatini BL. (2010). Competitive regulation of synaptic Ca2+ influx by D2 dopamine and A2A adenosine receptors. *Nat Neurosci* **13,** 958-966.

Hirschberg B, Maylie J, Adelman JP & Marrion NV. (1999). Gating properties of single SK channels in hippocampal CA1 pyramidal neurons. *Biophysical Journal* **77,** 1905-1913.

Hoffman DA, Magee JC, Colbert CM & Johnston D. (1997). K+ channel regulation of signal propagation in dendrites of hippocampal pyramidal neurons. *Nature* **387,** 869-875.

Holbro N, Grunditz A, Wiegert JS & Oertner TG. (2010). AMPA receptors gate spine Ca(2+) transients and spike-timing-dependent potentiation. *Proceedings of the National Academy of Sciences of the United States of America* **107,** 15975-15980.

Holthoff K, Kovalchuk Y, Yuste R & Konnerth A. (2004). Single-shock LTD by local dendritic spikes in pyramidal neurons of mouse visual cortex. *J Physiol* **560,** 27-36.

Holthoff K, Tsay D & Yuste R. (2002). Calcium dynamics of spines depend on their dendritic location. *Neuron* **33,** 425-437.

Holthoff K, Zecevic D & Konnerth A. (2010). Rapid time course of action potentials in spines and remote dendrites of mouse visual cortex neurons. *J Physiol* **588,** 1085-1096.

Holtmaat A, Wilbrecht L, Knott GW, Welker E & Svoboda K. (2006). Experience-dependent and cell-type-specific spine growth in the neocortex. *Nature* **441,** 979-983.

Holtmaat AJ, Trachtenberg JT, Wilbrecht L, Shepherd GM, Zhang X, Knott GW & Svoboda K. (2005). Transient and persistent dendritic spines in the neocortex in vivo. *Neuron* **45,** 279-291.

Hoogland TM & Saggau P. (2004). Facilitation of L-type Ca2+ channels in dendritic spines by activation of beta2 adrenergic receptors. *J Neurosci* **24,** 8416-8427.

Hu H, Shao LR, Chavoshy S, Gu N, Trieb M, Behrens R, Laake P, Pongs O, Knaus HG, Ottersen OP & Storm JF. (2001). Presynaptic Ca2+-activated K+ channels in glutamatergic hippocampal terminals and their role in spike repolarization and regulation of transmitter release. *J Neurosci* **21,** 9585-9597.

Huber KM, Roder JC & Bear MF. (2001). Chemical induction of mGluR5- and protein synthesis--dependent long-term depression in hippocampal area CA1. *J Neurophysiol* **86,** 321-325.

Isope P & Murphy TH. (2005). Low threshold calcium currents in rat cerebellar Purkinje cell dendritic spines are mediated by T-type calcium channels. *J Physiol* **562,** 257-269.

Jack JJB, Noble, D., Tsien, R.W. (1975). *Electric Current Flow in Excitable Cells* Oxford University Press, London.

Jaffe DB, Johnston D, Lasser-Ross N, Lisman JE, Miyakawa H & Ross WN. (1992). The spread of Na+ spikes determines the pattern of dendritic Ca2+ entry into hippocampal neurons. *Nature* **357,** 244-246.

Janssen WG, Vissavajjhala P, Andrews G, Moran T, Hof PR & Morrison JH. (2005). Cellular and synaptic distribution of NR2A and NR2B in macaque monkey and rat hippocampus as visualized with subunit-specific monoclonal antibodies. *Experimental Neurology* **191 Suppl 1,** S28-44.

Jaslove SW. (1992). The integrative properties of spiny distal dendrites. *Neuroscience* **47,** 495-519.

Jia H, Rochefort NL, Chen X & Konnerth A. (2010). Dendritic organization of sensory input to cortical neurons in vivo. *Nature* **464,** 1307-1312.

Johnston D, Hoffman DA, Magee JC, Poolos NP, Watanabe S, Colbert CM & Migliore M. (2000). Dendritic potassium channels in hippocampal pyramidal neurons. *J Physiol* **525 Pt 1,** 75-81.

Jourdain P, Fukunaga K & Muller D. (2003). Calcium/calmodulin-dependent protein kinase II contributes to activity-dependent filopodia growth and spine formation. *J Neurosci* **23,** 10645-10649.

Kampa BM, Clements J, Jonas P & Stuart GJ. (2004). Kinetics of Mg2+ unblock of NMDA receptors: implications for spike-timing dependent synaptic plasticity. *J Physiol* **556,** 337-345.

Kampa BM, Letzkus JJ & Stuart GJ. (2006). Requirement of dendritic calcium spikes for induction of spike-timing-dependent synaptic plasticity. *J Physiol* **574,** 283-290.

Kampa BM & Stuart GJ. (2006). Calcium spikes in basal dendrites of layer 5 pyramidal neurons during action potential bursts. *J Neurosci* **26,** 7424-7432.

Kang J, Huguenard JR & Prince DA. (1996). Two types of BK channels in immature rat neocortical pyramidal neurons. *J Neurophysiol* **76,** 4194-4197.

Kasai H, Fukuda M, Watanabe S, Hayashi-Takagi A & Noguchi J. (2010). Structural dynamics of dendritic spines in memory and cognition. *Trends Neurosci* **33,** 121-129.

Katz Y, Menon V, Nicholson DA, Geinisman Y, Kath WL & Spruston N. (2009). Synapse distribution suggests a two-stage model of dendritic integration in CA1 pyramidal neurons. *Neuron* **63,** 171-177.

Keen JE, Khawaled R, Farrens DL, Neelands T, Rivard A, Bond CT, Janowsky A, Fakler B, Adelman JP & Maylie J. (1999). Domains responsible for constitutive and Ca(2+)-dependent interactions between calmodulin and small conductance Ca(2+)-activated potassium channels. *J Neurosci* **19,** 8830-8838.

Koch C & Poggio T. (1983). A theoretical analysis of electrical properties of spines. *Proceedings of the Royal Society of London Series B, Containing papers of a Biological character Royal Society* **218,** 455-477.

Koch C, Poggio T & Torre V. (1983). Nonlinear interactions in a dendritic tree: localization, timing, and role in information processing. *Proceedings of the National Academy of Sciences of the United States of America* **80,** 2799-2802.

Koch C & Zador A. (1993). The function of dendritic spines: devices subserving biochemical rather than electrical compartmentalization. *J Neurosci* **13,** 413-422.

Koester HJ & Sakmann B. (1998). Calcium dynamics in single spines during coincident pre- and postsynaptic activity depend on relative timing of back-propagating action potentials and subthreshold excitatory postsynaptic potentials. *Proceedings of the National Academy of Sciences of the United States of America* **95,** 9596-9601.

Koester HJ & Sakmann B. (2000). Calcium dynamics associated with action potentials in single nerve terminals of pyramidal cells in layer 2/3 of the young rat neocortex. *J Physiol* **529 Pt 3,** 625-646.

Kohler M, Hirschberg B, Bond CT, Kinzie JM, Marrion NV, Maylie J & Adelman JP. (1996). Small-conductance, calcium-activated potassium channels from mammalian brain. *Science* **273,** 1709-1714.

Kole MH, Hallermann S & Stuart GJ. (2006). Single Ih channels in pyramidal neuron dendrites: properties, distribution, and impact on action potential output. *J Neurosci* **26,** 1677-1687.

Kole MH, Ilschner SU, Kampa BM, Williams SR, Ruben PC & Stuart GJ. (2008). Action potential generation requires a high sodium channel density in the axon initial segment. *Nat Neurosci* **11,** 178-186.

Korngreen A & Sakmann B. (2000). Voltage-gated K+ channels in layer 5 neocortical pyramidal neurones from young rats: subtypes and gradients. *J Physiol* **525 Pt 3,** 621-639.

Kovalchuk Y, Eilers J, Lisman J & Konnerth A. (2000). NMDA receptor-mediated subthreshold Ca(2+) signals in spines of hippocampal neurons. *J Neurosci* **20,** 1791-1799.

Kulik A, Nakadate K, Hagiwara A, Fukazawa Y, Lujan R, Saito H, Suzuki N, Futatsugi A, Mikoshiba K, Frotscher M & Shigemoto R. (2004). Immunocytochemical localization of the alpha 1A subunit of the P/Q-type calcium channel in the rat cerebellum. *The European Journal of Neuroscience* **19,** 2169-2178.

Kumar SS, Bacci A, Kharazia V & Huguenard JR. (2002). A developmental switch of AMPA receptor subunits in neocortical pyramidal neurons. *J Neurosci* **22,** 3005-3015.

Kwon HB & Sabatini BL. (2011). Glutamate induces de novo growth of functional spines in developing cortex. *Nature* **474,** 100-104.

Lancaster B & Nicoll RA. (1987). Properties of two calcium-activated hyperpolarizations in rat hippocampal neurones. *J Physiol* **389,** 187-203.

Larkman AU. (1991). Dendritic morphology of pyramidal neurones of the visual cortex of the rat: III. Spine distributions. *The Journal of Comparative Neurology* **306,** 332-343.

Larkum ME, Kaiser KM & Sakmann B. (1999). Calcium electrogenesis in distal apical dendrites of layer 5 pyramidal cells at a critical frequency of back-propagating action potentials. *Proceedings of the National Academy of Sciences of the United States of America* **96,** 14600-14604.

Larkum ME, Launey T, Dityatev A & Luscher HR. (1998). Integration of excitatory postsynaptic potentials in dendrites of motoneurons of rat spinal cord slice cultures. *J Neurophysiol* **80,** 924-935.

Larkum ME, Nevian T, Sandler M, Polsky A & Schiller J. (2009). Synaptic integration in tuft dendrites of layer 5 pyramidal neurons: a new unifying principle. *Science* **325,** 756-760.

Larkum ME, Watanabe S, Nakamura T, Lasser-Ross N & Ross WN. (2003). Synaptically activated Ca2+ waves in layer 2/3 and layer 5 rat neocortical pyramidal neurons. *J Physiol* **549,** 471-488.

Larkum ME, Waters J, Sakmann B & Helmchen F. (2007). Dendritic spikes in apical dendrites of neocortical layer 2/3 pyramidal neurons. *J Neurosci* **27,** 8999-9008.

Latorre R, Oberhauser A, Labarca P & Alvarez O. (1989). Varieties of calcium-activated potassium channels. *Annual Review of Physiology* **51,** 385-399.

Latorre R, Vergara C & Hidalgo C. (1982). Reconstitution in planar lipid bilayers of a Ca2+-dependent K+ channel from transverse tubule membranes isolated from rabbit skeletal muscle. *Proceedings of the National Academy of Sciences of the United States of America* **79,** 805-809.

Lavzin M, Rapoport S, Polsky A, Garion L & Schiller J. (2012). Nonlinear dendritic processing determines angular tuning of barrel cortex neurons in vivo. *Nature* **490,** 397-401.

Lee SJ, Escobedo-Lozoya Y, Szatmari EM & Yasuda R. (2009). Activation of CaMKII in single dendritic spines during long-term potentiation. *Nature* **458,** 299-304.

Legendre P, Rosenmund C & Westbrook GL. (1993). Inactivation of NMDA channels in cultured hippocampal neurons by intracellular calcium. *J Neurosci* **13,** 674-684.

Letzkus JJ, Kampa BM & Stuart GJ. (2006). Learning rules for spike timing-dependent plasticity depend on dendritic synapse location. *J Neurosci* **26,** 10420-10429.

Lev-Tov A, Miller JP, Burke RE & Rall W. (1983). Factors that control amplitude of EPSPs in dendritic neurons. *J Neurophysiol* **50,** 399-412.

Lin MT, Lujan R, Watanabe M, Adelman JP & Maylie J. (2008). SK2 channel plasticity contributes to LTP at Schaffer collateral-CA1 synapses. *Nat Neurosci* **11,** 170-177.

Lin MT, Lujan R, Watanabe M, Frerking M, Maylie J & Adelman JP. (2010). Coupled activity-dependent trafficking of synaptic SK2 channels and AMPA receptors. *J Neurosci* **30,** 11726-11734.

Liu L, Wong TP, Pozza MF, Lingenhoehl K, Wang Y, Sheng M, Auberson YP & Wang YT. (2004). Role of NMDA receptor subtypes in governing the direction of hippocampal synaptic plasticity. *Science* **304,** 1021-1024.

Llinas R, Hillman, D.E. (1969). Physiological and morphological organisation of the cerebellar circuits in various vertebrates. In *Neurobiology of Cerebellar Evolution and Development*, ed. Llinas R, pp. 43-73. Am. Med. Assoc. Edu. Res. Found, Chicago.

Lorincz A, Notomi T, Tamas G, Shigemoto R & Nusser Z. (2002). Polarized and compartment-dependent distribution of HCN1 in pyramidal cell dendrites. *Nat Neurosci* **5,** 1185-1193.

Losonczy A & Magee JC. (2006). Integrative properties of radial oblique dendrites in hippocampal CA1 pyramidal neurons. *Neuron* **50,** 291-307.

Losonczy A, Makara JK & Magee JC. (2008). Compartmentalized dendritic plasticity and input feature storage in neurons. *Nature* **452,** 436-441.

Lynch GS, Dunwiddie T & Gribkoff V. (1977). Heterosynaptic depression: a postsynaptic correlate of long-term potentiation. *Nature* **266,** 737-739.

Magee JC. (1998). Dendritic hyperpolarization-activated currents modify the integrative properties of hippocampal CA1 pyramidal neurons. *J Neurosci* **18,** 7613-7624.

Magee JC & Cook EP. (2000). Somatic EPSP amplitude is independent of synapse location in hippocampal pyramidal neurons. *Nat Neurosci* **3,** 895-903.

Magee JC & Johnston D. (1997). A synaptically controlled, associative signal for Hebbian plasticity in hippocampal neurons. *Science* **275,** 209-213.

Maingret F, Coste B, Hao J, Giamarchi A, Allen D, Crest M, Litchfield DW, Adelman JP & Delmas P. (2008). Neurotransmitter modulation of small-conductance Ca2+-activated K+ channels by regulation of Ca2+ gating. *Neuron* **59,** 439-449.

Markram H, Helm PJ & Sakmann B. (1995). Dendritic calcium transients evoked by single back-propagating action potentials in rat neocortical pyramidal neurons. *J Physiol* **485 (Pt 1),** 1-20.

Markram H, Lubke J, Frotscher M, Roth A & Sakmann B. (1997a). Physiology and anatomy of synaptic connections between thick tufted pyramidal neurones in the developing rat neocortex. *J Physiol* **500 (Pt 2),** 409-440.

Markram H, Lubke J, Frotscher M & Sakmann B. (1997b). Regulation of synaptic efficacy by coincidence of postsynaptic APs and EPSPs. *Science* **275,** 213-215.

Marrion NV & Tavalin SJ. (1998). Selective activation of Ca2+-activated K+ channels by co-localized Ca2+ channels in hippocampal neurons. *Nature* **395,** 900-905.

Marty A. (1981). Ca-dependent K channels with large unitary conductance in chromaffin cell membranes. *Nature* **291,** 497-500.

Massey PV, Johnson BE, Moult PR, Auberson YP, Brown MW, Molnar E, Collingridge GL & Bashir ZI. (2004). Differential roles of NR2A and NR2B-containing NMDA receptors in cortical long-term potentiation and long-term depression. *J Neurosci* **24,** 7821-7828.

Matsuzaki M, Ellis-Davies GC, Nemoto T, Miyashita Y, Iino M & Kasai H. (2001). Dendritic spine geometry is critical for AMPA receptor expression in hippocampal CA1 pyramidal neurons. *Nat Neurosci* **4,** 1086-1092.

Matsuzaki M, Honkura N, Ellis-Davies GC & Kasai H. (2004). Structural basis of long-term potentiation in single dendritic spines. *Nature* **429,** 761-766.

Mayer ML, Westbrook GL & Guthrie PB. (1984). Voltage-dependent block by Mg2+ of NMDA responses in spinal cord neurones. *Nature* **309,** 261-263.

Miller JP, Rall W & Rinzel J. (1985). Synaptic amplification by active membrane in dendritic spines. *Brain Res* **325,** 325-330.

Monyer H, Burnashev N, Laurie DJ, Sakmann B & Seeburg PH. (1994). Developmental and regional expression in the rat brain and functional properties of four NMDA receptors. *Neuron* **12,** 529-540.

Monyer H, Sprengel R, Schoepfer R, Herb A, Higuchi M, Lomeli H, Burnashev N, Sakmann B & Seeburg PH. (1992). Heteromeric NMDA receptors: molecular and functional distinction of subtypes. *Science* **256,** 1217-1221.

Nagerl UV, Eberhorn N, Cambridge SB & Bonhoeffer T. (2004). Bidirectional activity-dependent morphological plasticity in hippocampal neurons. *Neuron* **44,** 759-767.

Nagerl UV, Kostinger G, Anderson JC, Martin KA & Bonhoeffer T. (2007). Protracted synaptogenesis after activity-dependent spinogenesis in hippocampal neurons. *J Neurosci* **27,** 8149-8156.

Nagerl UV, Novo D, Mody I & Vergara JL. (2000). Binding kinetics of calbindin-D(28k) determined by flash photolysis of caged Ca(2+). *Biophysical Journal* **79,** 3009-3018.

Nakamura T, Barbara JG, Nakamura K & Ross WN. (1999). Synergistic release of Ca2+ from IP3-sensitive stores evoked by synaptic activation of mGluRs paired with backpropagating action potentials. *Neuron* **24,** 727-737.

Naraghi M & Neher E. (1997). Linearized buffered Ca2+ diffusion in microdomains and its implications for calculation of [Ca2+] at the mouth of a calcium channel. *J Neurosci* **17,** 6961-6973.

Neher E. (1986). *Concentration profiles of intracellular calcium in the presence of a diffusible chelator*. Springer-Verlag, Berlin.

Neher E. (1998). Vesicle pools and Ca2+ microdomains: new tools for understanding their roles in neurotransmitter release. *Neuron* **20,** 389-399.

Nevian T, Larkum ME, Polsky A & Schiller J. (2007). Properties of basal dendrites of layer 5 pyramidal neurons: a direct patch-clamp recording study. *Nat Neurosci* **10,** 206-214.

Nevian T & Sakmann B. (2004). Single spine Ca2+ signals evoked by coincident EPSPs and backpropagating action potentials in spiny stellate cells of layer 4 in the juvenile rat somatosensory barrel cortex. *J Neurosci* **24,** 1689-1699.

Nevian T & Sakmann B. (2006). Spine Ca2+ signaling in spike-timing-dependent plasticity. *J Neurosci* **26,** 11001-11013.

Ngo-Anh TJ, Bloodgood BL, Lin M, Sabatini BL, Maylie J & Adelman JP. (2005). SK channels and NMDA receptors form a Ca2+-mediated feedback loop in dendritic spines. *Nat Neurosci* **8,** 642-649.

Nicholson C & Llinas R. (1969). Inhibition of Purkinje cells in the cerebellum of elasmobranch fishes. *Brain Res* **12,** 477-481.

Nicholson DA, Trana R, Katz Y, Kath WL, Spruston N & Geinisman Y. (2006). Distance-dependent differences in synapse number and AMPA receptor expression in hippocampal CA1 pyramidal neurons. *Neuron* **50,** 431-442.

Nishiyama M, Hong K, Mikoshiba K, Poo MM & Kato K. (2000). Calcium stores regulate the polarity and input specificity of synaptic modification. *Nature* **408,** 584-588.

Nowak L, Bregestovski P, Ascher P, Herbet A & Prochiantz A. (1984). Magnesium gates glutamate-activated channels in mouse central neurones. *Nature* **307,** 462-465.

Ohtsuki G, Piochon C, Adelman JP & Hansel C. (2012). SK2 Channel Modulation Contributes to Compartment-Specific Dendritic Plasticity in Cerebellar Purkinje Cells. *Neuron* **75,** 108-120.

Palmer LM & Stuart GJ. (2006). Site of action potential initiation in layer 5 pyramidal neurons. *J Neurosci* **26,** 1854-1863.

Palmer LM & Stuart GJ. (2009). Membrane potential changes in dendritic spines during action potentials and synaptic input. *J Neurosci* **29,** 6897-6903.

Pedarzani P, Mosbacher J, Rivard A, Cingolani LA, Oliver D, Stocker M, Adelman JP & Fakler B. (2001). Control of electrical activity in central neurons by modulating the gating of small conductance Ca2+-activated K+ channels. *The Journal of Biological Chemistry* **276,** 9762-9769.

Perkel DH. (1982). Functional role of dendritic spines. *Journal de Physiologie* **78,** 695-699.

Perkel DH & Perkel DJ. (1985). Dendritic spines: role of active membrane in modulating synaptic efficacy. *Brain Res* **325,** 331-335.

Plant K, Pelkey KA, Bortolotto ZA, Morita D, Terashima A, McBain CJ, Collingridge GL & Isaac JT. (2006). Transient incorporation of native GluR2-lacking AMPA receptors during hippocampal long-term potentiation. *Nat Neurosci* **9,** 602-604.

Prakriya M & Lingle CJ. (1999). BK channel activation by brief depolarizations requires Ca2+ influx through L- and Q-type Ca2+ channels in rat chromaffin cells. *J Neurophysiol* **81,** 2267-2278.

Prakriya M & Lingle CJ. (2000). Activation of BK channels in rat chromaffin cells requires summation of Ca(2+) influx from multiple Ca(2+) channels. *J Neurophysiol* **84,** 1123-1135.

Precht W & Llinas R. (1969). Functional organization of the vestibular afferents to the cerebellar cortex of frog and cat. *Experimental Brain Research* **9,** 30-52.

Rah J-C, Bas E, Colonell J, Mishchenko Y, Karsh B, Fetter RD, Myers EW, Chklovskii DB, Svoboda K, Harris TD & Isaac JTR. (2013).

Thalamocortical input onto layer 5 pyramidal neurons measured using quantitative large-scale array tomography. *Frontiers in Neural Circuits* **7**.

Rall W. (1959). Branching dendritic trees and motoneuron membrane resistivity. *Experimental Neurology* **1,** 491-527.

Rall W. (1978). Dendritic spines and synaptic potency. In *Studies in Neurophysiology*, ed. Porter R, pp. 203-209. Cambridge University Press, New York.

Rall W, Rinzel, J. (1971). Dendritic spine function and synaptic attenuation calculations. *Soc Neurosci Abstr* **1**.

Rinzel J & Rall W. (1974). Transient response in a dendritic neuron model for current injected at one branch. *Biophysical Journal* **14,** 759-790.

Robbe D, Kopf M, Remaury A, Bockaert J & Manzoni OJ. (2002). Endogenous cannabinoids mediate long-term synaptic depression in the nucleus accumbens. *Proceedings of the National Academy of Sciences of the United States of America* **99,** 8384-8388.

Roberts TF, Tschida KA, Klein ME & Mooney R. (2010). Rapid spine stabilization and synaptic enhancement at the onset of behavioural learning. *Nature* **463,** 948-952.

Roberts WM. (1993). Spatial calcium buffering in saccular hair cells. *Nature* **363,** 74-76.

Roberts WM. (1994). Localization of calcium signals by a mobile calcium buffer in frog saccular hair cells. *J Neurosci* **14,** 3246-3262.

Roberts WM, Jacobs RA & Hudspeth AJ. (1990). Colocalization of ion channels involved in frequency selectivity and synaptic transmission at presynaptic active zones of hair cells. *J Neurosci* **10,** 3664-3684.

Robitaille R, Adler EM & Charlton MP. (1993). Calcium channels and calcium-gated potassium channels at the frog neuromuscular junction. *Journal of Physiology, Paris* **87,** 15-24.

Rosenmund C, Feltz A & Westbrook GL. (1995). Calcium-dependent inactivation of synaptic NMDA receptors in hippocampal neurons. *J Neurophysiol* **73,** 427-430.

Rosenmund C & Westbrook GL. (1993). Calcium-induced actin depolymerization reduces NMDA channel activity. *Neuron* **10,** 805-814.

Sabatini BL, Oertner TG & Svoboda K. (2002). The life cycle of Ca(2+) ions in dendritic spines. *Neuron* **33,** 439-452.

Sabatini BL & Svoboda K. (2000). Analysis of calcium channels in single spines using optical fluctuation analysis. *Nature* **408,** 589-593.

Safo PK & Regehr WG. (2005). Endocannabinoids control the induction of cerebellar LTD. *Neuron* **48,** 647-659.

Sah P & Davies P. (2000). Calcium-activated potassium currents in mammalian neurons. *Clin Exp Pharmacol Physiol* **27,** 657-663.

Sah P & McLachlan EM. (1991). Ca(2+)-activated K+ currents underlying the afterhyperpolarization in guinea pig vagal neurons: a role for Ca(2+)-activated Ca2+ release. *Neuron* **7,** 257-264.

Sailer CA, Hu H, Kaufmann WA, Trieb M, Schwarzer C, Storm JF & Knaus HG. (2002). Regional differences in distribution and functional expression of small-conductance Ca2+-activated K+ channels in rat brain. *J Neurosci* **22,** 9698-9707.

Schaefer AT, Helmstaedter M, Schmitt AC, Bar-Yehuda D, Almog M, Ben-Porat H, Sakmann B & Korngreen A. (2007). Dendritic voltage-gated K+ conductance gradient in pyramidal neurones of neocortical layer 5B from rats. *J Physiol* **579,** 737-752.

Schiller J, Major G, Koester HJ & Schiller Y. (2000). NMDA spikes in basal dendrites of cortical pyramidal neurons. *Nature* **404,** 285-289.

Schiller J, Schiller Y & Clapham DE. (1998). NMDA receptors amplify calcium influx into dendritic spines during associative pre- and postsynaptic activation. *Nat Neurosci* **1,** 114-118.

Schiller J, Schiller Y, Stuart G & Sakmann B. (1997). Calcium action potentials restricted to distal apical dendrites of rat neocortical pyramidal neurons. *J Physiol* **505 (Pt 3),** 605-616.

Schubert D, Staiger JF, Cho N, Kotter R, Zilles K & Luhmann HJ. (2001). Layer-specific intracolumnar and transcolumnar functional connectivity of layer V pyramidal cells in rat barrel cortex. *J Neurosci* **21,** 3580-3592.

Schwindt PC, Spain WJ, Foehring RC, Stafstrom CE, Chubb MC & Crill WE. (1988). Multiple potassium conductances and their functions in neurons from cat sensorimotor cortex in vitro. *J Neurophysiol* **59,** 424-449.

Segev I & Rall W. (1988). Computational study of an excitable dendritic spine. *J Neurophysiol* **60,** 499-523.

Seidler NW, Jona I, Vegh M & Martonosi A. (1989). Cyclopiazonic acid is a specific inhibitor of the Ca2+-ATPase of sarcoplasmic reticulum. *The Journal of Biological Chemistry* **264,** 17816-17823.

Shao LR, Halvorsrud R, Borg-Graham L & Storm JF. (1999). The role of BK-type Ca2+-dependent K+ channels in spike broadening during repetitive firing in rat hippocampal pyramidal cells. *J Physiol* **521 Pt 1,** 135-146.

Shepherd GM, Brayton RK, Miller JP, Segev I, Rinzel J & Rall W. (1985). Signal enhancement in distal cortical dendrites by means of interactions between active dendritic spines. *Proceedings of the National Academy of Sciences of the United States of America* **82,** 2192-2195.

Shouval HZ, Bear MF & Cooper LN. (2002). A unified model of NMDA receptor-dependent bidirectional synaptic plasticity. *Proceedings of the National Academy of Sciences of the United States of America* **99,** 10831-10836.

Sjostrom PJ & Hausser M. (2006). A cooperative switch determines the sign of synaptic plasticity in distal dendrites of neocortical pyramidal neurons. *Neuron* **51,** 227-238.

Sjostrom PJ, Turrigiano GG & Nelson SB. (2001). Rate, timing, and cooperativity jointly determine cortical synaptic plasticity. *Neuron* **32,** 1149-1164.

Sjostrom PJ, Turrigiano GG & Nelson SB. (2003). Neocortical LTD via coincident activation of presynaptic NMDA and cannabinoid receptors. *Neuron* **39,** 641-654.

Sjostrom PJ, Turrigiano GG & Nelson SB. (2004). Endocannabinoid-dependent neocortical layer-5 LTD in the absence of postsynaptic spiking. *J Neurophysiol* **92,** 3338-3343.

Skeberdis VA, Chevaleyre V, Lau CG, Goldberg JH, Pettit DL, Suadicani SO, Lin Y, Bennett MV, Yuste R, Castillo PE & Zukin RS. (2006). Protein kinase A regulates calcium permeability of NMDA receptors. *Nat Neurosci* **9,** 501-510.

Smith SL, Smith IT, Branco T & Hausser M. (2013). Dendritic spikes enhance stimulus selectivity in cortical neurons in vivo. *Nature* **503,** 115-120.

Sobczyk A, Scheuss V & Svoboda K. (2005). NMDA receptor subunit-dependent [Ca2+] signaling in individual hippocampal dendritic spines. *J Neurosci* **25,** 6037-6046.

Sobczyk A & Svoboda K. (2007). Activity-dependent plasticity of the NMDA-receptor fractional Ca2+ current. *Neuron* **53,** 17-24.

Solaro CR, Prakriya M, Ding JP & Lingle CJ. (1995). Inactivating and noninactivating Ca(2+)- and voltage-dependent K+ current in rat adrenal chromaffin cells. *J Neurosci* **15,** 6110-6123.

Song S, Miller KD & Abbott LF. (2000). Competitive Hebbian learning through spike-timing-dependent synaptic plasticity. *Nat Neurosci* **3,** 919-926.

Sorra KE & Harris KM. (2000). Overview on the structure, composition, function, development, and plasticity of hippocampal dendritic spines. *Hippocampus* **10,** 501-511.

Spruston N. (2008). Pyramidal neurons: dendritic structure and synaptic integration. *Nat Rev Neurosci* **9,** 206-221.

Spruston N, Jaffe DB & Johnston D. (1994). Dendritic attenuation of synaptic potentials and currents: the role of passive membrane properties. *Trends Neurosci* **17,** 161-166.

Spruston N, Schiller Y, Stuart G & Sakmann B. (1995). Activity-dependent action potential invasion and calcium influx into hippocampal CA1 dendrites. *Science* **268,** 297-300.

Stackman RW, Hammond RS, Linardatos E, Gerlach A, Maylie J, Adelman JP & Tzounopoulos T. (2002). Small conductance Ca2+-activated K+ channels modulate synaptic plasticity and memory encoding. *J Neurosci* **22,** 10163-10171.

Stocker M, Krause M & Pedarzani P. (1999). An apamin-sensitive Ca2+-activated K+ current in hippocampal pyramidal neurons. *Proceedings of the National Academy of Sciences of the United States of America* **96,** 4662-4667.

Stocker M & Pedarzani P. (2000). Differential distribution of three Ca(2+)-activated K(+) channel subunits, SK1, SK2, and SK3, in the adult rat central nervous system. *Molecular and Cellular Neurosciences* **15,** 476-493.

Storm JF. (1987a). Action potential repolarization and a fast after-hyperpolarization in rat hippocampal pyramidal cells. *J Physiol* **385,** 733-759.

Storm JF. (1987b). Phorbol esters broaden the action potential in CA1 hippocampal pyramidal cells. *Neuroscience letters* **75,** 71-74.

Stuart G. (1999). Voltage-activated sodium channels amplify inhibition in neocortical pyramidal neurons. *Nat Neurosci* **2,** 144-150.

Stuart GJ, Dodt HU & Sakmann B. (1993). Patch-clamp recordings from the soma and dendrites of neurons in brain slices using infrared video microscopy. *Pflugers Arch* **423,** 511-518.

Stuart G & Sakmann B. (1995). Amplification of EPSPs by axosomatic sodium channels in neocortical pyramidal neurons. *Neuron* **15,** 1065-1076.

Stuart G, Schiller J & Sakmann B. (1997). Action potential initiation and propagation in rat neocortical pyramidal neurons. *J Physiol* **505 (Pt 3),** 617-632.

Stuart GJ & Hausser M. (2001). Dendritic coincidence detection of EPSPs and action potentials. *Nat Neurosci* **4,** 63-71.

Stuart GJ & Sakmann B. (1994). Active propagation of somatic action potentials into neocortical pyramidal cell dendrites. *Nature* **367,** 69-72.

Sun X, Gu XQ & Haddad GG. (2003). Calcium influx via L- and N-type calcium channels activates a transient large-conductance Ca2+-activated K+ current in mouse neocortical pyramidal neurons. *J Neurosci* **23,** 3639-3648.

Sun XP, Yazejian B & Grinnell AD. (2004). Electrophysiological properties of BK channels in Xenopus motor nerve terminals. *J Physiol* **557,** 207-228.

Svoboda K, Tank DW & Denk W. (1996). Direct measurement of coupling between dendritic spines and shafts. *Science* **272,** 716-719.

Tadross MR, Tsien RW & Yue DT. (2013). Ca2+ channel nanodomains boost local Ca2+ amplitude. *Proceedings of the National Academy of Sciences of the United States of America* **110,** 15794-15799.

Thiagarajan TC, Lindskog M & Tsien RW. (2005). Adaptation to synaptic inactivity in hippocampal neurons. *Neuron* **47,** 725-737.

Thompson SM, Masukawa LM & Prince DA. (1985). Temperature dependence of intrinsic membrane properties and synaptic potentials in hippocampal CA1 neurons in vitro. *J Neurosci* **5,** 817-824.

Thurbon D, Luscher HR, Hofstetter T & Redman SJ. (1998). Passive electrical properties of ventral horn neurons in rat spinal cord slices. *J Neurophysiol* **79,** 2485-2502.

Tonnesen J, Katona G, Rozsa B & Nagerl UV. (2014). Spine neck plasticity regulates compartmentalization of synapses. *Nat Neurosci* **advance online publication**.

Trachtenberg JT, Chen BE, Knott GW, Feng G, Sanes JR, Welker E & Svoboda K. (2002). Long-term in vivo imaging of experience-dependent synaptic plasticity in adult cortex. *Nature* **420,** 788-794.

Tsay D & Yuste R. (2002). Role of dendritic spines in action potential backpropagation: a numerical simulation study. *J Neurophysiol* **88,** 2834-2845.

Vargas-Caballero M & Robinson HP. (2003). A slow fraction of Mg2+ unblock of NMDA receptors limits their contribution to spike generation in cortical pyramidal neurons. *J Neurophysiol* **89,** 2778-2783.

Wang K, Lin MT, Adelman JP & Maylie J. (2014). Distinct Ca(2+) Sources in Dendritic Spines of Hippocampal CA1 Neurons Couple to SK and Kv4 Channels. *Neuron* **81,** 379-387.

Wang SS, Denk W & Hausser M. (2000). Coincidence detection in single dendritic spines mediated by calcium release. *Nat Neurosci* **3,** 1266-1273.

Wickens J. (1988). Electrically coupled but chemically isolated synapses: dendritic spines and calcium in a rule for synaptic modification. *Progress in Neurobiology* **31,** 507-528.

Wilbrecht L, Holtmaat A, Wright N, Fox K & Svoboda K. (2010). Structural plasticity underlies experience-dependent functional plasticity of cortical circuits. *J Neurosci* **30,** 4927-4932.

Williams SR & Stuart GJ. (2000). Site independence of EPSP time course is mediated by dendritic I(h) in neocortical pyramidal neurons. *J Neurophysiol* **83,** 3177-3182.

Williams SR & Stuart GJ. (2002). Dependence of EPSP efficacy on synapse location in neocortical pyramidal neurons. *Science* **295,** 1907-1910.

Wilson CJ. (1986). Three dimensional analysis of dendritic spines by means of HVEM. *J Electron Microsc* **35,** 1151-1155.

Wolfart J & Roeper J. (2002). Selective coupling of T-type calcium channels to SK potassium channels prevents intrinsic bursting in dopaminergic midbrain neurons. *J Neurosci* **22,** 3404-3413.

Womack MD, Chevez C & Khodakhah K. (2004). Calcium-activated potassium channels are selectively coupled to P/Q-type calcium channels in cerebellar Purkinje neurons. *J Neurosci* **24,** 8818-8822.

Womack MD & Khodakhah K. (2003). Somatic and Dendritic Small-Conductance Calcium-Activated Potassium Channels Regulate the Output of Cerebellar Purkinje Neurons. *J Neurosci* **23,** 2600-2607.

Xia XM, Fakler B, Rivard A, Wayman G, Johnson-Pais T, Keen JE, Ishii T, Hirschberg B, Bond CT, Lutsenko S, Maylie J & Adelman JP. (1998). Mechanism of calcium gating in small-conductance calcium-activated potassium channels. *Nature* **395,** 503-507.

Xu NL, Harnett MT, Williams SR, Huber D, O'Connor DH, Svoboda K & Magee JC. (2012). Nonlinear dendritic integration of sensory and motor input during an active sensing task. *Nature* **492,** 247-251.

Yang G, Pan F & Gan WB. (2009). Stably maintained dendritic spines are associated with lifelong memories. *Nature* **462,** 920-924.

Yang SN, Tang YG & Zucker RS. (1999). Selective induction of LTP and LTD by postsynaptic [Ca2+]i elevation. *J Neurophysiol* **81,** 781-787.

Yang Y, Wang XB & Zhou Q. (2010). Perisynaptic GluR2-lacking AMPA receptors control the reversibility of synaptic and spines modifications. *Proceedings of the National Academy of Sciences of the United States of America* **107,** 11999-12004.

Yasuda R, Nimchinsky EA, Scheuss V, Pologruto TA, Oertner TG, Sabatini BL & Svoboda K. (2004). Imaging Calcium Concentration Dynamics in Small Neuronal Compartments. *Sci STKE* **2004,** pl5-.

Yasuda R, Sabatini BL & Svoboda K. (2003). Plasticity of calcium channels in dendritic spines. *Nat Neurosci* **6,** 948-955.

Yazejian B, DiGregorio DA, Vergara JL, Poage RE, Meriney SD & Grinnell AD. (1997). Direct measurements of presynaptic calcium and calcium-activated potassium currents regulating neurotransmitter release at cultured Xenopus nerve-muscle synapses. *J Neurosci* **17,** 2990-3001.

Yazejian B, Sun XP & Grinnell AD. (2000). Tracking presynaptic Ca2+ dynamics during neurotransmitter release with Ca2+-activated K+ channels. *Nat Neurosci* **3,** 566-571.

Yu Y, Maureira C, Liu X & McCormick D. (2010). P/Q and N channels control baseline and spike-triggered calcium levels in neocortical axons and synaptic boutons. *J Neurosci* **30,** 11858-11869.

Yuste R & Denk W. (1995). Dendritic spines as basic functional units of neuronal integration. *Nature* **375,** 682-684.

Yuste R, Majewska A, Cash SS & Denk W. (1999). Mechanisms of calcium influx into hippocampal spines: heterogeneity among spines, coincidence detection by NMDA receptors, and optical quantal analysis. *J Neurosci* **19,** 1976-1987.

Zhao S, Ting JT, Atallah HE, Qiu L, Tan J, Gloss B, Augustine GJ, Deisseroth K, Luo M, Graybiel AM & Feng G. (2011). Cell type-specific channelrhodopsin-2 transgenic mice for optogenetic dissection of neural circuitry function. *Nat Methods* **8,** 745-752.

Zito K, Scheuss V, Knott G, Hill T & Svoboda K. (2009). Rapid functional maturation of nascent dendritic spines. *Neuron* **61,** 247-258.

Zucker RS. (1999). Calcium- and activity-dependent synaptic plasticity. *Current Opinion in Neurobiology* **9,** 305-313.